

## ELECTRONIC SUPPORTING INFORMATION

### Pnictogen-Functionalised Isocyanide Ligands

Ryan M. Kirk and Anthony F. Hill\*

## 1 Experimental

### 1.0 General considerations

Unless otherwise stated, all manipulations were carried out under an inert atmosphere of commercially purified argon using standard Schlenk techniques; the air stability/sensitivity of each compound is explicitly stated in the accompanying text. Anaerobic flash chromatography was conducted using a 30 x 5 cm Schlenk column loaded with oven-dried (120 °C) silica gel which had previously been degassed *in situ* by placing under vacuum for *ca* 60 minutes followed by flushing the apparatus with argon for a further *ca* 10 minutes. Reagents and materials were purchased from chemical vendors and used as-supplied without further purification: [Cr(CO)<sub>6</sub>], [Mo(CO)<sub>6</sub>], [W(CO)<sub>6</sub>], [Fe(CO)<sub>5</sub>], [Re<sub>2</sub>(CO)<sub>10</sub>] (Strem); [Mn(CO)<sub>3</sub>(η<sup>5</sup>-C<sub>5</sub>H<sub>5</sub>)], Na[N(SiMe<sub>3</sub>)<sub>2</sub>], ClP<sup>t</sup>Bu<sub>2</sub>, AsCl<sub>3</sub>, SbCl<sub>3</sub>, <sup>t</sup>BuMgCl solution (2 M in Et<sub>2</sub>O), silica gel 230–400 mesh, celite 545 (diatomaceous earth) (Sigma-Aldrich). [Fe(CO)<sub>4</sub>(PPh<sub>3</sub>)]<sup>1</sup> and [Re(CO)<sub>3</sub>(η<sup>5</sup>-C<sub>5</sub>H<sub>5</sub>)]<sup>2</sup> were prepared according to literature procedures. HPLC-grade solvents were purchased from Merck and re-distilled from an appropriate desiccant under nitrogen: THF, Et<sub>2</sub>O (sodium/benzophenone); toluene, tmeda, *n*-hexane (sodium); CH<sub>2</sub>Cl<sub>2</sub>, *n*-pentane (P<sub>2</sub>O<sub>5</sub>). Re-distilled solvents were then stored over an appropriate desiccant: THF, Et<sub>2</sub>O, *n*-pentane, *n*-hexane, toluene (sodium mirror); TMEDA, CH<sub>2</sub>Cl<sub>2</sub> (4 Å molecular sieves). Deuterated solvents were purchased from Cambridge Isotopes Laboratories and re-distilled under argon from an appropriate desiccant under nitrogen: C<sub>6</sub>D<sub>6</sub> (sodium); CDCl<sub>3</sub>, CD<sub>2</sub>Cl<sub>2</sub> (P<sub>2</sub>O<sub>5</sub>); CD<sub>3</sub>CN (CaCl<sub>2</sub>). ClAs<sup>t</sup>Bu<sub>2</sub> and ClSb<sup>t</sup>Bu<sub>2</sub> were prepared from AsCl<sub>3</sub> or SbCl<sub>3</sub>, respectively, and two equivalents of <sup>t</sup>BuMgCl in Et<sub>2</sub>O at 0 °C and purified by vacuum distillation.

**ClAs<sup>t</sup>Bu<sub>2</sub>:** Quantities used: 2.00 mL AsCl<sub>3</sub> (23.8 mmol), 23.8 mL <sup>t</sup>BuMgCl solution (2.0 M, 47.6 mmol). Isolated yield: 3.60 g (15.9 mmol, 67%). NMR: <sup>1</sup>H (C<sub>6</sub>D<sub>6</sub>, 400 MHz, 25 °C) δ<sub>H</sub> = 1.12 ppm; <sup>13</sup>C{<sup>1</sup>H} (C<sub>6</sub>D<sub>6</sub>, 101 MHz, 25 °C) δ<sub>C</sub> = 39.5, 27.9 ppm.

**ClSb<sup>t</sup>Bu<sub>2</sub>:** Quantities used: 3.00 g SbCl<sub>3</sub> (13.2 mmol), 13.2 mL <sup>t</sup>BuMgCl solution (2.0 M, 26.4 mmol). Isolated yield: 1.80 g (51%, 6.6 mmol). NMR: <sup>1</sup>H (C<sub>6</sub>D<sub>6</sub>, 400 MHz, 25 °C) δ<sub>H</sub> = 1.20 ppm; <sup>13</sup>C{<sup>1</sup>H} (C<sub>6</sub>D<sub>6</sub>, 101 MHz, 25 °C) δ<sub>C</sub> = 38.4, 28.8 ppm.

Solution NMR spectroscopy was conducted on Bruker Avance 400 (400 MHz for <sup>1</sup>H, 101 MHz for <sup>13</sup>C, 162 MHz for <sup>31</sup>P) or 800 (201 MHz for <sup>13</sup>C) instruments. Spectra were processed using the MestReNova suite and are referenced to the residual *proto*-solvent impurity (for <sup>1</sup>H), the solvent itself (for <sup>13</sup>C), or an external standard (for <sup>31</sup>P: 85% aqueous H<sub>3</sub>PO<sub>4</sub>). Chemical shifts are reported to 2 d.p. for <sup>1</sup>H, and 1 d.p. for <sup>13</sup>C, <sup>31</sup>P, and also coupling constants. We thank Dr Doug Lawes of the ANU for helpful discussion and assistance. Solution and solid-state IR

spectroscopies were conducted on Perkin Elmer Spectrum One and Spectrum Two instruments, respectively, and bond stretching frequencies are reported to the nearest whole number. The following abbreviations are used to denote relative absorption intensities: w (weak), m (medium), s (strong), vs (very strong). High-resolution mass spectrometry was conducted by the Joint Mass Spectrometry Facility at the Research School of Chemistry (ANU) using a Waters Synapt G2-Si HDMS LC-Q/TOF MS-MS spectrometer. Ion signals are reported to 4 d.p. and specific isotopomers are given for non-C,H,N,O elements. We thank Mrs Anitha Jeyasingham of the ANU for acquisition and processing of spectra. Elemental microanalytical data (duplicate runs) were provided by the Chemical Analysis Facility at the Department of Molecular Sciences, Macquarie University (NSW, Australia). Analyses are given to 2 d.p. Single crystal X-ray diffraction was conducted at 150 K on an Agilent Technologies Supernova equipped with a Rigaku HyPix 6000HE detector using graphite-monochromatised Cu-Kα radiation ( $\lambda$  = 1.5406 Å), or New Xcalibur equipped with an Atlas CCD detector using graphite-monochromatised Mo-Kα radiation ( $\lambda$  = 0.7107 Å). Selected crystals were mounted in oil on nylon loops and fixed under a cold stream of nitrogen. Data were processed within the CrysAlisPRO-CCD and -RED software packages.<sup>4</sup> Structures were solved within Olex<sup>25</sup> with SHELXT using intrinsic phasing and refined with SHELXL<sup>6</sup> using full-matrix least-squares against  $F^2$  in an anisotropic (for non-hydrogen atoms) approximation. Hydrogen atom positions were refined in isotropic approximation in a “riding” model with the  $U_{\text{iso}}(\text{H})$  parameters fixed to 1.2 (for aromatic hydrogens) or 1.5 (for aliphatic hydrogens)  $U_{\text{eq}}(\text{C}_i)$ , where  $U_{\text{eq}}(\text{C}_i)$  is the equivalent thermal parameter of the carbon atom to which the corresponding H atom is bonded. Specific absorption correction methods are stated for each crystalline sample in the accompanying text. POV-RAY images of crystal structures were rendered in ORTEP-3 (v2020.1)<sup>7</sup> or Mercury.<sup>8</sup> We thank Dr Michael Gardiner of the ANU for helpful discussion and assistance.

### 1.2 Synthesis of homoleptic cyanometallate salts

As these intermediates were identical or similar to previously reported salts, elemental microanalytical data were not pursued.

The procedure is a slight modification of that previously described by King<sup>3</sup>. To a solution of Na[N(SiMe<sub>3</sub>)<sub>2</sub>] in toluene was added one equivalent of the appropriate homoleptic metal carbonyl ([Cr(CO)<sub>6</sub>], [Mo(CO)<sub>6</sub>], [W(CO)<sub>6</sub>] or [Fe(CO)<sub>5</sub>]) at ambient temperature resulting in pale-yellow suspensions after the prescribed time. For Cr, Mo, and W the mixtures were

vigorously stirred for 48–72 hours (extended reaction times are due to the moderate solubility of the metal carbonyls in toluene), whereas for Fe only 16 hours reaction time was required. The supernatants were then decanted, and the solids were re-suspended in fresh toluene and collected on a medium-porosity frit under argon. Copious washing with toluene then *n*-hexane followed by drying *in vacuo* afforded the cyanometallate salts as air-sensitive solids which were stored in an argon-filled glovebox. All are soluble in donor solvents including THF, Et<sub>2</sub>O, acetone, acetonitrile, TMEDA, DME, and water. Proton NMR spectra with 4-iodoanisole as an internal standard confirmed the as-isolated products were unsolvated. **Caution should be exercised when handling these metal cyanide salts as their toxicological properties are unknown.**

### 1.2.1 Na[Cr(CN)(CO)<sub>5</sub>]

Quantities used: 4.00 g Na[N(SiMe<sub>3</sub>)<sub>2</sub>] (21.8 mmol), 4.80 g [Cr(CO)<sub>6</sub>] (21.8 mmol). The product is encountered as a white solid which is pale yellow in solution. Isolated yield: 4.70 g (19.4 mmol, 88%).

NMR: <sup>1</sup>H (CD<sub>3</sub>CN, 400 MHz, 25 °C) quiescent; <sup>13</sup>C{<sup>1</sup>H} (CD<sub>3</sub>CN, 201 MHz, 25 °C) δ<sub>C</sub> = 222.0 (CO<sub>ax</sub>), 219.0 (CO<sub>eq</sub>) 153.0 (CN) ppm. IR (THF, 25 °C): ν<sub>CO</sub> 2054(w), 1928(vs), 1898(s) cm<sup>-1</sup>, ν<sub>CN</sub> 2112(w) cm<sup>-1</sup>; IR (ATR, 25 °C): ν<sub>CO</sub> 2069(w), 1965(vs), 1892(vs), 1800(vs) cm<sup>-1</sup>, ν<sub>CN</sub> 2110(s) cm<sup>-1</sup>.

### 1.2.2 Na[Mo(CN)(CO)<sub>5</sub>]

Quantities used: 4.00 g Na[N(SiMe<sub>3</sub>)<sub>2</sub>] (21.8 mmol), 5.76 g [Mo(CO)<sub>6</sub>] (21.8 mmol). The product is encountered as a white solid which is pale yellow in solution. Isolated yield: 5.20 g (18.2 mmol, 83%).

NMR: <sup>1</sup>H (CD<sub>3</sub>CN, 400 MHz, 25 °C) quiescent; <sup>13</sup>C{<sup>1</sup>H} (CD<sub>3</sub>CN, 201 MHz, 25 °C) δ 211.7 (CO<sub>ax</sub>), 207.3 (CO<sub>eq</sub>), 148.5 (CN) ppm. IR (THF, 25 °C): ν<sub>CO</sub> 2060(w), 1930(vs), 1899(s) cm<sup>-1</sup>, ν<sub>CN</sub> 2114(w) cm<sup>-1</sup>; IR (ATR, 25 °C): ν<sub>CO</sub> 2075(w), 1968(vs), 1898(vs), 1799(vs) cm<sup>-1</sup>, ν<sub>CN</sub> 2113(w) cm<sup>-1</sup>.

### 1.2.3 Na[W(CN)(CO)<sub>5</sub>]

Quantities used: 5.00 g Na[N(SiMe<sub>3</sub>)<sub>2</sub>] (27.2 mmol), 9.60 g [W(CO)<sub>6</sub>] (27.2 mmol). The product is encountered as a white solid which is pale yellow in solution. Isolated yield: 9.30 g (24.9 mmol, 92%).

NMR: <sup>1</sup>H (CD<sub>3</sub>CN, 400 MHz, 25 °C) quiescent; <sup>13</sup>C{<sup>1</sup>H} (CD<sub>3</sub>CN, 201 MHz, 25 °C) δ<sub>C</sub> = 201.0 (<sup>1</sup>J<sub>WC</sub> = 140.6 Hz, CO<sub>ax</sub>), 197.5 (<sup>1</sup>J<sub>WC</sub> = 123.7 Hz, CO<sub>eq</sub>) 139.8 (<sup>1</sup>J<sub>WC</sub> = 92.6 Hz, CN) ppm. IR (THF, 25 °C): ν<sub>CO</sub> 2058(w), 1922(vs), 1896(s) cm<sup>-1</sup>, ν<sub>CN</sub> 2117(w) cm<sup>-1</sup>; IR (ATR, 25 °C): ν<sub>CO</sub> 2073(w), 1957(vs), 1884(vs), 1792(vs) cm<sup>-1</sup>, ν<sub>CN</sub> 2116(s) cm<sup>-1</sup>.

### 1.2.4 Na[Fe(CN)(CO)<sub>5</sub>]

Quantities used: 3.00 g Na[N(SiMe<sub>3</sub>)<sub>2</sub>] (16.3 mmol), 2.20 mL [Fe(CO)<sub>5</sub>] (17 mmol). The product is encountered as a light brown solid which is light orange in solution. Isolated yield: 6.30 g (29.0 mmol, 85%).

NMR: <sup>1</sup>H (CD<sub>3</sub>CN, 400 MHz, 25 °C) quiescent; <sup>13</sup>C{<sup>1</sup>H} (CD<sub>3</sub>CN, 201 MHz, 25 °C) δ<sub>C</sub> = 217.0 (CO), 144.1 (CN) ppm. IR (THF, 25 °C):

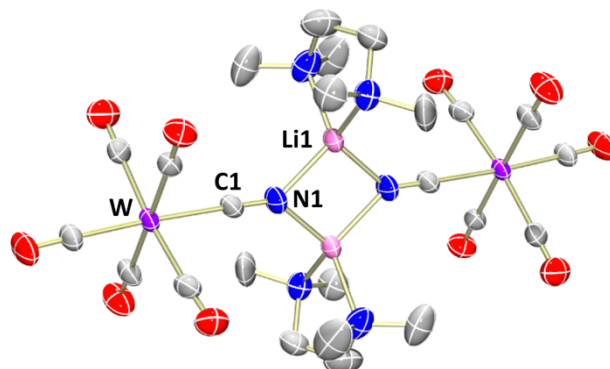
ν<sub>CO</sub> 2038(s), 1950(s), 1930(vs) cm<sup>-1</sup>, ν<sub>CN</sub> 2120(w) cm<sup>-1</sup>; the compound was too air sensitive for ATR IR measurements, where rapid oxidation occurred (signalled by a dark brown cast forming on the sample almost instantly) and ν<sub>CO</sub> and ν<sub>CN</sub> assignments could not be made in confidence.

### 1.2.5 [LiW(μ-CN)(CO)<sub>5</sub>·TMEDA]<sub>2</sub>

A solution of Li[N(SiMe<sub>3</sub>)<sub>2</sub>] in 25 mL THF was prepared from 0.60 mL HN(SiMe<sub>3</sub>)<sub>2</sub> (2.8 mmol) and 1.2 mL *n*-BuLi solution (2.8 mmol, 2.5 M in hexanes) at 0 °C. To this was added 0.50 mL tmdea (3.1 mmol) and 1.00 g [W(CO)<sub>6</sub>] (2.8 mmol) and the mixture stirred overnight, becoming light yellow. After this time volatiles were removed under reduced pressure and the residue triturated in *n*-hexane resulting in precipitation of off-white solids which were collected on a glass frit under argon and washed copiously with *n*-hexane and dried *in vacuo*. Isolated yield: 0.87 g (0.91 mmol, 65%). Encountered as an off-white solid which is pale yellow in solution. A <sup>1</sup>H NMR spectrum containing a known quantity of 4-iodoanisole as an internal standard confirmed the product to be (empirically) a TMEDA monosolvate.

NMR: <sup>1</sup>H (CD<sub>3</sub>CN, 400 MHz, 25 °C) δ<sub>H</sub> = 2.35 (s, 4H, C<sub>2</sub>H<sub>4</sub>), 2.22 (s, 12H, CH<sub>3</sub>) ppm; <sup>13</sup>C{<sup>1</sup>H} (CD<sub>3</sub>CN, 201 MHz, 25 °C) δ<sub>C</sub> = 200.9 (<sup>1</sup>J<sub>WC</sub> = 139.1 Hz, CO<sub>ax</sub>), 197.8 (<sup>1</sup>J<sub>WC</sub> = 125.0 Hz, CO<sub>eq</sub>), 141.8 (<sup>1</sup>J<sub>WC</sub> = 93.1 Hz, CN), 57.4 (C<sub>2</sub>H<sub>4</sub>), 46.1 (CH<sub>3</sub>) ppm. IR (THF, 25 °C) ν<sub>CO</sub> 2059(m), 1925(vs), 1900(s) cm<sup>-1</sup>, ν<sub>CN</sub> 2123(w) cm<sup>-1</sup>; IR (ATR, 25 °C) ν<sub>CO</sub> 2053(s), 1984(s), 1880(vs, br) cm<sup>-1</sup>, ν<sub>CN</sub> 2108(m) cm<sup>-1</sup>.

Single crystals were grown by layering a THF solution with *n*-hexane at -30 °C. The TMEDA ethylene bridge was disordered over two positions in a *ca* 80:20 occupancy ratio, and the minor component was modelled isotropically. The asymmetric unit contains one-half of a dimeric complex. *Crystal Data for* C<sub>24</sub>H<sub>32</sub>Li<sub>2</sub>N<sub>6</sub>O<sub>10</sub>W<sub>2</sub> (*M*<sub>w</sub> = 946.13 gmol<sup>-1</sup>): colourless prism 0.42 × 0.19 × 0.11 mm, triclinic, space group P-1 (no. 2), *a* = 8.71120(10) Å, *b* = 10.7852(2) Å, *c* = 11.3689(2) Å, α = 112.5180(10)°, β = 111.564(2)°, γ = 93.9840(10)°, *V* = 889.73(3) Å<sup>3</sup>, *Z* = 1, spherical correction *T*<sub>min</sub>/*T*<sub>max</sub> = 0.183/0.277, μ(Cu-Kα) = 12.236 mm<sup>-1</sup>, ρ<sub>calc</sub> = 1.766 Mg m<sup>-3</sup>, 10566 reflections measured (9.154° ≤ 2θ ≤ 156.102°), 3729 unique (*R*<sub>int</sub> = 0.0422, *R*<sub>sigma</sub> = 0.0308) which were used in all calculations against 218 parameters. The final *R*<sub>1</sub> was 0.0362 (*I* > 2σ(*I*)) and *wR*<sub>2</sub> was 0.0945 (all data), *GOF*(*F*<sup>2</sup>) = 1.055, *D*<sub>min</sub>/*D*<sub>max</sub> = -2.72/1.21 eÅ<sup>-3</sup>. CCDC number 2403970.

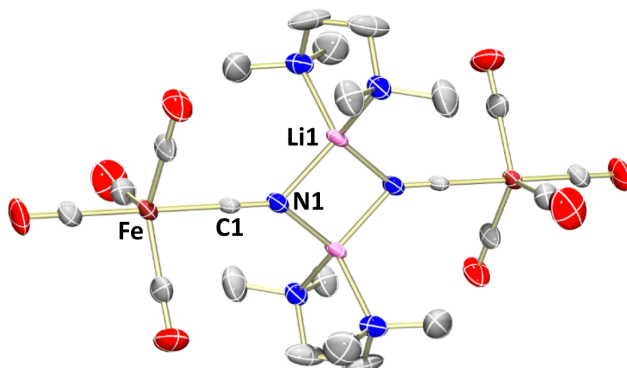


**Figure S1:** Molecular structure of centrosymmetric  $\{\text{Li}(\text{tmeda})[\mathbf{1}_\text{W}]\}_2$ .**1.2.6  $[\text{LiFe}(\mu\text{-CN})(\text{CO})_4\text{-tmeda}]_2$** 

Prepared and purified as described above, except  $\text{Et}_2\text{O}$  was used as the reaction medium. Quantities used: 3.0 mL  $n\text{-BuLi}$  solution (7.6 mmol, 2.5 M in hexanes), 1.6 mL  $\text{HN}(\text{SiMe}_3)_2$  (7.6 mmol), 1.2 mL tmeda (8.0 mmol), 1.0 mL  $[\text{Fe}(\text{CO})_5]$  (7.6 mmol). Isolated yield: 1.8 g (2.7 mmol, 71%). Encountered as a pale yellow solid which is yellow in solution.

NMR:  $^1\text{H}$  ( $\text{CD}_3\text{CN}$ , 400 MHz, 25 °C)  $\delta$  2.36 (s, 4H,  $\text{C}_2\text{H}_4$ ), 2.23 (s, 12H,  $\text{CH}_3$ ) ppm;  $^{13}\text{C}\{^1\text{H}\}$  ( $\text{CD}_3\text{CN}$ , 400 MHz, 25 °C)  $\delta$  217.0 (CO), 146.4 (CN), 57.4 ( $\text{C}_2\text{H}_4$ ), 46.0 ( $\text{CH}_3$ ) ppm. IR (THF, 25 °C)  $\nu_{\text{CO}}$  2040(s), 1954(s), 1933(vs) cm<sup>-1</sup>;  $\nu_{\text{CN}}$  2126(w) cm<sup>-1</sup>; IR (ATR, 25 °C)  $\nu_{\text{CO}}$  2036(s), 1929(vs, br) cm<sup>-1</sup>,  $\nu_{\text{CN}}$  2107(m) cm<sup>-1</sup>.

Single crystals were grown by layering a THF solution with  $n$ -hexane at -30 °C. The selected crystal proved to be twinned, and data was processed accordingly. The asymmetric unit contains one-half of a dimeric molecule. *Crystal data for*  $\text{C}_{22}\text{H}_{32}\text{Fe}_2\text{Li}_2\text{N}_6\text{O}_8$  ( $M_w = 634.11 \text{ gmol}^{-1}$ ): colourless plate  $0.269 \times 0.105 \times 0.061$  mm, triclinic, space group  $P\bar{1}$  (no. 2),  $a = 9.6531(15)$  Å,  $b = 9.7961(15)$  Å,  $c = 10.6609(13)$  Å,  $\alpha = 116.394(14)$ °,  $\beta = 108.038(12)$ °,  $\gamma = 97.046(13)$ °,  $V = 817.6(2)$  Å<sup>3</sup>,  $Z = 1$ , multi-scan correction  $T_{\min}/T_{\max} = 0.784/1.000$ ,  $\mu(\text{Mo-K}\alpha) = 0.934 \text{ mm}^{-1}$ ,  $\rho_{\text{calc}} = 1.288 \text{ Mg m}^{-3}$ , 8226 reflections measured ( $6.932^\circ \leq 2\theta \leq 59.626^\circ$ ), 8226 unique ( $R_{\text{sigma}} = 0.0718$ ) which were used in all calculations against 186 parameters. The final  $R_1$  was 0.0644 ( $I > 2\sigma(I)$ ) and  $wR_2$  was 0.1797 (all data),  $GOF(F^2) = 0.944$ ,  $D_{\min}/D_{\max} = -0.73/1.15 \text{ e}/\text{\AA}^3$ . CCDC number 2403969.

**Figure S2:** Molecular structure of centrosymmetric  $\{\text{Li}(\text{tmeda})[\mathbf{1}_\text{Fe}]\}_2$ .

Dimeric arrangements are found for  $\{\text{Li}(\text{tmeda})[\mathbf{1}_\text{W}]\}_2$  and  $\{\text{Li}(\text{tmeda})[\mathbf{1}_\text{Fe}]\}_2$  in the solid state with the cyanide N-termini bridging a pair of tetrahedral lithium cations; a crystallographic inversion centre is found at the midpoints of the (N1-Li1)<sub>2</sub> rhomboids which have side lengths *ca* 2.0 Å, and the metal-cyanide carbon distances of 2.161(7) (M = W) and 1.911(5) Å (M = Fe) are not especially remarkable. Formal C≡N bonds are measured which are essentially indistinguishable between the two metals (*ca* 1.15–1.16 Å), as dictated by the modest  $\pi$ -acceptor character of the cyanide ligand (*viz.* the axial position

in  $[\mathbf{1}_\text{Fe}]^-$ ) and in spite the disparate retrodative properties of the  $\text{W}(\text{CO})_5$  and  $\text{Fe}(\text{CO})_4$  centres.

**1.3 Synthesis of heteroleptic cyanometallate salts**

These cyanometallates were prepared and purified similarly to those above, except the mixtures in toluene were warmed to reflux for 16 h. **Caution should be exercised when handling these metal cyanide salts as their toxicological properties are unknown.**

**1.3.1  $\text{Na}[\text{Fe}(\text{CN})(\text{CO})_3(\text{PPh}_3)]$** 

Quantities used: 1.00 g  $[\text{Fe}(\text{CO})_4(\text{PPh}_3)]$  (2.4 mmol), 0.425 g  $\text{Na}[\text{N}(\text{SiMe}_3)_2]$  (2.34 mmol). The product is encountered as a beige solid which is dark orange in solution. Isolated yield: 0.80 g (1.77 mmol, 74%).

NMR:  $^1\text{H}$  ( $\text{CD}_3\text{CN}$ , 400 MHz, 25 °C)  $\delta_\text{H} = 7.47\text{--}7.43$  (m, 6H,  $\text{C}_6\text{H}_5$ ), 7.34–7.32 (m, 9H,  $\text{C}_6\text{H}_5$ ) ppm;  $^{13}\text{C}\{^1\text{H}\}$  ( $\text{CD}_3\text{CN}$ , 201 MHz, 25 °C)  $\delta_\text{C} = 218.8$  (d,  $^{2}\text{J}_\text{PC} = 27.3$  Hz, CO), 152.2 (d,  $^{2}\text{J}_\text{PC} = 6.8$  Hz, CN), 138.5 (d,  $^{1}\text{J}_\text{PC} = 43.0$  Hz, *ipso*- $\text{C}_6\text{H}_5$ ), 133.8 (d,  $^{2}\text{J}_\text{PC} = 10.4$  Hz, *ortho*- $\text{C}_6\text{H}_5$ ), 130.5 (*para*- $\text{C}_6\text{H}_5$ ), 128.9 (d,  $^{4}\text{J}_\text{PC} = 9.7$  Hz, *meta*- $\text{C}_6\text{H}_5$ ) ppm;  $^{31}\text{P}\{^1\text{H}\}$  ( $\text{CD}_3\text{CN}$ , 162 MHz, 25 °C)  $\delta_\text{P} = 84.3$  ppm. IR (THF)  $\nu_{\text{CO}}$  1780(vs), 1726(s) cm<sup>-1</sup>,  $\nu_{\text{CN}}$  2117(w) cm<sup>-1</sup>; IR (ATR)  $\nu_{\text{CO}}$  1991(s), 1909(s), 1895(vs), 1845(vs), 1789(vs) cm<sup>-1</sup>,  $\nu_{\text{CN}}$  2070(s), 2060(s) cm<sup>-1</sup>.

**1.3.2  $\text{Na}[\text{Mn}(\text{CN})(\text{CO})_2(\eta^5\text{-C}_5\text{H}_5)]$** 

Quantities used: 1.50 g  $[\text{Mn}(\text{CO})_3(\eta^5\text{-C}_5\text{H}_5)]$  (7.3 mmol), 1.35 g  $\text{Na}[\text{N}(\text{SiMe}_3)_2]$  (7.3 mmol). Encountered as a beige solid which is dark yellow in solution. Isolated yield: 1.21 g (5.3 mmol, 72%).

NMR:  $^1\text{H}$  ( $\text{CD}_3\text{CN}$ , 400 MHz, 25 °C)  $\delta_\text{H} = 4.41$  ( $\eta^5\text{-C}_5\text{H}_5$ ) ppm;  $^{13}\text{C}\{^1\text{H}\}$  ( $\text{CD}_3\text{CN}$ , 201 MHz, 25 °C)  $\delta_\text{C} = 236.4$  (CO), 165.6 (CN), 82.1 ( $\eta^5\text{-C}_5\text{H}_5$ ) ppm. IR (THF)  $\nu_{\text{CO}}$  1915(vs), 1845(vs) cm<sup>-1</sup>,  $\nu_{\text{CN}}$  2075(m) cm<sup>-1</sup>; IR (ATR)  $\nu_{\text{CO}}$  2047(s), 1899(vs), 1836(s), 1820(vs) cm<sup>-1</sup>,  $\nu_{\text{CN}}$  2057(s) cm<sup>-1</sup>.

**1.3.3  $\text{Na}[\text{Re}(\text{CN})(\text{CO})_2(\eta^5\text{-C}_5\text{H}_5)]$** 

Quantities used: 1.50 g  $[\text{Re}(\text{CO})_3(\eta^5\text{-C}_5\text{H}_5)]$  (4.4 mmol), 0.82 g  $\text{Na}[\text{N}(\text{SiMe}_3)_2]$  (4.4 mmol). Encountered as beige solid which is dark yellow in solution. Isolated yield: 1.30 g (3.6 mmol, 81%).

NMR:  $^1\text{H}$  ( $\text{CD}_3\text{CN}$ , 400 MHz, 25 °C)  $\delta$  5.07 ( $\eta^5\text{-C}_5\text{H}_5$ ) ppm;  $^{13}\text{C}\{^1\text{H}\}$  ( $\text{CD}_3\text{CN}$ , 201 MHz, 25 °C)  $\delta$  205.4 (CO), 133.1 (CN), 82.9 ( $\eta^5\text{-C}_5\text{H}_5$ ) ppm. IR (THF)  $\nu_{\text{CO}}$  1905(vs), 1836(vs) cm<sup>-1</sup>,  $\nu_{\text{CN}}$  2080(m) cm<sup>-1</sup>; IR (ATR)  $\nu_{\text{CO}}$  2058(s), 1890(vs), 1812(s), 1773(s) cm<sup>-1</sup>,  $\nu_{\text{CN}}$  2065(s) cm<sup>-1</sup>.

**1.4 General observations on cyanometallates**

In  $\text{CD}_3\text{CN}$  solution the presumably nitrile-solvated  $\text{Na}[\mathbf{1}_\text{M}]$  salts display  $^{13}\text{C}$  signals for the cyanide carbon nuclei in the neighbourhood of ~165–130 ppm (Table ), with a lower chemical shift loosely correlating with increasing metal basicity *i.e.*,  $[\mathbf{1}_\text{M}]^- > [\mathbf{1}_\text{Cr}]^- > [\mathbf{1}_\text{Fe}^\text{P}]^- \approx [\mathbf{1}_\text{Fe}]^- > [\mathbf{1}_\text{Mo}]^- > [\mathbf{1}_\text{Re}]^- > [\mathbf{1}_\text{W}]^-$ . The same overall trend is observed for the carbonyl  $^{13}\text{C}$  resonances. One-bond  $^{14}\text{N},^{13}\text{C}$  couplings were not resolved (at 201 MHz) and

these signals appeared with moderate line-broadening, although for Na[1<sub>W</sub>] <sup>183</sup>W satellites ( $I = \frac{1}{2}$ ) are observed with  ${}^1J_{WC} \approx 90$  Hz (cf.  ${}^1J_{WC} \approx 140$ –120 Hz for the carbonyl signals). Solution IR spectra (in THF) reveal a subtle but monotonous increase in  $\nu_{CN}$  energies with increasing metal *d*-occupancy, though the presence of an additional cyclopentadienyl ligand shifts  $\nu_{CN}$  to appreciably lower wavenumbers for [1<sub>Mn</sub>]<sup>–</sup> and [1<sub>Re</sub>]<sup>–</sup>.

**Table S1:** Selected spectroscopic data for all cyanometallates prepared herein.

	$\delta_{CN}^a$	$\delta_{CO}^a$	$\nu_{CN}^b$	$\nu_{CO}^b$
Na[1 <sub>Cr</sub> ]	153.0	222.0, 219.0	2112(w)	2054(w), 1928(vs), 1898(s)
Na[1 <sub>Mo</sub> ]	148.5	211.7, 207.3	2114(w)	2060(w), 1930(vs), 1899(s)
Na[1 <sub>W</sub> ]	139.8 ( ${}^1J_{WC}$ $= 92.6$ Hz)	201.0 ( ${}^1J_{WC}$ $= 140.6$ Hz), 197.5 ( ${}^1J_{WC}$ $= 123.7$ Hz)	2117(w)	2058(w), 1922(vs), 1896(s)
Na[1 <sub>Fe</sub> ]	144.1	217.0	2120(w)	2038(s), 1950(s), 1930(vs)
Na[1 <sub>Fe</sub> P]	152.2 ( ${}^2J_{PC}$ $= 6.8$ Hz)	218.8 ( ${}^2J_{PC}$ $= 27.3$ Hz)	2117(w)	1780(vs), 1726(m)
Na[1 <sub>Mn</sub> ]	165.3	236.4	2075(m)	1915(vs), 1845(vs)
Na[1 <sub>Re</sub> ]	133.1	205.4	2080(m)	1905(vs), 1836(vs)

a) CD<sub>3</sub>CN solution, 25 °C, ppm; b) THF solution, 25 °C, cm<sup>–1</sup>.

#### 1.4 Synthesis of pnictogeno-isocyanide complexes

##### 1.4.1 Synthesis of [M(CNA<sup>t</sup>Bu<sub>2</sub>)(CO)<sub>5</sub>] (M = Cr, Mo, W; A = P, As, Sb)

The procedure given here is broadly general for all combinations of metal “M” and pnictogen “A” described here. To a solution of Na[M(CO)<sub>5</sub>(CN)] (Na[1<sub>M</sub>]) in *ca* 50 mL THF cooled to 0 °C was added one equivalent of ClEt<sup>t</sup>Bu<sub>2</sub>, also dissolved in *ca* 5 mL THF. Mixtures were allowed to warm with stirring overnight to ambient temperature, becoming turbid although their colours did not noticeably change. After this time volatiles were removed *in vacuo* and the residues were extracted with 2:1 *n*-hexane/Et<sub>2</sub>O and purified by anaerobic flash chromatography on silica gel (10 x 5 cm; see note in *General Considerations*), eluting with the same solvent mixture (approximately 200–400 mL eluent was typically used depending on the scale of the reaction; the solvent should be rigorously deoxygenated). Slow concentration of the eluate under reduced pressure deposited the products as large colourless (A = P) or pale-yellow (A = As, Sb) crystals which were collected and dried. All [M(CNA<sup>t</sup>Bu<sub>2</sub>)(CO)<sub>5</sub>] are encountered as air-sensitive crystalline solids which are readily soluble in common organic solvents. All were stored at -30 °C in an argon-filled glovebox where they were indefinitely stable.

##### 1.4.2 [Cr(CNP<sup>t</sup>Bu<sub>2</sub>)(CO)<sub>5</sub>]

Quantities used: 2.00 g Na[Cr(CO)<sub>5</sub>(CN)] (8.30 mmol), 1.50 g ClP<sup>t</sup>Bu<sub>2</sub> (8.30 mmol). Isolated yield: 2.30 g (6.30 mmol, 76%).

NMR:  ${}^1H$  (C<sub>6</sub>D<sub>6</sub>, 400 MHz, 25 °C)  $\delta_H = 0.92$  (d,  ${}^3J_{PH} = 13.0$  Hz, 18H, C(CH<sub>3</sub>)<sub>3</sub> ppm;  ${}^{13}C\{{}^1H\}$  {C<sub>6</sub>D<sub>6</sub>, 201 MHz, 25 °C}  $\delta_C = 216.6$  (CO<sub>ax</sub>), 215.0 (CO<sub>eq</sub>) 189.0 ( ${}^1J_{NP} = 21.6$  Hz,  ${}^2J_{PC} = 29.9$  Hz, CN), 34.9 (d,  ${}^1J_{PC} = 25.4$  Hz, C(CH<sub>3</sub>)<sub>3</sub>), 27.3 (d,  ${}^2J_{PC} = 15.9$  Hz, C(CH<sub>3</sub>)<sub>3</sub>) ppm;  ${}^{31}P\{{}^1H\}$  (C<sub>6</sub>D<sub>6</sub>, 162 MHz, 25 °C)  $\delta_P = 104.6$  (t,  ${}^1J_{NP} = 59.2$  Hz) ppm. IR (*n*-hexane, 25 °C):  $\nu_{CO}$  2023(s), 1961(vs), 1932(s) cm<sup>–1</sup>,  $\nu_{CN}$  2102(w) cm<sup>–1</sup>; IR (ATR, 25 °C):  $\nu_{CO}$  2035(s), 1947(s), 1906(vs, br) cm<sup>–1</sup>,  $\nu_{CN}$  2105(s) cm<sup>–1</sup>. HR-MS (ESI, MeCN, +ve ion) found *m/z* 364.0396 (calc. for C<sub>14</sub>H<sub>19</sub>NO<sub>5</sub>P<sup>52</sup>Cr [M + H]<sup>+</sup>: 364.0400). Analysis found 46.26% C, 5.63% H, 3.69% N (calc. for C<sub>14</sub>H<sub>18</sub>CrNO<sub>5</sub>P: 46.29% C, 4.99% H, 3.86% N).

Single crystals were grown by slow evaporation of a benzene solution. The asymmetric unit comprises one-half of a molecule. *Crystal data* for C<sub>14</sub>H<sub>18</sub>NO<sub>5</sub>PCr (*M<sub>w</sub>* = 363.26 gmol<sup>–1</sup>): colourless prism 0.547 × 0.244 × 0.118 mm, orthorhombic, space group *Pnma* (no. 62),  $a = 21.7679(3)$  Å,  $b = 13.5735(2)$  Å,  $c = 5.92480(10)$  Å,  $V = 1750.58(5)$  Å<sup>3</sup>,  $Z = 4$ , spherical correction  $T_{min}/T_{max} = 0.279/0.358$ ,  $\mu(\text{Cu-K}\alpha) = 6.431$  mm<sup>–1</sup>,  $\rho_{\text{calc}} = 1.378$  Mgm<sup>–3</sup>, 7056 reflections measured (8.124° ≤ 2θ ≤ 155.768°), 1919 unique ( $R_{\text{int}} = 0.0555$ ,  $R_{\text{sigma}} = 0.0384$ ) which were used in all calculations against 112 parameters. The final  $R_1$  was 0.0379 ( $I > 2\sigma(I)$ ) and  $wR_2$  was 0.1100 (all data),  $GOF(F^2) = 1.101$ ,  $D_{\text{min}}/D_{\text{max}} = -0.61/0.51$  eÅ<sup>–3</sup>. CCDC number 2403973.

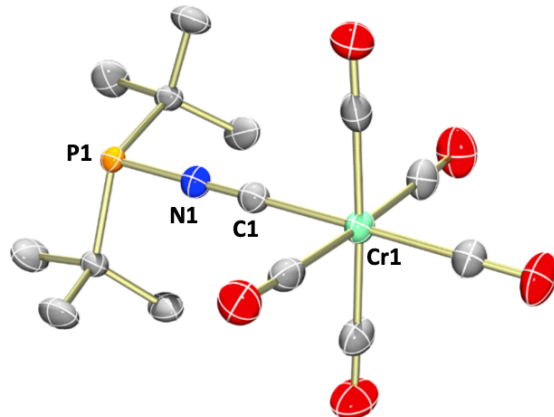


**Figure S3:** The molecular structure of 2CrP in a crystal. Hydrogen atoms omitted for clarity and ellipsoids shown at 50% displacement. Only one half of the molecule is crystallographically unique (in *Pnma*) due to the presence of an internal symmetry plane which bifurcates the Cr1, C1, N1 and P1 atoms. Selected distances (Å) and angles (°): Cr1-C1 1.973(2), C1-N1 1.165(3), N1-P1 1.725(2), Cr1-C1-N1 177.5(2), C1-N1-P1 178.5(2).

##### 1.4.3 [Mo(CNP<sup>t</sup>Bu<sub>2</sub>)(CO)<sub>5</sub>]

Quantities used: 1.00 g Na[Mo(CO)<sub>5</sub>(CN)] (3.50 mmol), 0.63 g ClP<sup>t</sup>Bu<sub>2</sub> (3.50 mmol). Isolated yield: 1.00 g (2.45 mmol, 71%).

NMR:  ${}^1H$  (C<sub>6</sub>D<sub>6</sub>, 400 MHz, 25 °C)  $\delta_H = 0.91$  (d,  ${}^3J_{PH} = 13.0$  Hz, 18H, C(CH<sub>3</sub>)<sub>3</sub> ppm;  ${}^{13}C\{{}^1H\}$  {C<sub>6</sub>D<sub>6</sub>, 201 MHz, 25 °C}  $\delta_C = 206.4$  (CO<sub>ax</sub>), 204.0 (CO<sub>eq</sub>), 179.9 ( ${}^2J_{PC} = 30.7$  Hz, CN;  ${}^1J_{NC}$  unresolved), 34.8 (d,  ${}^1J_{PC} = 24.6$  Hz, C(CH<sub>3</sub>)<sub>3</sub>), 27.3 (d,  ${}^2J_{PC} = 15.4$  Hz, C(CH<sub>3</sub>)<sub>3</sub>) ppm;  ${}^{31}P\{{}^1H\}$  (C<sub>6</sub>D<sub>6</sub>, 162 MHz, 25 °C)  $\delta_P = 103.5$  ( ${}^1J_{NP} = 58.9$  Hz)

ppm. IR (*n*-hexane, 25 °C)  $\nu_{\text{CO}}$  2025(s), 1963(vs), 1934(s) cm<sup>-1</sup>,  $\nu_{\text{CN}}$  2104(w) cm<sup>-1</sup>; IR (ATR, 25 °C)  $\nu_{\text{CO}}$  2039(s), 1948(s), 1897(vs, br) cm<sup>-1</sup>,  $\nu_{\text{CN}}$  2107(s) cm<sup>-1</sup>. HR-MS (ESI, MeCN, +ve ion) found  $m/z$  410.0044 (calc. for  $\text{C}_{14}\text{H}_{19}\text{NO}_5\text{P}^{98}\text{Mo}$  [M + H]<sup>+</sup>: 410.0049). Analysis found 39.80% C, 5.10% H, 2.80% N (calc. for  $\text{C}_{14}\text{H}_{18}\text{MoNO}_5\text{P}$ : 41.29% C, 4.49% H, 3.44% N). Satisfactory microanalytical data not acquired, most likely due to adventitious oxidation.

Single crystals were grown by slow evaporation of benzene solution. The asymmetric unit comprises one-half of a molecule. *Crystal data for*  $\text{C}_{14}\text{H}_{18}\text{Mo}_1\text{N}_1\text{O}_5\text{P}_1$  ( $M_w = 407.20$  gmol<sup>-1</sup>): colourless block 0.45 × 0.319 × 0.169 mm, orthorhombic, space group *Pnma* (no. 62),  $a = 22.1456(2)$  Å,  $b = 13.6345(2)$  Å,  $c = 5.93730(10)$  Å,  $V = 1792.73(4)$  Å<sup>3</sup>,  $Z = 4$ , spherical correction  $T_{\min}/T_{\max} = 0.183/0.277$ ,  $\mu(\text{Cu-K}\alpha) = 7.016$  mm<sup>-1</sup>,  $\rho_{\text{calc}} = 1.509$  Mgm<sup>-3</sup>, 7801 reflections measured (7.984° ≤ 2θ ≤ 156.02°), 1971 unique ( $R_{\text{int}} = 0.0377$ ,  $R_{\text{sigma}} = 0.0240$ ) which were used in all calculations against 112 parameters. The final  $R_1$  was 0.0328 ( $I > 2\sigma(I)$ ) and  $wR_2$  was 0.0904 (all data),  $GOF(F^2) = 1.111$ ,  $D_{\min}/D_{\max} = -1.11/0.43$  eÅ<sup>-3</sup>. CCDC number 2403976.

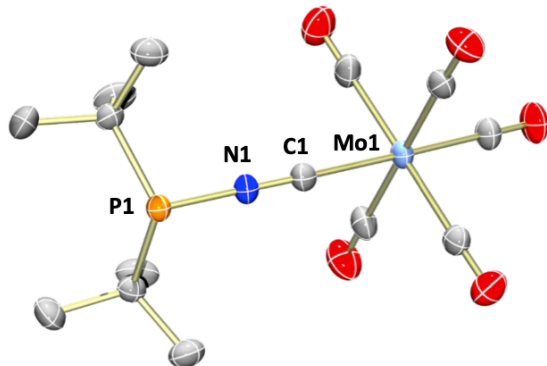


**Figure S4:** The molecular structure of  $\text{2}_{\text{MoP}}$  in a crystal. Hydrogen atoms omitted for clarity and ellipsoids shown at 50% displacement. Only one half of the molecule is crystallographically unique (in *Pnma*) due to the presence of an internal symmetry plane which bifurcates the Mo1, C1, N1 and P1 atoms. Selected distances (Å) and angles (°): Mo1-C1 2.130(3), C1-N1 1.156(4), N1-P1 1.728(3), Mo1-C1-N1 176.6(3), C1-N1-P1 178.4(3)

#### 1.4.4 $[\text{W}(\text{CNP}^t\text{Bu}_2)(\text{CO})_5]$

Quantities used: 2.60 g Na[W(CO)<sub>5</sub>(CN)] (6.90 mmol), 1.25 g ClP<sup>t</sup>Bu<sub>2</sub> (6.90 mmol). Isolated yield: 2.40 g (4.8 mmol, 70%). The reaction was repeated a further three times (on smaller scales) with isolated yields typically 60–70%.

NMR:  $^1\text{H}$  (C<sub>6</sub>D<sub>6</sub>, 400 MHz, 25 °C)  $\delta_{\text{H}} = 0.89$  (d,  $^3J_{\text{PH}} = 12.9$  Hz, 18H, C(CH<sub>3</sub>)<sub>3</sub>) ppm;  $^{13}\text{C}\{\text{H}\}$  (C<sub>6</sub>D<sub>6</sub>, 201 MHz, 25 °C)  $\delta_{\text{C}} = 196.1$  ( $^1J_{\text{WC}} = 132.2$  Hz, CO<sub>ax</sub>), 194.3 ( $^1J_{\text{WC}} = 124.2$  Hz, CO<sub>eq</sub>), 168.9 ( $^1J_{\text{NC}} = 25.9$  Hz,  $^2J_{\text{PC}} = 29.3$  Hz, CN;  $^1J_{\text{WC}}$  unresolved), 35.0 (d,  $^1J_{\text{PC}} = 15.0$  Hz, C(CH<sub>3</sub>)<sub>3</sub>), 27.3 (d,  $^2J_{\text{PC}} = 15.4$  Hz, C(CH<sub>3</sub>)<sub>3</sub>) ppm;  $^{31}\text{P}\{\text{H}\}$  (C<sub>6</sub>D<sub>6</sub>, 162 MHz, 25 °C)  $\delta_{\text{P}} = 103.4$  ( $^1J_{\text{NP}} = 59.5$  Hz) ppm. IR (*n*-hexane, 25 °C):  $\nu_{\text{CO}}$  = 2020(s), 1957(vs), 1928(w) cm<sup>-1</sup>,  $\nu_{\text{CN}}$  = 2107(w) cm<sup>-1</sup>. IR (ATR, 25 °C):  $\nu_{\text{CO}}$  2035(s), 1942(s), 1894(vs, br) cm<sup>-1</sup>,  $\nu_{\text{CN}}$  2109(s) cm<sup>-1</sup>. HR-MS (ESI, MeCN, +ve ion) found  $m/z$  495.0442 (calc. for  $\text{C}_{14}\text{H}_{18}\text{NO}_5\text{P}^{184}\text{W}$  [M]<sup>+</sup>: 495.0432). Analysis found 34.56% C, 3.85% H, 2.72% N (calc. for  $\text{C}_{14}\text{H}_{18}\text{NO}_5\text{PW}$ : 33.96% C, 3.66% H, 2.83% N). Satisfactory microanalytical data not

acquired, most likely due trace contamination with HPO<sup>t</sup>Bu<sub>2</sub> (see Figure S53 Calc for C<sub>8</sub>H<sub>19</sub>PO: 59.24% C, 11.81% H).

Single crystals were grown by slow evaporation of *n*-pentane solution at -30 °C. The asymmetric unit comprises one-half of a molecule. *Crystal data for*  $\text{C}_{14}\text{H}_{18}\text{NO}_5\text{PW}$  ( $M_w = 495.11$  gmol<sup>-1</sup>): colourless plate 0.26 × 0.1 × 0.02 mm, orthorhombic, space group *Pnma* (no. 62),  $a = 22.1015(3)$  Å,  $b = 13.5912(2)$  Å,  $c = 5.92670(10)$  Å,  $V = 1780.30(5)$  Å<sup>3</sup>,  $Z = 4$ , Gaussian correction  $T_{\min}/T_{\max} = 0.127/1.000$ ,  $\mu(\text{Cu-K}\alpha) = 13.064$  mm<sup>-1</sup>,  $\rho_{\text{calc}} = 1.847$  Mgm<sup>-3</sup>, 21172 reflections measured (8° ≤ 2θ ≤ 156.164°), 1978 unique ( $R_{\text{int}} = 0.0851$ ,  $R_{\text{sigma}} = 0.0408$ ) which were used in all calculations against 112 parameters. The final  $R_1$  was 0.0338 ( $I > 2\sigma(I)$ ) and  $wR_2$  was 0.0902 (all data),  $GOF(F^2) = 1.052$ ,  $D_{\min}/D_{\max} = -1.65/1.29$  eÅ<sup>-3</sup>. CCDC number 2403979. For the molecular geometry see Figure 2 in main article.

#### 1.4.5 $[\text{W}(\text{CNASt}^t\text{Bu}_2)(\text{CO})_5]$

Quantities used: 1.60 g Na[W(CO)<sub>5</sub>(CN)] (4.30 mmol), 0.90 g ClAs<sup>t</sup>Bu<sub>2</sub> (4.00 mmol). Isolated yield: 1.60 g (3.00 mmol, 75%).

NMR:  $^1\text{H}$  (C<sub>6</sub>D<sub>6</sub>, 400 MHz, 25 °C)  $\delta_{\text{H}} = 0.91$  (s, 18H, C(CH<sub>3</sub>)<sub>3</sub>) ppm;  $^{13}\text{C}\{\text{H}\}$  (C<sub>6</sub>D<sub>6</sub>, 201 MHz, 25 °C)  $\delta_{\text{C}} = 196.6$  ( $^1J_{\text{WC}} = 135.3$  Hz, CO<sub>ax</sub>), 194.9 ( $^1J_{\text{WC}} = 124.6$  Hz, CO<sub>eq</sub>), 165.3 ( $^1J_{\text{WC}} = 109.4$  Hz, CN;  $^1J_{\text{NC}}$  unresolved), 40.6 (C(CH<sub>3</sub>)<sub>3</sub>), 27.4 (C(CH<sub>3</sub>)<sub>3</sub>) ppm. IR (*n*-hexane, 25 °C)  $\nu_{\text{CO}}$  2027(s), 1953(vs), 1924(s) cm<sup>-1</sup>,  $\nu_{\text{CN}}$  2108(w) cm<sup>-1</sup>; IR (ATR, 25 °C)  $\nu_{\text{CO}}$  2042(s), 1937(s), 1892(vs, br) cm<sup>-1</sup>,  $\nu_{\text{CN}}$  2112(s) cm<sup>-1</sup>. HR-MS (EI, MeCN, +ve ion) found  $m/z$  539.9973 (calc. for  $\text{C}_{14}\text{H}_{19}\text{NO}_5^{75}\text{As}^{184}\text{W}$  [M + H]<sup>+</sup>: 539.9983). Analysis found 31.23% C, 3.60% H, 2.30% N (calc. for  $\text{C}_{14}\text{H}_{18}\text{AsNO}_5\text{W}$ : 31.19% C, 3.37% H, 2.60% N).

Single crystals were grown by slow evaporation of benzene solution. The asymmetric unit comprises one-half of a molecule. *Crystal data for*  $\text{C}_{14}\text{H}_{18}\text{NO}_5\text{AsW}$  ( $M_w = 539.06$  gmol<sup>-1</sup>): yellow prism 0.33 × 0.231 × 0.049 mm, orthorhombic, space group *Pnma* (no. 62),  $a = 22.2713(2)$  Å,  $b = 13.80740(10)$  Å,  $c = 5.94700(10)$  Å,  $V = 1828.75(4)$  Å<sup>3</sup>,  $Z = 4$ , spherical correction  $T_{\min}/T_{\max} = 0.269/0.349$ ,  $\mu(\text{Cu-K}\alpha) = 13.901$  mm<sup>-1</sup>,  $\rho_{\text{calc}} = 1.958$  Mgm<sup>-3</sup>, 7592 reflections measured (7.94° ≤ 2θ ≤ 156.102°), 2010 unique ( $R_{\text{int}} = 0.0292$ ,  $R_{\text{sigma}} = 0.0225$ ) which were used in all calculations against 112 parameters. The final  $R_1$  was 0.0351 ( $I > 2\sigma(I)$ ) and  $wR_2$  was 0.0944 (all data),  $GOF(F^2) = 1.124$ ,  $D_{\min}/D_{\max} = -1.35/2.70$  eÅ<sup>-3</sup>. CCDC number 2403977. For the molecular geometry see Figure 2 in main article.

#### 1.4.6 $[\text{W}(\text{CNSb}^t\text{Bu}_2)(\text{CO})_5]$

Quantities used: 1.00 g Na[W(CO)<sub>5</sub>(CN)] (2.68 mmol), 0.73 g ClSb<sup>t</sup>Bu<sub>2</sub> (2.68 mmol). Isolated yield: 1.04 g (1.77 mmol, 66%).

NMR:  $^1\text{H}$  (C<sub>6</sub>D<sub>6</sub>, 400 MHz, 25 °C)  $\delta_{\text{H}} = 1.04$  (s, 18H, C(CH<sub>3</sub>)<sub>3</sub>) ppm;  $^{13}\text{C}\{\text{H}\}$  (C<sub>6</sub>D<sub>6</sub>, 201 MHz, 25 °C)  $\delta_{\text{C}} = 196.9$  ( $^1J_{\text{WC}} = 135.2$  Hz, CO<sub>ax</sub>), 195.2 ( $^1J_{\text{WC}} = 125.1$  Hz, CO<sub>eq</sub>), 167.0 ( $^1J_{\text{WC}} = 96.6$  Hz, CN;  $^1J_{\text{NC}}$  unresolved), 41.2 (C(CH<sub>3</sub>)<sub>3</sub>), 28.7 (C(CH<sub>3</sub>)<sub>3</sub>) ppm. IR (*n*-hexane, 25 °C)  $\nu_{\text{CO}}$  2023(s), 1951(vs), 1922(w) cm<sup>-1</sup>,  $\nu_{\text{CN}}$  2104(w) cm<sup>-1</sup>; IR (ATR, 25 °C)  $\nu_{\text{CO}}$  2039(s), 1933(vs), 1889(vs) cm<sup>-1</sup>,  $\nu_{\text{CN}}$  2109(s) cm<sup>-1</sup>. HR-MS (ESI, MeCN, +ve ion) found  $m/z$  584.9193 (calc. for  $\text{C}_{14}\text{H}_{18}\text{NO}_5^{121}\text{Sb}^{184}\text{W}$  [M]<sup>+</sup>: 584.9732). Analysis found

28.71% C, 3.16% H, 2.31% N (calc. for  $C_{14}H_{18}NO_5SbW$ : 28.70% C, 3.10% H, 2.39% N).

Single crystals were grown by slow evaporation of benzene solution. The asymmetric unit comprises one-half of a molecule. *Crystal data for  $C_{14}H_{18}NO_5SbW$*  ( $M_w = 585.89$  gmol $^{-1}$ ): colourless prism  $0.492 \times 0.152 \times 0.098$  mm, orthorhombic, space group  $Pnma$  (no. 62),  $a = 22.5380(2)$  Å,  $b = 14.13850(14)$  Å,  $c = 6.04179(5)$  Å,  $V = 1925.24(3)$  Å $^3$ ,  $Z = 4$ , spherical correction  $T_{\min}/T_{\max} = 0.043/0.143$ ,  $\mu(\text{Cu-K}\alpha) = 22.182$  mm $^{-1}$ ,  $\rho_{\text{calc}} = 2.021$  Mgm $^{-3}$ , 8281 reflections measured ( $7.846^\circ \leq 2\Theta \leq 156.078^\circ$ ), 2113 unique ( $R_{\text{int}} = 0.0385$ ,  $R_{\text{sigma}} = 0.0269$ ) which were used in all calculations against 112 parameters. The final  $R_1$  was 0.0362 ( $I > 2\sigma(I)$ ) and  $wR_2$  was 0.1003 (all data),  $GOF(F^2) = 1.070$ ,  $D_{\min}/D_{\max} = -0.74/1.55$  eÅ $^{-3}$ . CCDC number 2403975. For the molecular geometry see Figure 2 in main article.

#### 1.4.7 [Fe(CNP $t$ Bu $_2$ )(CO) $_4$ ]

This compound was prepared similarly to the Group 6 congeners, however decomposes rapidly on contact with silica gel forming immobile materials. Instead, the dried reaction residue was extracted with portions of *n*-pentane and filtered through a Celite® plug (2.5 x 2.5 cm) under positive pressure of argon. Concentration of the filtrate and storage at -20 °C overnight deposited large dark orange crystals which were isolated and dried *in vacuo*. The product is air-sensitive and readily soluble in common organic solvents. The product was stored at -30 °C in an argon-filled glovebox; samples kept at ambient temperature for extended periods of time (> 24 h) slowly acquired a brown cast though without noticeable change to the NMR spectra.

Quantities used: 1.00 g Na[Fe(CO) $_4$ (CN)] (4.60 mmol), 0.80 g CNP $t$ Bu $_2$  (4.4 mmol). Isolated yield: 0.75 g (1.6 mmol, 43%). The reaction was repeated a further two times (on smaller scales) with isolated yields *ca* 30–40%. The reduced yields here compared to the Group 6 complexes are probably due to losses incurred by fractional re-crystallisation.

NMR:  $^1\text{H}$  (C $_6$ D $_6$ , 400 MHz, 25 °C)  $\delta_{\text{H}} = 0.92$  (d,  $^3J_{\text{PH}} = 13.1$  Hz, 18H, C(CH $_3$ ) $_3$ ) ppm;  $^{13}\text{C}\{^1\text{H}\}$  (C $_6$ D $_6$ , 201 MHz, 25 °C)  $\delta_{\text{C}} = 213.1$  (CO), 183.8 ( $^1J_{\text{NC}} = 29.9$  Hz,  $^2J_{\text{PC}} = 29.7$  Hz, CN), 35.2 (d,  $^1J_{\text{PC}} = 25.7$  Hz, C(CH $_3$ ) $_3$ ), 27.3 (d,  $^2J_{\text{PC}} = 15.5$  Hz, C(CH $_3$ ) $_3$ ) ppm;  $^{31}\text{P}\{^1\text{H}\}$  (C $_6$ D $_6$ , 162 MHz, 25 °C)  $\delta_{\text{P}} = 108.7$  ( $^1J_{\text{NP}} = 60.2$  Hz) ppm. IR (*n*-hexane, 25 °C):  $\nu_{\text{CO}}$  2034(vs), 1998(s), 1970(vs), 1935(m) cm $^{-1}$ ,  $\nu_{\text{CN}}$  2110(w) cm $^{-1}$ ; IR (ATR, 25 °C):  $\nu_{\text{CO}}$  2033(vs), 1986(s), 1941(vs, br) cm $^{-1}$ ,  $\nu_{\text{CN}}$  2114(s) cm $^{-1}$ . HR-MS (EI, MeCN, +ve ion) found  $m/z$  339.0331 (calc. for  $C_{13}H_{18}NO_4^{56}\text{Fe}^{31}\text{P}$ , [M] $^+$ : 339.0323). Satisfactory elemental microanalysis could not be obtained due to thermal and aerobic instability such that samples consistently underestimated carbon content by ~5%.

Single crystals were grown by slow evaporation of *n*-pentane solution at -30 °C. *Crystal data for  $C_{13}H_{18}FeNO_4P$*  ( $M_w = 339.10$  gmol $^{-1}$ ): orange prism  $0.215 \times 0.21 \times 0.115$  mm, orthorhombic, space group  $Pbcn$  (no. 60),  $a = 20.8819(5)$  Å,  $b = 10.0111(3)$  Å,  $c = 16.0053(4)$  Å,  $V = 3345.92(15)$  Å $^3$ ,  $Z = 8$ , spherical correction  $T_{\min}/T_{\max} = 0.308/0.383$ ,  $\mu(\text{Cu-K}\alpha) = 8.237$  mm $^{-1}$ ,  $\rho_{\text{calc}} = 1.346$  Mgm $^{-3}$ , 13826 reflections measured (8.468°

$\leq 2\Theta \leq 156.258^\circ$ ), 3503 unique ( $R_{\text{int}} = 0.0508$ ,  $R_{\text{sigma}} = 0.0435$ ) which were used in all calculations against 187 parameters. The final  $R_1$  was 0.0461 ( $I > 2\sigma(I)$ ) and  $wR_2$  was 0.1360 (all data),  $GOF(F^2) = 1.063$ ,  $D_{\min}/D_{\max} = -0.55/0.40$  eÅ $^{-3}$ . CCDC number 2403975. For the molecular geometry, see Figure 5 in the main article.

#### 1.4.8 trans-[Fe(CNP $t$ Bu $_2$ )(CO) $_3$ (PPh $_3$ )]

NMR:  $^1\text{H}$  (C $_6$ D $_6$ , 400 MHz, 25 °C)  $\delta_{\text{H}} = 7.77$ –7.72 (m, 6H, C $_6$ H $_5$ ), 7.00–6.98 (m, 9H, C $_6$ H $_5$ ), 1.05 (d,  $^3J_{\text{PH}} = 12.7$  Hz, 18H, C(CH $_3$ ) $_3$ ) ppm;  $^{13}\text{C}\{^1\text{H}\}$  (C $_6$ D $_6$ , 201 MHz, 25 °C)  $\delta_{\text{C}} = 215.4$  (d,  $^2J_{\text{PC}} = 27.5$  Hz, CO), 194.2 (overlapping dd,  $^2J_{\text{PtBu}_2\text{C}} \approx 2^2J_{\text{PPh}_3\text{C}} \approx 28$  Hz, CN), 136.2 (d,  $^1J_{\text{PC}} = 46.2$  Hz, *ipso*-P(C $_6$ H $_5$ ) $_3$ ), 133.7 (d,  $^3J_{\text{PC}} = 10.6$  Hz, *meta*-P(C $_6$ H $_5$ ) $_3$ ), 130.5 (d,  $^4J_{\text{PC}} = 1.5$  Hz, *para*-P(C $_6$ H $_5$ ) $_3$ ), 128.6 (d,  $^2J_{\text{PC}} = 10.0$  Hz, *ortho*-P(C $_6$ H $_5$ ) $_3$ ), 35.1 (d,  $^1J_{\text{PC}} = 25.1$  Hz, C(CH $_3$ ) $_3$ ), 27.6 (d,  $^2J_{\text{PC}} = 15.6$  Hz, C(CH $_3$ ) $_3$ ) ppm;  $^{31}\text{P}\{^1\text{H}\}$  (C $_6$ D $_6$ , 162 MHz, 25 °C)  $\delta_{\text{P}} = 102.6$  ( $^1J_{\text{NP}} = 57.4$  Hz, CNP), 77.7 (PPh $_3$ ) ppm. IR (*n*-hexane, 25 °C)  $\nu_{\text{CO}}$  1974(s), 1962(m), 1934(s), 1921(vs) cm $^{-1}$ ,  $\nu_{\text{CN}}$  2060(s), 2041(m) cm $^{-1}$ ; IR (ATR, 25 °C)  $\nu_{\text{CO}}$  1969(s), 1899(vs), 1872(s) cm $^{-1}$ ,  $\nu_{\text{CN}}$  2061(s) cm $^{-1}$ . HR-MS (ESI, MeCN, +ve ion) found  $m/z$  574.1343 (calc. for  $C_{20}H_{34}NO_3P_2^{56}\text{Fe}$  [M + H] $^+$ : 574.1357). Analysis found 62.68% C, 6.08% H, 2.19% N (calc. for  $C_{30}H_{33}FeNO_3P_2$ : 62.84% C, 5.80% H, 2.44% N).

Single crystals were grown by layering a CH $_2$ Cl $_2$  solution with *n*-hexane at -30 °C. The asymmetric unit contains one-half of an *n*-hexane solvate molecule. *Crystal data for  $C_{30}H_{33}NO_3P_2\text{Fe}\cdot 0.5C_6H_{14}$*  ( $M_w = 616.45$  gmol $^{-1}$ ): yellow prism  $0.807 \times 0.299 \times 0.212$  mm, monoclinic, space group  $P2_1/c$  (no. 14),  $a = 17.9002(17)$  Å,  $b = 10.5291(9)$  Å,  $c = 18.4283(19)$  Å,  $\beta = 110.203(12)^\circ$ ,  $V = 3259.5(6)$  Å $^3$ ,  $Z = 4$ , multi-scan correction  $T_{\min}/T_{\max} = 0.919/1.000$ ,  $\mu(\text{Mo-K}\alpha) = 0.593$  mm $^{-1}$ ,  $\rho_{\text{calc}} = 1.256$  Mgm $^{-3}$ , 34437 reflections measured ( $7.138^\circ \leq 2\Theta \leq 59.228^\circ$ ), 7761 unique ( $R_{\text{int}} = 0.0527$ ,  $R_{\text{sigma}} = 0.0508$ ) which were used in all calculations against 368 parameters. The final  $R_1$  was 0.0498 ( $I > 2\sigma(I)$ ) and  $wR_2$  was 0.1348 (all data),  $GOF(F^2) = 1.046$ ,  $D_{\min}/D_{\max} = -0.42/0.50$  eÅ $^{-3}$ . CCDC number 2403974. For the molecular geometry, see Figure 5 in the main article

#### 1.4.9 [Mn(CNP $t$ Bu $_2$ )(CO) $_2$ ( $\eta^5\text{-C}_5\text{H}_5$ )]

NMR:  $^1\text{H}$  (C $_6$ D $_6$ , 400 MHz, 25 °C)  $\delta_{\text{H}} = 4.22$  (s, 5H,  $\eta^5\text{-C}_5\text{H}_5$ ), 1.07 ( $^3J_{\text{PH}} = 12.5$  Hz, C(CH $_3$ ) $_3$ ) ppm;  $^{13}\text{C}\{^1\text{H}\}$  (C $_6$ D $_6$ , 201 MHz, 25 °C)  $\delta_{\text{C}} = 229.5$  (CO), 206.4 (d,  $^2J_{\text{PC}} = 26.6$  Hz, CN), 82.2 ( $\eta^5\text{-C}_5\text{H}_5$ ), 35.1 (d,  $^1J_{\text{PC}} = 24.8$  Hz, C(CH $_3$ ) $_3$ ), 27.6 (d,  $^2J_{\text{PC}} = 15.8$  Hz, C(CH $_3$ ) $_3$ ) ppm;  $^{31}\text{P}\{^1\text{H}\}$  (C $_6$ D $_6$ , 162 MHz, 25 °C)  $\delta_{\text{P}} = 100.2$  ( $^1J_{\text{NP}} = 55.8$  Hz) ppm. IR (*n*-hexane, 25 °C)  $\nu_{\text{CO}}$  1937(vs), 1915(vs) cm $^{-1}$ ,  $\nu_{\text{CN}}$  2027(s) cm $^{-1}$ ; IR (ATR, 25 °C)  $\nu_{\text{CO}}$  1917(s), 1879(vs), 1853(s) cm $^{-1}$ ,  $\nu_{\text{CN}}$  2066(s) cm $^{-1}$ . HR-MS (ESI, MeCN, +ve ion) found  $m/z$  348.0905 (calc. for  $C_{16}H_{24}NO_2P^{55}\text{Mn}$  [M + H] $^+$ : 348.0917). Analysis found 55.44% C, 6.60% H, 3.95% N (calc. for  $C_{16}H_{23}\text{MnNO}_2\text{P}$ : 55.34% C, 6.68% H, 4.03% N).

Single crystals were grown by evaporation of an *n*-hexane solution at -30 °C. *Crystal data for  $C_{16}H_{23}\text{NO}_2\text{PMn}$*  ( $M = 347.26$  gmol $^{-1}$ ): yellow prism  $0.36 \times 0.23 \times 0.09$  mm, monoclinic, space group  $P2_1/c$  (no. 14),  $a = 10.3531(6)$  Å,  $b = 6.3326(3)$  Å,  $c = 26.3915(13)$  Å,  $\beta = 91.390(5)^\circ$ ,  $V = 1729.77(16)$  Å $^3$ ,  $Z = 4$ , multi-scan correction  $T_{\min}/T_{\max} = 0.713/1.000$ ,  $\mu(\text{Mo-K}\alpha) = 0.859$  mm $^{-1}$ .

<sup>1</sup>,  $\rho_{\text{calc}} = 1.333 \text{ Mgm}^{-3}$ , 22496 reflections measured ( $4.944^\circ \leq 2\Theta \leq 61.776^\circ$ ), 4339 unique ( $R_{\text{int}} = 0.0881$ ,  $R_{\text{sigma}} = 0.0641$ ) which were used in all calculations against 196 parameters. The final  $R_1$  was 0.0444 ( $I > 2\sigma(I)$ ) and  $wR_2$  was 0.1017 (all data),  $GOF(F^2) = 1.020$ ,  $D_{\text{min}}/D_{\text{max}} = -0.34/0.51 \text{ e}/\text{\AA}^3$ . CCDC number 2403971. For the molecular geometry, see Figure 4 in the main article.

#### 1.4.10 [Re(CN<sup>t</sup>Bu<sub>2</sub>)(CO)<sub>2</sub>(η<sup>5</sup>-C<sub>5</sub>H<sub>5</sub>)]

NMR: <sup>1</sup>H (C<sub>6</sub>D<sub>6</sub>, 400 MHz, 25 °C)  $\delta_H = 4.66$  (s, 5H, η<sup>5</sup>-C<sub>5</sub>H<sub>5</sub>), 1.09 (d, <sup>3</sup>J<sub>PH</sub> = 12.5 Hz, 18H, C(CH<sub>3</sub>)<sub>3</sub>) ppm; <sup>13</sup>C{<sup>1</sup>H} (C<sub>6</sub>D<sub>6</sub>, 201 MHz, 25 °C)  $\delta_C = 198.5$  (CO), 172.3 (<sup>2</sup>J<sub>PC</sub> = 24.4 Hz, CN), 83.5 (η<sup>5</sup>-C<sub>5</sub>H<sub>5</sub>), 35.2 (d, <sup>1</sup>J<sub>PC</sub> = 24.8 Hz, C(CH<sub>3</sub>)<sub>3</sub>), 27.7 (d, <sup>2</sup>J<sub>PC</sub> = 15.7 Hz, C(CH<sub>3</sub>)<sub>3</sub>) ppm; <sup>31</sup>P{<sup>1</sup>H} (C<sub>6</sub>D<sub>6</sub>, 162 MHz, 25 °C)  $\delta_P = 98.7$  (<sup>1</sup>J<sub>NP</sub> = 53.4 Hz) ppm. IR (n-hexane, 25 °C)  $\nu_{\text{CO}}$  1930(vs), 1909(vs) cm<sup>-1</sup>,  $\nu_{\text{CN}}$  2031(s) cm<sup>-1</sup>; IR (ATR, 25 °C)  $\nu_{\text{CO}}$  1904(vs), 1864(vs) cm<sup>-1</sup>,  $\nu_{\text{CN}}$  2030(s) cm<sup>-1</sup>. HR-MS (ESI, MeCN, +ve ion) found *m/z* 480.1102 (calc. for C<sub>16</sub>H<sub>23</sub>NO<sub>2</sub>P<sup>187</sup>Re [M]<sup>+</sup>: 480.1103). Analysis found 40.09% C, 4.70% H, 2.86% N (calc. for C<sub>16</sub>H<sub>23</sub>NO<sub>2</sub>PRE: 40.16% C, 4.84% H, 2.93% N).

Single crystals were grown by slow evaporation of an n-hexane solution at -30 °C. Crystal data for C<sub>16</sub>H<sub>23</sub>NO<sub>2</sub>PRE ( $M_w = 478.52 \text{ gmol}^{-1}$ ): colourless block 0.341 × 0.233 × 0.195 mm, triclinic, space group P-1 (no. 2),  $a = 6.5007(4) \text{ \AA}$ ,  $b = 10.3978(6) \text{ \AA}$ ,  $c = 12.9967(6) \text{ \AA}$ ,  $\alpha = 91.653(4)^\circ$ ,  $\beta = 94.080(4)^\circ$ ,  $\gamma = 93.172(5)^\circ$ ,  $V = 874.44(8) \text{ \AA}^3$ ,  $Z = 2$ , Gaussian correction  $T_{\text{min}}/T_{\text{max}} = 0.182/0.367$ ,  $\mu(\text{Mo-K}\alpha) = 7.043 \text{ mm}^{-1}$ ,  $\rho_{\text{calc}} = 1.817 \text{ Mgm}^{-3}$ , 7683 reflections measured ( $6.828^\circ \leq 2\Theta \leq 58.546^\circ$ ), 3780 unique ( $R_{\text{int}} = 0.0476$ ,  $R_{\text{sigma}} = 0.0799$ ) which were used in all calculations against 190 parameters. The final  $R_1$  was 0.0404 ( $I > 2\sigma(I)$ ) and  $wR_2$  was 0.0824 (all data),  $GOF(F^2) = 1.040$ ,  $D_{\text{min}}/D_{\text{max}} = -2.13/1.35 \text{ e}/\text{\AA}^3$ . CCDC number 2403972. For the molecular geometry, see Figure 4 in the main article.

### 1.5 Synthesis of model isocyanide and nitrile complexes

#### 1.5.1 [W(CNMes)(CO)<sub>5</sub>] (Mes = C<sub>6</sub>H<sub>2</sub>Me<sub>3</sub>-2,4,6)

A yellow solution of [W(THF)(CO)<sub>5</sub>] was prepared by UV-photolysis of 0.25 g [W(CO)<sub>6</sub>] (7.1 mmol) in 30 mL THF. To this was added 0.12 g CNMes (8.2 mmol, ~1.1 eq.) and the mixture allowed to stir at ambient temperature overnight. After this time volatiles were removed by rotary evaporation and the residue purified by flash column chromatography on silica gel (25 x 2.5 cm) with petroleum ether eluent giving a faint yellow band which was collected and dried. Re-crystallisation from n-hexane at 0 °C deposited large colourless plates. Isolated yield: 0.25 g (5.3 mmol, 75%). The product is readily soluble in common organic solvents and is air stable.

NMR: <sup>1</sup>H (C<sub>6</sub>D<sub>6</sub>, 400 MHz, 25 °C)  $\delta_H = 6.36$  (s, 2H, 3,5-C<sub>6</sub>H<sub>2</sub>Me<sub>3</sub>), 1.93 (s, 6H, 2,6-C<sub>6</sub>H<sub>2</sub>(CH<sub>3</sub>)<sub>3</sub>), 1.92 (s, 3H, 4-C<sub>6</sub>H<sub>2</sub>(CH<sub>3</sub>)<sub>3</sub>) ppm; <sup>13</sup>C{<sup>1</sup>H} (C<sub>6</sub>D<sub>6</sub>, 176 MHz, 25 °C)  $\delta_C = 196.4$  (<sup>1</sup>J<sub>WC</sub> = 133.2 Hz, CO<sub>ax</sub>), 194.1 (<sup>1</sup>J<sub>WC</sub> = 126.5 Hz, CO<sub>eq</sub>), 153.5 (CN, <sup>1</sup>J<sub>WC</sub> and <sup>1</sup>J<sub>NC</sub> unresolved), 139.0 (4-C<sub>6</sub>H<sub>2</sub>Me<sub>3</sub>), 134.9 (2,6-C<sub>6</sub>H<sub>2</sub>Me<sub>3</sub>), 128.7 (3,5-C<sub>6</sub>H<sub>2</sub>Me<sub>3</sub>), 124.9 (1-C<sub>6</sub>H<sub>2</sub>Me<sub>3</sub>), 20.9 (4-C<sub>6</sub>H<sub>2</sub>(CH<sub>3</sub>)<sub>3</sub>), 18.2 (2,6-C<sub>6</sub>H<sub>2</sub>(CH<sub>3</sub>)<sub>3</sub>) ppm. IR (n-hexane, 25 °C)  $\nu_{\text{CO}}$  2054(s), 1957(vs),

1926(s) cm<sup>-1</sup>,  $\nu_{\text{CN}}$  2134(w) cm<sup>-1</sup>; IR (ATR, 25 °C)  $\nu_{\text{CO}}$  2059(s), 1895 (vs, br) cm<sup>-1</sup>,  $\nu_{\text{CN}}$  2143(s) cm<sup>-1</sup>.

Crystal data for C<sub>15</sub>H<sub>11</sub>NO<sub>5</sub>W ( $M_w = 469.10 \text{ gmol}^{-1}$ ): 0.245 × 0.196 × 0.098 mm, monoclinic, space group P2<sub>1</sub>/n,  $a = 9.21210(10) \text{ \AA}$ ,  $b = 15.24780(10) \text{ \AA}$ ,  $c = 11.81920(10) \text{ \AA}$ ,  $\beta = 103.5200(10)^\circ$ ,  $V = 1614.17(3) \text{ \AA}^3$ ,  $Z = 4$ , Gaussian correction,  $\mu(\text{Cu-K}\alpha) = 13.468 \text{ mm}^{-1}$ ,  $\rho_{\text{calc}} = 1.930 \text{ Mgm}^{-3}$ , 12081 reflections measured ( $9.638^\circ \leq 2\Theta \leq 156.284^\circ$ ), 3408 unique ( $R_{\text{int}} = 0.0218$ ,  $R_{\text{sigma}} = 0.0181$ ) which were used in all calculations against 202 parameters. The final  $R_1$  was 0.0208 ( $I > 2\sigma(I)$ ) and  $wR_2$  was 0.0553 (all data),  $GOF(F^2) = 1.089$ ,  $D_{\text{min}}/D_{\text{max}} = -1.22/0.46 \text{ e}/\text{\AA}^3$ . CCDC number 2403978.

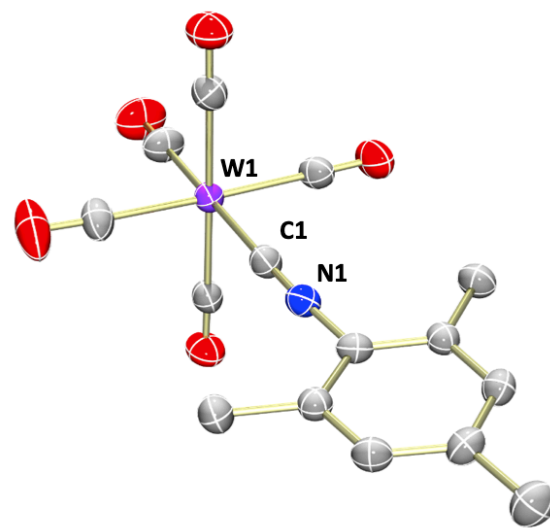


Figure S5: The molecular structure of [W(CNMes)(CO)<sub>5</sub>] in a crystal. Hydrogen atoms omitted for clarity and ellipsoids shown at 50% displacement. Selected distances (Å) and angles (°): W1-C1 2.124(3), C1-N1 1.165(4), W1-C1-N1 175.6(2).

#### 1.5.2 [W(NCPPh)(CO)<sub>5</sub>]

Prepared and purified in an identical manner to that above (1.5.1). Quantities used: 0.25 g [W(CO)<sub>6</sub>] (7.1 mmol), 0.15 g NCPPh (14.2 mmol, 2 eq.). Re-crystallisation from n-hexane at 0 °C deposited large light-yellow plates. Isolated yield: 0.16 g (3.7 mmol, 52%). The product is readily soluble in common organic solvents and is air stable in solution for short periods of time.

NMR: <sup>1</sup>H (C<sub>6</sub>D<sub>6</sub>, 400 MHz, 25 °C)  $\delta_H = 6.81$ –6.77 (m, 1H, 4-C<sub>6</sub>H<sub>5</sub>), 6.57–6.53 (m, 2H, 3,5-C<sub>6</sub>H<sub>5</sub>), 6.45–6.41 (m, 2H, 2,6-C<sub>6</sub>H<sub>5</sub>) ppm; <sup>13</sup>C{<sup>1</sup>H} (C<sub>6</sub>D<sub>6</sub>, 176 MHz, 25 °C)  $\delta_C = 199.9$  (<sup>1</sup>J<sub>WC</sub> = 152.8 Hz, CO<sub>ax</sub>), 196.9 (<sup>1</sup>J<sub>WC</sub> = 129.7 Hz, CO<sub>eq</sub>), 133.4 (4-C<sub>6</sub>H<sub>5</sub>), 132.5 (2,6-C<sub>6</sub>H<sub>5</sub>), 128.8 (3,5-C<sub>6</sub>H<sub>5</sub>), 124.7 (1-C<sub>6</sub>H<sub>5</sub>), 109.8 (NC) ppm. IR (n-hexane, 25 °C)  $\nu_{\text{CO}}$  1946(vs), 1928(s) cm<sup>-1</sup>,  $\nu_{\text{CN}}$  2075(w) cm<sup>-1</sup>; IR (ATR, 25 °C)  $\nu_{\text{CO}}$  1888(vs, br) cm<sup>-1</sup>,  $\nu_{\text{CN}}$  2074(w) cm<sup>-1</sup>.

Crystal data for C<sub>12</sub>H<sub>5</sub>NO<sub>5</sub>W ( $M_w = 427.02 \text{ gmol}^{-1}$ ): 0.17 × 0.13 × 0.06 mm, monoclinic, space group P2<sub>1</sub>/c,  $a = 10.33250(10) \text{ \AA}$ ,  $b = 10.33250(10) \text{ \AA}$ ,  $c = 9.66530(10) \text{ \AA}$ ,  $\beta = 100.7130(10)^\circ$ ,  $V = 1320.61(3) \text{ \AA}^3$ ,  $Z = 4$ , Gaussian correction,  $\mu(\text{Cu-K}\alpha) = 16.379 \text{ mm}^{-1}$ ,  $\rho_{\text{calc}} = 2.148 \text{ Mgm}^{-3}$ , 9690 reflections measured ( $8.71^\circ \leq 2\Theta \leq 155.736^\circ$ ), 2774 unique ( $R_{\text{int}} = 0.0327$ ,  $R_{\text{sigma}} = 0.0301$ ) which were used in all calculations against 172 parameters. The final  $R_1$  was 0.0339 ( $I > 2\sigma(I)$ ) and  $wR_2$  was

0.0891 (all data),  $GOF(F^2) = 1.071$ ,  $D_{\min}/D_{\max} = -1.15/2.77 \text{ e}\AA^{-3}$ .  
CCDC number 2403981.

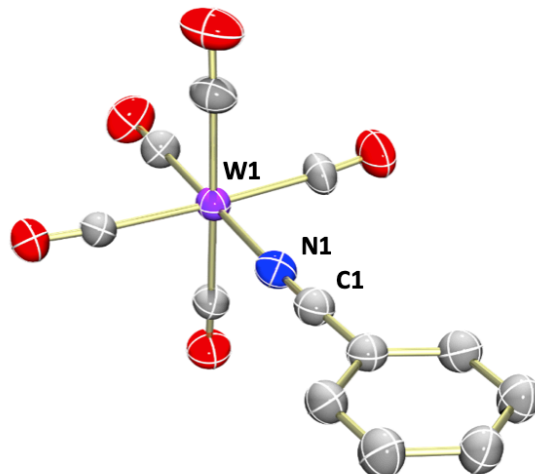


**Figure S6:** The molecular structure of  $[W(NCPh)(CO)_5]$  in a crystal. Hydrogen atoms omitted for clarity and ellipsoids shown at 50% displacement. Selected distances ( $\text{\AA}$ ) and angles ( $^\circ$ ): W1-N1 2.175(4), N1-C1 1.166(7), W1-N1-C1 177.8(4).

## 2 Computational Studies

Computational studies were performed by using the SPARTAN24 suite of programs.<sup>9</sup> In the first instance, geometry optimisations (gas phase) were performed at the DFT level of theory using the exchange functional (M06-2X) of Truhlar.<sup>10</sup> The Los Alamos effective core potential type basis set (LANL2D $\zeta$ ) of Hay and Wadt<sup>11</sup> was used for W, Sb and Bi; the Pople 6-31G\* basis sets<sup>12</sup> were used for all other atoms. Geometry optimisations and single-point energy calculations were performed at the M06-2X/6-31G\*/LANL2D $\zeta$ (W,Sb,Bi) level; frequency calculations were performed to confirm that the optimized structures were local minima and to identify vibrational modes of interest. For the method's typical reflection of phenomenological Lewis bonds, Löwdin bond orders,<sup>13</sup> which emphasise covalency were also calculated. The calculations follow a very similar form to the Wiberg indices, except using the Löwdin symmetrically orthogonalized basis set instead of the natural basis.

**Table S2** Data calculated for the model complexes  $[W(CNAME_2)(CO)_5]$ .

A	Z <sub>w</sub>	Z <sub>c</sub>	Z <sub>A</sub>	r <sub>wc</sub>	$\Sigma^a A^c$	v <sub>co</sub> <sup>d,e</sup>	v <sub>co</sub> <sup>d,e</sup>	f(A)
	e <sup>b</sup>	e	e	Å	°	cm <sup>-1</sup>	cm <sup>-1</sup>	e
N	-0.06	0.19	-0.30	2.149	334.5	2164	2075, 2010, <b>1987</b> , 1979	0.07
P	-0.06	0.24	1.09	2.122	294.3	2032 <sup>f</sup>	2108 <sup>f</sup> , 2011, <b>1986</b> , 1981	0.03
As	-0.06	0.23	1.21	2.133	287.7	2036 <sup>f</sup>	2108 <sup>f</sup> , 2009, <b>1980</b> , 1978	0.02
Sb	-0.06	0.21	1.53	2.136	279.7	2030 <sup>f</sup>	2105 <sup>f</sup> , 2010, <b>1979</b> , 1979	0.02
Bi	-0.06	0.19	1.53	2.146	277.1	2040 <sup>f</sup>	2108 <sup>f</sup> , 2009, <b>1978</b> , 1977	0.02

<sup>a</sup> DFT:M06-2X/6-31G\*/LANL2D $\zeta$ (W,Sb,Bi)/gas phase. <sup>b</sup> 1 a.u. (e) = 0.1602 aC. <sup>c</sup> Angle sum at pnictogen A. <sup>d</sup>  $\lambda = 0.9297$ . <sup>e</sup> A<sub>1</sub> mode corresponding to *trans* v<sub>to</sub> in bold. <sup>f</sup> Pronounced Fermi resonance.

**Table S3** Löwdin Bond Orders along the O–C–W–C–N–A spines of  $[W(CNAME_2)(CO)_5]$ .<sup>a</sup>

A	O–C	C–W	W–C	C–N	N–E
N	2.58	1.31	1.02	2.60	1.20
P	2.59	1.28	1.07	2.62	0.95
As	2.59	1.30	1.05	2.67	0.90
Sb	2.59	1.29	1.03	2.71	0.84
Bi	2.58	1.30	1.01	2.75	0.78

<sup>a</sup> DFT:M06-2X/6-31G\*/LANL2D $\zeta$ (W,Sb,Bi)/gas phase.

**Observations:** The bonding in the carbonyl ligand *trans* to the CNAME<sub>2</sub> ligand is essentially invariant down the series, as the W–C bond of the CNAME<sub>2</sub> ligand. A rather monotonic decrease in the N–A bond order down the group is accompanied by a rather modest increase in the CN multiple bonding.

## 2.1 $[W(CNNMe_2)(CO)_5]$

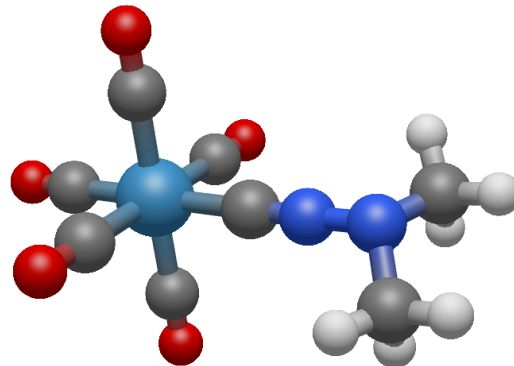


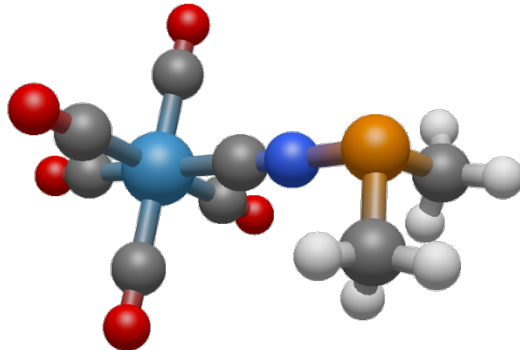
**Figure S7.** Optimised geometry for  $[W(CNNMe_2)(CO)_5]$  at the M06-2X/6-31G\*/LANL2D $\zeta$ (W) level of DFT. Selected distances ( $\text{\AA}$ ) and angles ( $^\circ$ ): W–C 2.149, C–N 1.169, N–N 1.347, W–C–N 179.7, C–N–N 176.0.

**Table S4.** Cartesian Coordinates for  $[W(CNNMe_2)(CO)_5]$

Atom	x	y	z
W	-2.036839	-0.076090	0.751499
N	2.131821	-0.078342	-1.338100
N	0.957037	-0.078318	-0.678845
O	-2.999844	2.197181	-1.297663
O	-1.059230	-2.343776	2.796775
C	-0.099225	-0.077654	-0.178816
C	-2.653290	1.384673	-0.569756
C	-1.404547	-1.533062	2.065169
C	3.044446	-1.070410	-0.761811
O	-4.910753	-0.071626	2.123501
C	-3.875396	-0.073120	1.628139
O	-3.004644	-2.348421	-1.296806
O	-1.056367	2.191223	2.796000
C	-2.656523	-1.536028	-0.569331
C	-1.402067	1.380809	2.064338
C	2.693756	1.274809	-1.385814
H	1.965488	1.941872	-1.848021
H	2.954741	1.645592	-0.385658
H	3.588503	1.234658	-2.009413
H	3.936360	-1.096710	-1.389857
H	3.324510	-0.819359	0.269926
H	2.562062	-2.047902	-0.785457

**Table S5.** Thermodynamic data (298.15 K) for  $[W(CNNMe_2)(CO)_5]$  at the M06-2X/6-31G\*/LANL2D $\zeta$ (W)

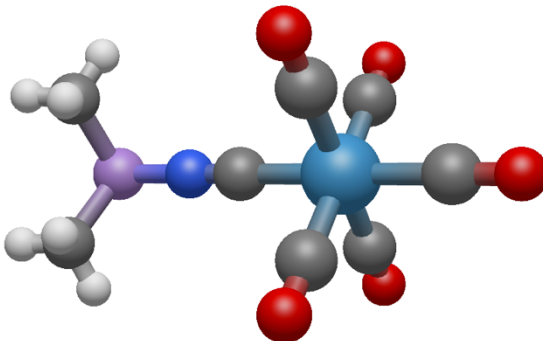
<b>Zero Point Energy :</b>	358.26 kJ/mol
<b>Temperature Correction :</b>	42.79 kJ/mol
<b>Enthalpy Correction :</b>	401.05 kJ/mol
<b>Enthalpy :</b>	-861.354002 au
<b>Entropy :</b>	514.56 J/mol•K
<b>Gibbs Energy :</b>	-861.412434 au
<b>C<sub>v</sub>:</b>	267.22 J/mol•K

**2.2  $[W(CNPMMe_2)(CO)_5]$** **Figure S8.** Optimised geometry for  $[W(CNPMMe_2)(CO)_5]$  at the M06-2X/6-31G\*/LANL2D $\zeta$ (W) level of DFT. Selected distances ( $\text{\AA}$ ) and angles ( $^\circ$ ): W–C 2.122, C–N 1.175, N–P 1.730, W–C–N 179.3, C–N–P 176.2.**Table S6.** Cartesian Coordinates for  $[W(CNPMMe_2)(CO)_5]$ 

Atom	x	y	z
W	-2.125643	0.000476	0.720791
P	2.174463	0.001201	-1.879685
N	0.729651	-0.000072	-0.927399
O	-3.253466	2.281855	-1.235334
O	-0.967159	-2.271124	2.665679
C	-0.292799	-0.001245	-0.347623
C	-2.849615	1.466391	-0.541641
C	-1.381686	-1.460489	1.971996
C	3.015694	-1.410672	-1.036253
O	-4.890349	0.001727	2.323162
C	-3.898253	0.001152	1.748562
O	-3.256890	-2.271753	-1.243763
O	-0.963204	2.266123	2.670452
C	-2.852402	-1.458868	-0.547544
C	-1.377751	1.456638	1.975399
C	3.017826	1.407610	-1.032185
H	2.507962	2.342309	-1.276103
H	3.039581	1.278054	0.052488
H	4.042545	1.470363	-1.410791
H	4.039196	-1.474523	-1.418078
H	3.040383	-1.282685	0.048934
H	2.501708	-2.342694	-1.281475

**Table S7.** Thermodynamic data (298.15 K) for  $[W(CNAsMe_2)(CO)_5]$  at the M06-2X/6-31G\*/LANL2D $\zeta$ (W)

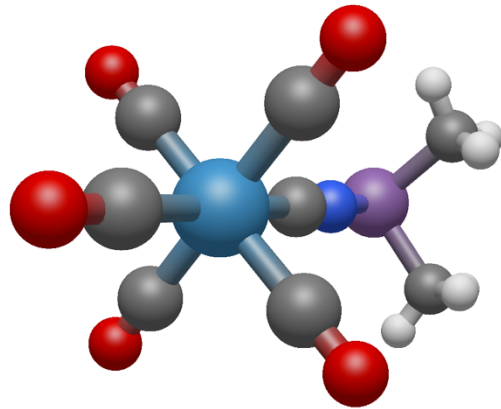
<b>Zero Point Energy :</b>	340.74 kJ/mol
<b>Temperature Correction :</b>	44.76 kJ/mol
<b>Enthalpy Correction :</b>	385.50 kJ/mol
<b>Enthalpy :</b>	-1148.012082 au
<b>Entropy :</b>	529.21 J/mol•K
<b>Gibbs Energy :</b>	-1148.072179 au
<b>C<sub>v</sub>:</b>	281.58 J/mol•K

**2.3  $[W(CNAsMe_2)(CO)_5]$** **Figure S9.** Optimised geometry for  $[W(CNAsMe_2)(CO)_5]$  at the M06-2X/6-31G\*/LANL2D $\zeta$ (W) level of DFT. Selected distances ( $\text{\AA}$ ) and angles ( $^\circ$ ): W–C 2.133, C–N 1.174, N–As 1.881, W–C–N 179.3, C–N–As 176.2.**Table S8.** Cartesian Coordinates for  $[W(CNAsMe_2)(CO)_5]$ 

Atom	x	y	z
W	2.173192	-0.027673	0.734633
As	-2.228205	-0.029516	-2.006928
N	-0.670578	-0.028526	-0.952339
O	3.320481	-2.300913	-1.218050
O	0.985329	2.239934	2.666121
C	0.343337	-0.028169	-0.360937
C	2.910379	-1.488280	-0.524225
C	1.410008	1.429759	1.977383
C	-3.045659	1.510068	-1.112137
O	4.918842	-0.025981	2.362224
C	3.931087	-0.026637	1.778890
O	3.318094	2.250871	-1.213391
O	0.991933	-2.301442	2.663071
C	2.908971	1.435864	-0.521695
C	1.413753	-1.488444	1.975780
C	-3.133357	-1.431579	-0.980197
H	-2.649392	-2.391844	-1.165713
H	-3.109942	-1.207393	0.087746
H	-4.170826	-1.489925	-1.320812
H	-4.078578	1.599320	-1.459733
H	-3.033130	1.381214	-0.028429
H	-2.505739	2.419293	-1.381262

**Table S9.** Thermodynamic data (298.15 K) for  $[W(CNPMe_2)(CO)_5]$  at the M06-2X/6-31G\*/LANL2D $\zeta$ (W)

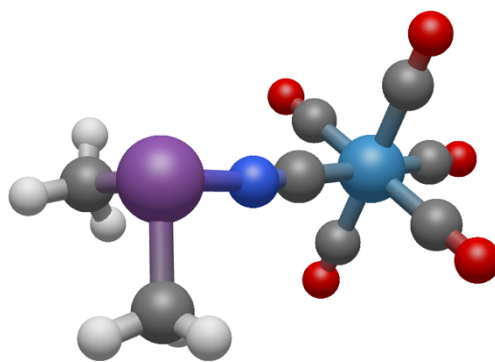
Zero Point Energy :	335.60 kJ/mol
Temperature Correction :	45.69 kJ/mol
Enthalpy Correction :	381.28 kJ/mol
Enthalpy :	-3042.290376 au
Entropy :	540.20 J/mol•K
Gibbs Energy :	-3042.351721 au
$C_v$ :	287.61 J/mol•K

**2.4  $[W(CNSbMe_2)(CO)_5]$** **Figure S10.** Optimised geometry for  $[W(CNSbMe_2)(CO)_5]$  at the M06-2X/6-31G\*/LANL2D $\zeta$ (W,Sb) level of DFT. Selected distances ( $\text{\AA}$ ) and angles ( $^\circ$ ): W–C 2.136, C–N 1.175, N–Sb 2.071, W–C–N 178.9, C–N–Sb 174.8.**Table S10.** Cartesian Coordinates for  $[W(CNSbMe_2)(CO)_5]$ 

Atom	x	y	z
W	-0.289241	-0.024141	2.342624
Sb	-0.993938	0.130634	-2.985494
N	-0.628926	0.035529	-0.949332
O	-2.750591	2.014562	2.628358
O	2.165778	-2.060376	2.000993
C	-0.522949	0.015006	0.220236
C	-1.872542	1.286917	2.525795
C	1.289106	-1.333928	2.124055
C	0.289818	-1.539496	-3.392927
O	0.068616	-0.076553	5.512856
C	-0.060759	-0.058414	4.372860
O	-2.327410	-2.497221	2.504094
O	1.740837	2.450433	2.129784
C	-1.599300	-1.615525	2.445602
C	1.015560	1.567566	2.206905
C	0.535641	1.605959	-3.278434
H	0.196754	2.583069	-2.928301
H	1.432651	1.314571	-2.728344
H	0.773292	1.678126	-4.343807
H	0.505176	-1.576958	-4.464881
H	1.225595	-1.425751	-2.841750
H	-0.193167	-2.474010	-3.100892

**Table S11.** Thermodynamic data (298.15 K) for  $[W(CNSbMe_2)(CO)_5]$  at the M06-2X/6-31G\*/LANL2D $\zeta$ (W,Sb)

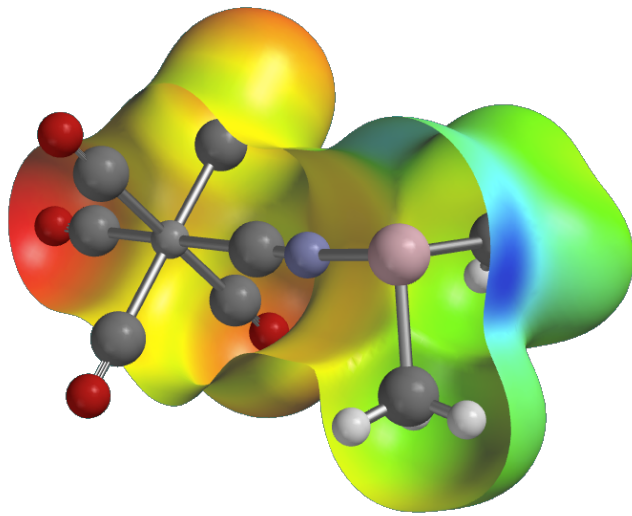
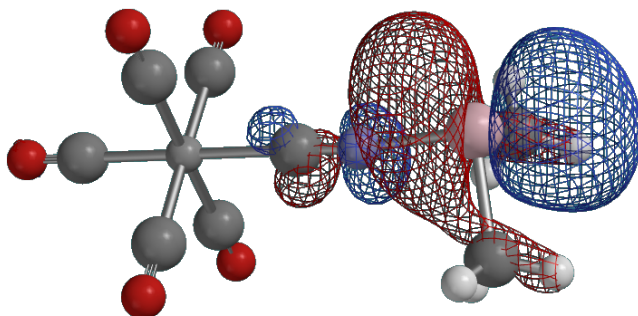
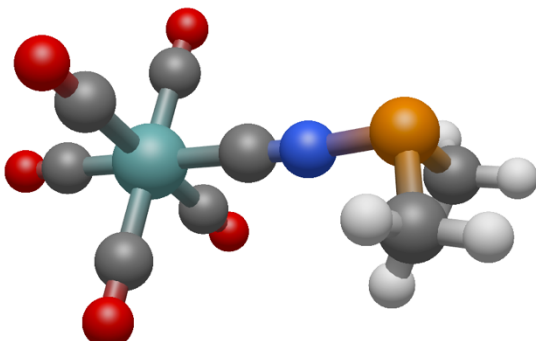
Zero Point Energy :	329.53 kJ/mol
Temperature Correction :	46.28 kJ/mol
Enthalpy Correction :	375.81 kJ/mol
Enthalpy :	-812.080457 au
Entropy :	549.47 J/mol•K
Gibbs Energy :	-812.142854 au
$C_v$ :	289.45 J/mol•K

**2.5  $[W(CNBiMe_2)(CO)_5]$** **Figure S11.** Optimised geometry for  $[W(CNBiMe_2)(CO)_5]$  at the M06-2X/6-31G\*/LANL2D $\zeta$ (W,Bi) level of DFT. Selected distances ( $\text{\AA}$ ) and angles ( $^\circ$ ): W–C 2.136, C–N 1.175, N–Bi 2.071, W–C–N 178.9, C–N–Bi 174.8.**Table S12.** Cartesian Coordinates for  $[W(CNBiMe_2)(CO)_5]$ 

Atom	x	y	z
W	-0.441627	0.041977	-2.375895
C	1.619729	0.069671	-2.317797
O	2.764572	0.083612	-2.288879
C	-0.468860	2.103579	-2.370254
O	-0.482734	3.248883	-2.369057
C	-0.403714	0.031538	-4.415314
O	-0.383630	0.025340	-5.563277
C	-2.502481	0.013062	-2.398146
O	-3.647784	-0.001616	-2.411277
C	-0.412727	-2.019391	-2.347195
O	-0.398532	-3.164597	-2.333408
C	-0.490389	0.055274	-0.230715
N	-0.510663	0.062085	0.942728
Bi	-0.843249	0.103595	3.073538
C	0.813907	1.540493	3.387688
H	1.634755	1.278487	2.717784
H	1.156837	1.472089	4.423911
H	0.486262	2.561532	3.184623
C	0.463013	-1.659855	3.382476
H	1.397313	-1.509678	2.838438
H	-0.028295	-2.564928	3.021084
H	0.678295	-1.771151	4.448944

**Table S13.** Thermodynamic data (298.15 K) for  $[W(CNSbMe_2)(CO)_5]$  at the M06-2X/6-31G\*/LANL2D $\zeta$ (W,Sb)

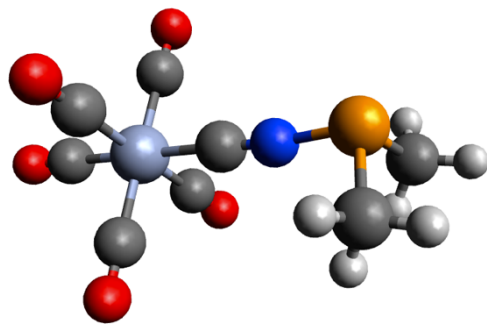
<b>Zero Point Energy :</b>	327.80 kJ/mol
<b>Temperature Correction :</b>	46.43 kJ/mol
<b>Enthalpy Correction :</b>	374.23 kJ/mol
<b>Enthalpy :</b>	-812.115692 au
<b>Entropy :</b>	554.41 J/mol•K
<b>Gibbs Energy :</b>	-812.178650 au
<b>C<sub>v</sub>:</b>	295.29 J/mol•K

**Figure S12.** Optimised geometry for  $[W(CNBiMe_2)(CO)_5]$  at the M06-2X/6-31G\*/LANL2D $\zeta$ (W,Bi) level of DFT showing the  $\sigma$ -hole on bismuth opposite to the N–Bi bond.**Figure S13.** Optimised geometry for  $[W(CNBiMe_2)(CO)_5]$  at the M06-2X/6-31G\*/LANL2D $\zeta$ (W,Bi) level of DFT showing LUMO predominately comprising the N–Bi  $\sigma^*$ -antibond.**2.6 [Mo(CNPM<sub>2</sub>)(CO)<sub>5</sub>]****Figure S14.** Optimised geometry for  $[Mo(CNPM_2)(CO)_5]$  at the M06-2X/6-31G\*/LANL2D $\zeta$ (Mo) level of DFT. Selected distances (Å) and angles (°): Mo–C 2.145, C–N 1.175, N–P 1.733, Mo–C–N 178.9, C–N–Bi 174.0.**Table S14.** Cartesian Coordinates for  $[Mo(CNPM_2)(CO)_5]$ 

Atom	x	y	z
Mo	-2.143848	-0.000921	0.734467
P	2.175986	-0.002229	-1.876764
N	0.750290	0.002130	-0.891584
O	-3.253724	2.291560	-1.237918
O	-0.999994	-2.288536	2.687000
C	-0.281384	0.000881	-0.328707
C	-2.860016	1.474964	-0.542223
C	-1.408941	-1.474514	1.996348
C	3.035302	-1.408315	-1.043529
O	-4.930784	0.007949	2.308581
C	-3.933274	0.003843	1.746435
O	-3.260253	-2.281102	-1.248694
O	-0.978330	2.270118	2.693474
C	-2.863340	-1.470295	-0.548138
C	-1.395613	1.463650	1.998889
C	3.038008	1.408086	-1.053718
H	2.519476	2.340686	-1.287216
H	3.087464	1.280506	0.030779
H	4.053072	1.471953	-1.458307
H	4.050338	-1.475159	-1.447315
H	3.084013	-1.273790	0.040132
H	2.515553	-2.341468	-1.271992

**Table S15.** Thermodynamic data (298.15 K) for  $[Mo(CNPM_2)(CO)_5]$  at the M06-2X/6-31G\*/LANL2D $\zeta$ (Mo)

<b>Zero Point Energy :</b>	338.57 kJ/mol
<b>Temperature Correction :</b>	45.66 kJ/mol
<b>Enthalpy Correction :</b>	384.23 kJ/mol
<b>Enthalpy :</b>	-1147.719987 au
<b>Entropy :</b>	531.68 J/mol•K
<b>Gibbs Energy :</b>	-1147.780365 au
<b>C<sub>v</sub>:</b>	284.72 J/mol•K

2.7 [Cr(CNPM<sub>2</sub>)(CO)<sub>5</sub>]

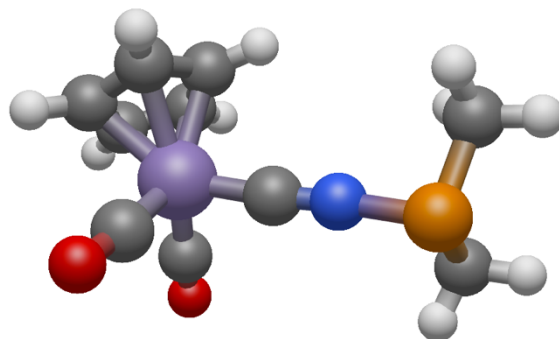
**Figure S15.** Optimised geometry for  $[\text{Cr}(\text{CNPM}_2)(\text{CO})_5]$  at the M06-2X/6-31G\*/LANL2D $_{\zeta}^{\text{c}}$ (Cr) level of DFT. Selected distances ( $\text{\AA}$ ) and angles ( $^{\circ}$ ): Cr–C 1.992, C–N 1.175, N–P 1.732, Cr–C–N 178.8, C–N–P 173.9.

**Table S16.** Cartesian Coordinates for  $[\text{Cr}(\text{CNPM}_2)(\text{CO})_5]$

Atom	x	y	z
Cr	-2.091664	0.000524	0.711172
P	2.087133	0.001517	-1.837171
N	0.665851	0.001286	-0.847659
O	-3.141594	2.181829	-1.175202
O	-0.973660	-2.175248	2.560715
C	-0.364700	0.001111	-0.282428
C	-2.751753	1.367631	-0.474358
C	-1.394258	-1.363839	1.873696
C	2.950409	-1.408457	-1.016185
O	-4.737306	0.000903	2.232425
C	-3.744266	0.000457	1.663157
O	-3.147077	-2.170518	-1.184200
O	-0.968146	2.164664	2.570967
C	-2.755763	-1.359130	-0.480945
C	-1.390551	1.356859	1.880793
C	2.952671	1.407280	-1.010133
H	2.434443	2.341442	-1.238313
H	3.005116	1.275369	0.073740
H	3.966366	1.471560	-1.417436
H	3.964733	-1.472390	-1.422268
H	3.002007	-1.281434	0.068296
H	2.432009	-2.341416	-1.248664

**Table S17.** Thermodynamic data (298.15 K) for  $[\text{Cr}(\text{CNPM}_2)(\text{CO})_5]$  at the M06-2X/6-31G\*/LANL2D $_{\zeta}^{\text{c}}$ (Cr)

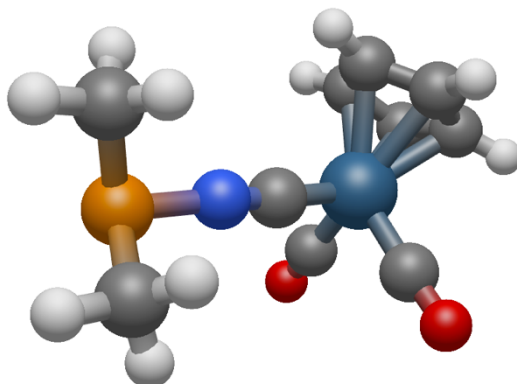
Zero Point Energy :	341.35 kJ/mol
Temperature Correction :	44.90 kJ/mol
Enthalpy Correction :	386.25 kJ/mol
Enthalpy :	-2124.556700 au
Entropy :	524.07 J/mol•K
Gibbs Energy :	-2124.616213 au
C <sub>v</sub> :	281.20 J/mol•K

2.8  $[\text{Mn}(\text{CNPM}_2)(\text{CO})_2(\eta^5\text{-C}_5\text{H}_5)]$ 

**Figure S16.** Optimised geometry for  $[\text{Mn}(\text{CNPM}_2)(\text{CO})_2(\eta^5\text{-C}_5\text{H}_5)]$  at the M06-2X/6-31G\*/LANL2D $_{\zeta}^{\text{c}}$ (Mn) level of DFT. Selected distances ( $\text{\AA}$ ) and angles ( $^{\circ}$ ): Mn–C 1.876, C–N 1.179, N–P 1.723, Mn–C–N 175.5, C–N–P 172.7.

**Table S18.** Cartesian Coordinates for  $[\text{Mn}(\text{CNPM}_2)(\text{CO})_2(\eta^5\text{-C}_5\text{H}_5)]$

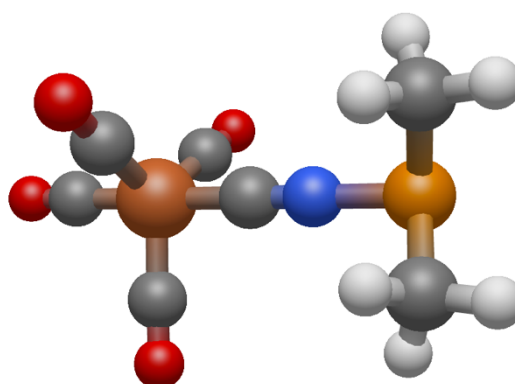
Atom	x	y	z
Mn	1.042289	1.248208	-0.098497
H	3.146967	2.336523	-1.818362
C	2.149074	1.920726	-1.864777
C	0.944922	2.651163	-1.776097
H	2.527772	-0.271134	-2.141751
H	0.860440	3.722532	-1.650837
C	-0.141473	1.731332	-1.881731
H	-1.193191	1.981213	-1.866208
C	0.411037	0.438154	-2.042338
H	-0.152974	-0.480981	-2.135556
C	1.824115	0.541096	-2.025303
C	0.244275	2.430319	1.023630
O	-0.302264	3.214650	1.658100
C	2.571308	1.120741	0.880449
O	3.579179	1.052966	1.422893
C	0.250906	-0.226869	0.747743
N	-0.291317	-1.171038	1.199830
P	-0.902028	-2.579728	1.982391
C	-1.630340	-3.394558	0.491318
H	-0.829578	-3.747870	-0.162466
H	-2.282296	-2.716734	-0.066270
H	-2.208759	-4.263081	0.821270
C	-2.437811	-1.831562	2.685863
H	-2.169687	-1.136568	3.484915
H	-3.045877	-2.631799	3.118997
H	-3.019050	-1.302929	1.925640

2.9 [Re(CNPM<sub>2</sub>)(CO)<sub>2</sub>(η<sup>5</sup>-C<sub>5</sub>H<sub>5</sub>)]

**Figure S17.** Optimised geometry for [Re(CNPM<sub>2</sub>)(CO)<sub>2</sub>(η<sup>5</sup>-C<sub>5</sub>H<sub>5</sub>)] at the M06-2X/6-31G\*/LANL2D<sub>C</sub>(Re) level of DFT. Selected distances (Å) and angles (°): Re–C 1.945, C–N 1.185, N–P 1.719, Re–C–N 176.8, C–N–P 166.0.

**Table S19.** Cartesian Coordinates for [Re(CNPM<sub>2</sub>)(CO)<sub>2</sub>(η<sup>5</sup>-C<sub>5</sub>H<sub>5</sub>)]

Atom	x	y	z
Re	-0.178390	-1.012593	-1.231057
H	-1.897018	-3.285684	-2.316331
C	-2.025685	-2.282980	-1.932461
C	-2.012104	-1.089456	-2.697616
H	-2.338037	-2.628099	0.261954
H	-1.871887	-1.023917	-3.767733
C	-2.233211	0.012434	-1.809263
H	-2.294465	1.053493	-2.092293
C	-2.372134	-0.518750	-0.499071
H	-2.534385	0.062593	0.398887
C	-2.254684	-1.934741	-0.562614
C	0.047770	-0.159047	-2.405245
O	1.748302	0.381921	-3.147706
C	1.033488	-2.463687	-1.026714
O	1.727968	-3.379948	-0.916092
C	0.664069	-0.121666	0.278503
N	1.118671	0.451581	1.210651
P	1.899122	0.898460	2.675362
C	0.631310	2.089798	3.294487
H	-0.260975	1.544994	3.611346
H	0.356981	2.823720	2.531972
H	1.040156	2.609709	4.166739
C	3.104202	2.105174	1.964940
H	3.864950	1.567344	1.394227
H	3.599571	2.625651	2.790494
H	2.614000	2.834859	1.315008

2.10 [Fe(CNPM<sub>2</sub>)(CO)<sub>4</sub>]

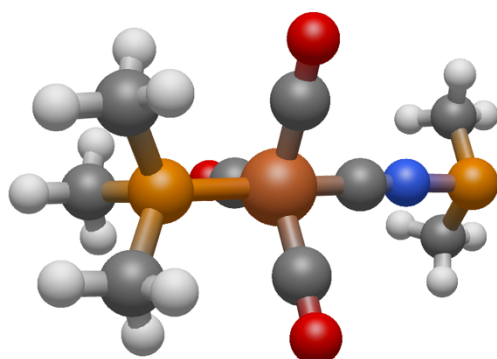
**Figure S18.** Optimised geometry for [Fe(CNPM<sub>2</sub>)(CO)<sub>4</sub>] at the M06-2X/6-31G\*/LANL2D<sub>C</sub>(Fe) level of DFT. Selected distances (Å) and angles (°): Fe–C 1.916, C–N 1.172, N–P 1.735, Fe–C–N 179.5, C–N–P 173.1.

**Table S20.** Cartesian Coordinates for [Fe(CNPM<sub>2</sub>)(CO)<sub>4</sub>]

Atom	x	y	z
Fe	-0.356387	-0.001311	-2.379522
C	-0.305721	-0.021292	-4.227439
O	-0.275645	-0.034661	-5.365823
C	-1.941801	-0.885782	-2.386660
O	-2.945469	-1.436272	-2.354131
C	-0.353890	1.807392	-2.360137
O	-0.349771	2.952269	-2.319691
C	1.222573	-0.887623	-2.296639
O	2.223013	-1.440075	-2.213524
C	-0.418713	-0.002294	-0.464048
N	-0.447329	-0.004143	0.707301
P	-0.697102	-0.008713	2.424410
C	0.426394	-1.417341	2.828261
H	-0.011581	-2.350105	2.466049
H	0.510723	-1.480499	3.917523
H	1.421341	-1.289140	2.394481
C	0.416217	1.407142	2.833297
H	-0.026651	2.337499	2.470753
H	1.413346	1.285692	2.402624
H	0.496453	1.469258	3.922915

**Table S21.** Thermodynamic data (298.15 K) for [Fe(CNPM<sub>2</sub>)(CO)<sub>4</sub>] at the M06-2X/6-31G\*/LANL2D<sub>C</sub>(Fe)

Zero Point Energy :	315.93 kJ/mol
Temperature Correction :	41.15 kJ/mol
Enthalpy Correction :	357.07 kJ/mol
Enthalpy :	-2230.402717 au
Entropy :	499.27 J/mol•K
Gibbs Energy :	-2230.459414 au
C <sub>v</sub> :	252.12 J/mol•K

2.11 *trans*-[Fe(CNPM<sub>2</sub>)(CO)<sub>3</sub>(PMe<sub>3</sub>)]

**Figure S19.** Optimised geometry for *trans*-[Fe(CNPM<sub>2</sub>)(CO)<sub>3</sub>(PMe<sub>3</sub>)] at the M06-2X/6-31G\*/LANL2D $\zeta$ (Fe) level of DFT. Selected distances ( $\text{\AA}$ ) and angles ( $^{\circ}$ ): Fe-C 1.880, C-N 1.175, N-P 1.726, Fe-C-N 178.8, C-N-P 174.0.

**Table S22.** Cartesian Coordinates for *trans*-[Fe(CNPM<sub>2</sub>)(CO)<sub>3</sub>(PMe<sub>3</sub>)]

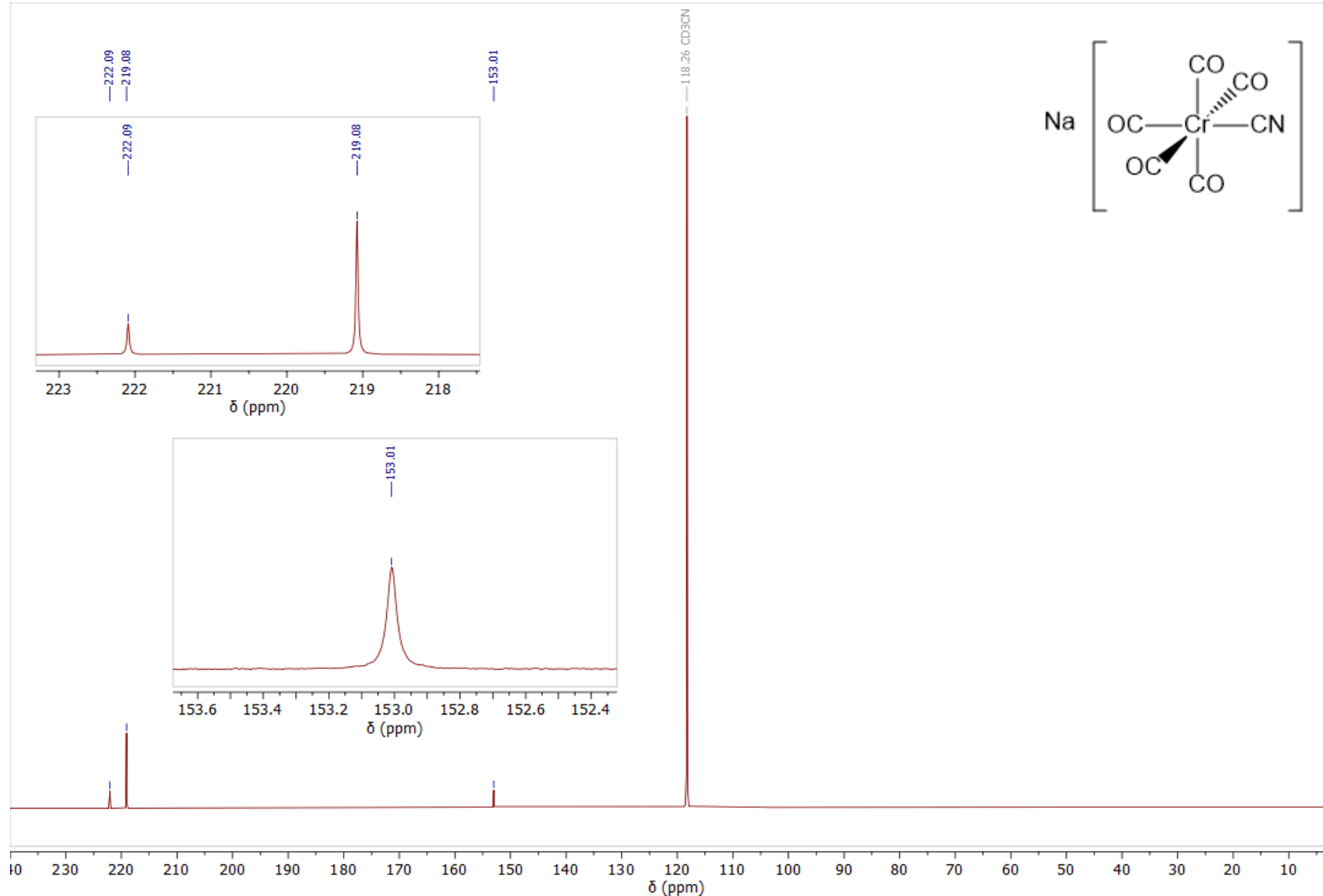
Atom	x	y	z
Fe	-0.233753	0.198534	-0.311907
C	-1.953564	-0.321375	-0.388813
O	-3.053657	-0.644876	-0.490426
C	0.157204	1.946332	-0.375028
O	0.420397	3.064569	-0.456782
C	1.103959	-0.998707	-0.293715
O	1.965655	-1.762780	-0.320263
C	-0.278391	0.222980	1.567064
N	-0.283213	0.232892	2.741967
P	-0.460104	0.304034	4.457102
C	-0.401993	-1.512383	4.784385
H	-1.320158	-1.979835	4.421395
H	-0.345908	-1.664258	5.866792
H	0.459426	-1.985336	4.305695
C	1.290983	0.734199	4.862074
H	1.502122	1.755740	4.537684
H	1.998050	0.049295	4.386751
H	1.413777	0.687740	5.948570
P	-0.174998	0.148030	-2.621746
C	0.253633	1.722434	-3.462010
H	-0.464359	2.495178	-3.173381
H	0.246280	1.606947	-4.550119
H	1.246105	2.050072	-3.139819
C	-1.735754	-0.311840	-3.471408
H	-2.052230	-1.305779	-3.143397
H	-1.609831	-0.311101	-4.558327
H	-2.521305	0.398011	-3.197338
C	1.021951	-1.021907	-3.375582
H	0.790793	-2.039155	-3.046793
H	2.032365	-0.780181	-3.034485
H	0.986302	-0.977474	-4.468140

**Table S23.** Thermodynamic data (298.15 K) for *trans*-[Fe(CNPM<sub>2</sub>)(CO)<sub>3</sub>(PMe<sub>3</sub>)] at the M06-2X/6-31G\*/LANL2D $\zeta$ (Fe)

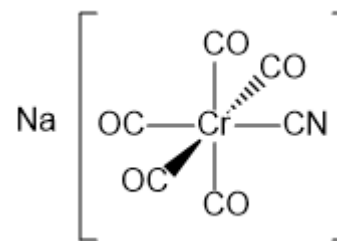
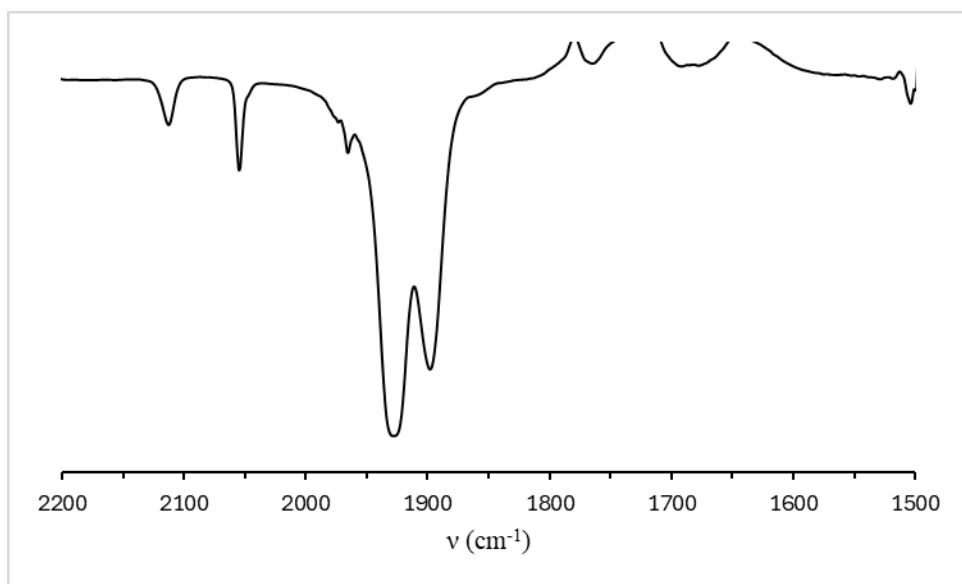
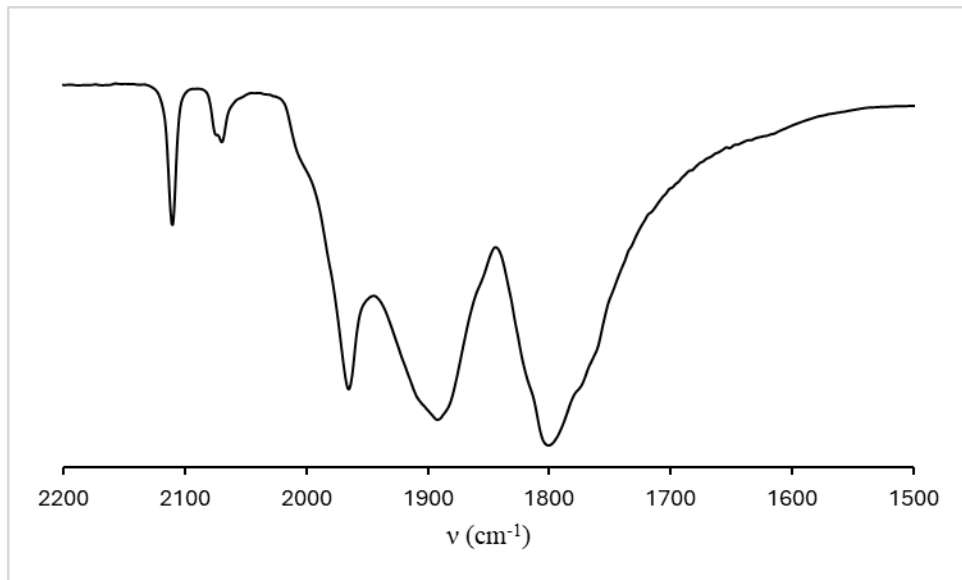
Zero Point Energy :	603.46 kJ/mol
Temperature Correction :	52.10 kJ/mol
Enthalpy Correction :	655.56 kJ/mol
Enthalpy :	-2578.003465 au
Entropy :	571.69 J/mol•K
Gibbs Energy :	-2578.068386 au
C <sub>v</sub> :	332.80 J/mol•K

## References

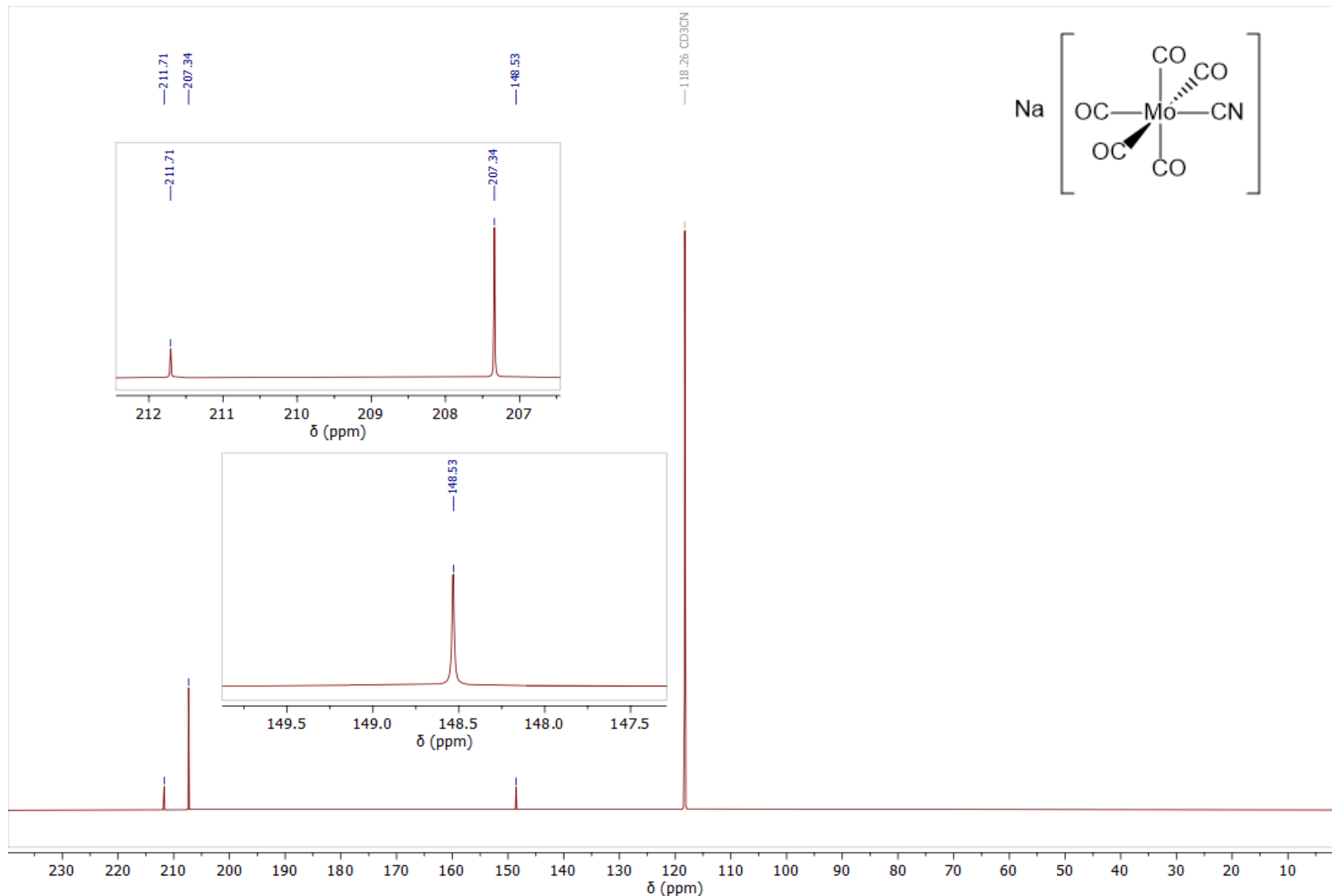
- 1 H. L. Conder and M. Y. Darensbourg, *J. Organomet. Chem.*, 1974, **67**, 93-97.
- 2 R. R. Cesati and J. A. Katzenellenbogen, *J. Am. Chem. Soc.*, 2001, **123**, 4093-4094.
- 3 R. B. King, *Inorg. Chem.*, 1967, **6**, 25-29.
- 4 CrysAlisPRO®, Oxford Diffraction/Agilent Technologies UK Ltd., Yarnton, England, 2010.
- 5 O. V. Dolomanov, L. J. Bourhis, R. J. Gildea, J. A. K. Howard and H. Puschmann, *J. Appl. Crystallogr.*, 2009, **42**, 339-341.
- 6 G. M. Sheldrick, *Acta Crystallogr. Sect. C: Cryst. Struct. Commun.*, 2015, **71**, 3-8.
- 7 ORTEP3
- 8 C. F. Macrae, I. J. Bruno, J. A. Chisholm, P. R. Edgington, P. McCabe, E. Pidcock, L. Rodriguez-Monge, R. Taylor, J. van de Streek and P. A. Wood, *J. Appl. Crystallogr.*, 2008, **41**, 466-470.
- 9 Spartan 24® (2024) Wavefunction, Inc., 18401 Von Karman Ave., Suite 370 Irvine, CA 92612 U.S.A.
- 10 Y. Zhao and D. G. Truhlar, *Theor. Chem. Acc.*, 2008, **120**, 215-241.
- 11 a) P. J. Hay and W.R. Wadt, *J. Chem. Phys.*, 1985, **82**, 270-283; b) W. R. Wadt and P. J. Hay, *J. Chem. Phys.* 1985, **82**, 284-298; c) P. J. Hay, W. R. Wadt, *J. Chem. Phys.*, 1985, **82**, 299-310.
- 12 a) W. J. Hehre, R. Ditchfield and J. A. Pople, *J. Chem. Phys.*, 1972, **56**, 2257-2261. b) Hariharan, P. C., Pople, J. A., *Theor. Chim. Acta.*, 1973, **28**, 213-222
- 13 a) Löwdin, P.-O., *J. Mol. Spec.*, 1963, **10**, 12-33; b) Löwdin, P.-O., *J. Mol. Spec.*, 1964, **13**, 320-337; c) Löwdin, P.-O., *J. Math. Phys.*, 1962, **3**, 969-982; d) Löwdin, P.-O., *J. Mol. Spec.*, 1964, **14**, 112-118.



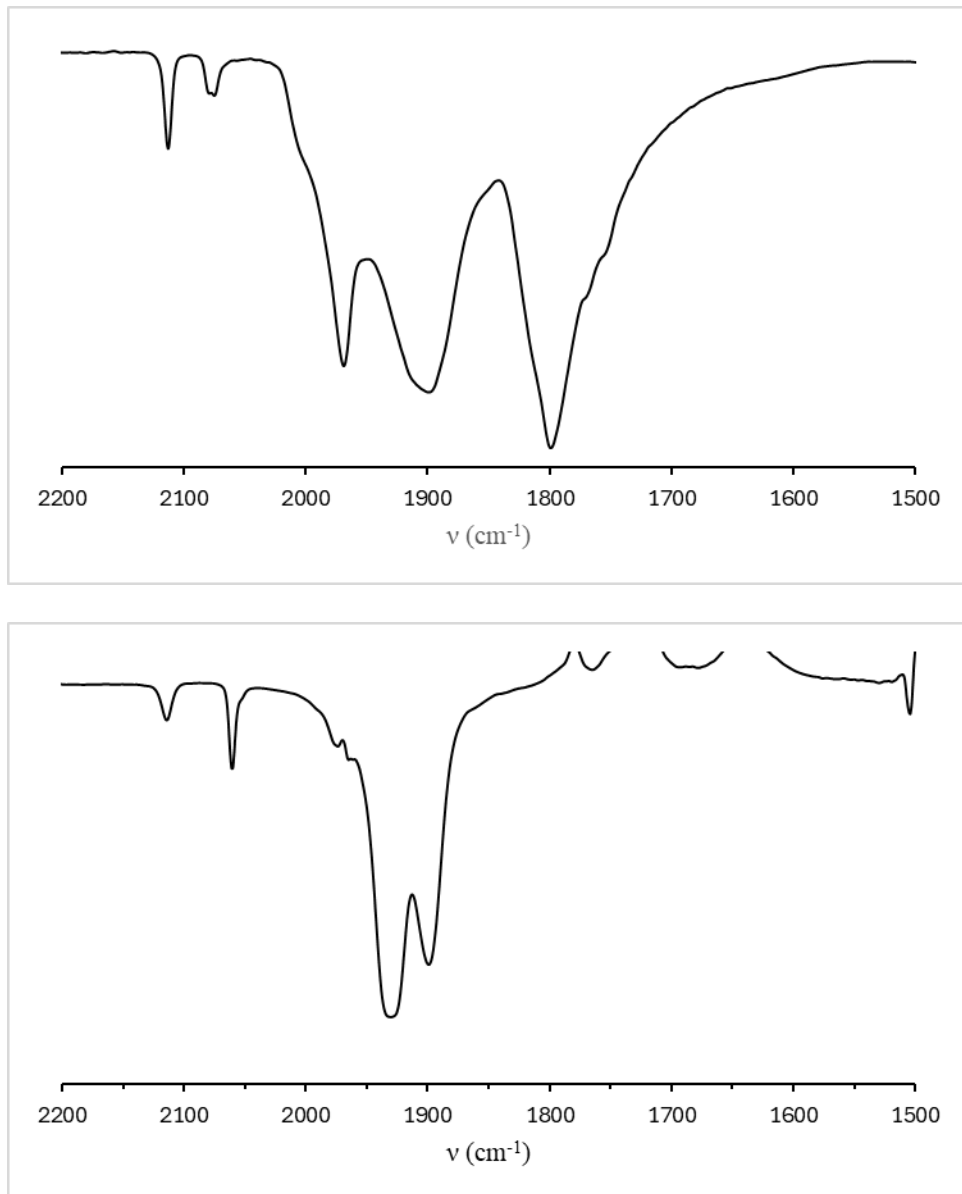
**Figure S20:** The  $^{13}\text{C}\{^1\text{H}\}$  NMR spectrum of  $\text{Na}[\text{Cr}(\text{CO})_5(\text{CN})]$  ( $\text{CD}_3\text{CN}$ , 201 MHz, 25 °C).



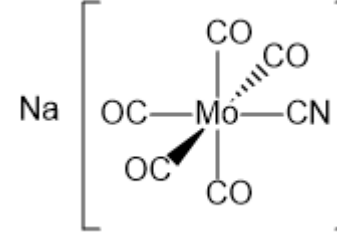
**Figure S21:** The solid state ATR-IR (top) and solution FT-IR (THF; bottom) spectra of  $\text{Na}[\text{Cr}(\text{CN})(\text{CO})_5]$  in the carbonyl region (25 °C).



**Figure S22:** The  $^{13}\text{C}\{^1\text{H}\}$  NMR spectrum of  $\text{Na}[\text{Mo}(\text{CO})_5(\text{CN})]$  ( $\text{CD}_3\text{CN}$ , 201 MHz, 25 °C).



**Figure S23:** The solid state ATR-IR (top) and solution FT-IR (THF; bottom) spectra of  $\text{Na}[\text{Mo}(\text{CN})(\text{CO})_5]$  in the carbonyl region (25 °C).



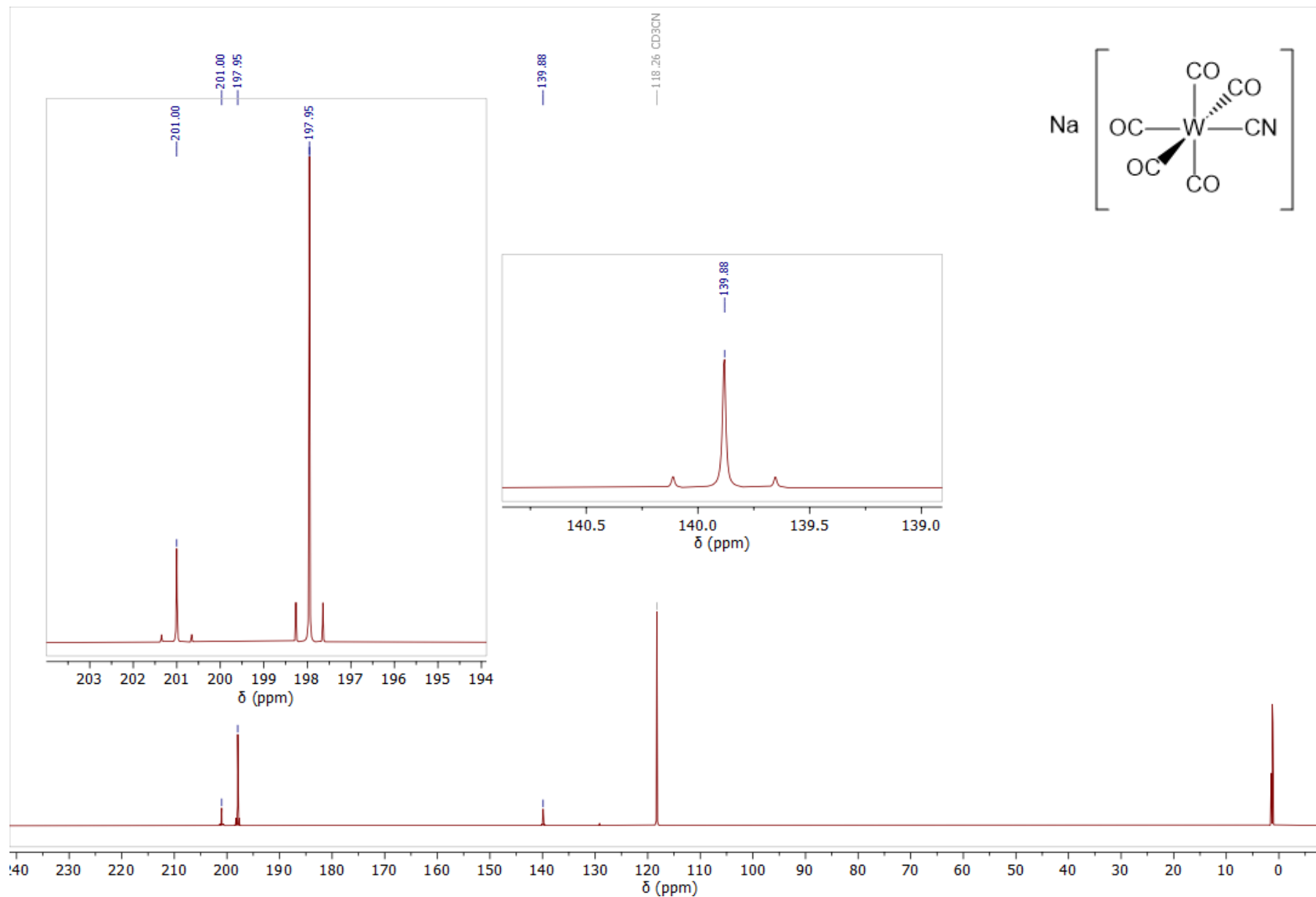


**Figure 24:** The  $^{13}\text{C}\{^1\text{H}\}$  NMR spectrum of  $\text{Na}[\text{W}(\text{CO})_5(\text{CN})]$  ( $\text{CD}_3\text{CN}$ , 201 MHz, 25 °C).

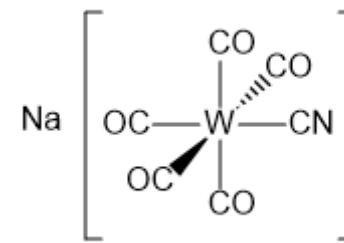
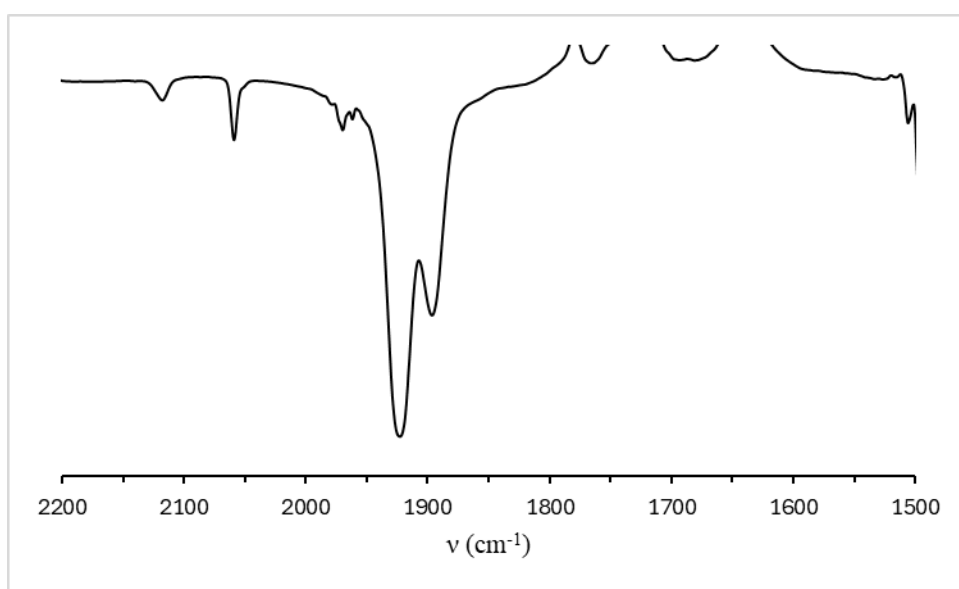
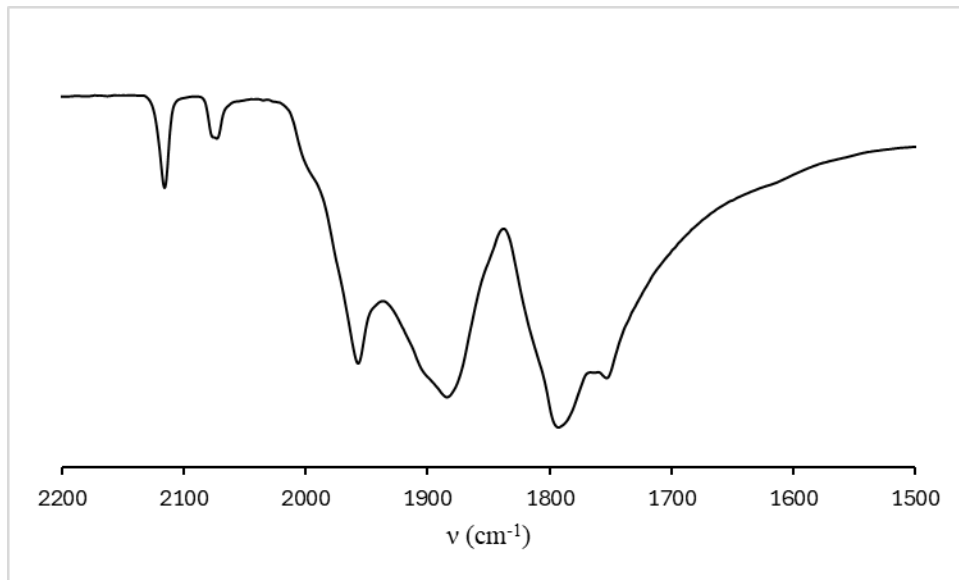


**Figure S25:** The solid state ATR-IR (top) and solution FT-IR (THF; bottom) spectra of  $\text{Na}[\text{W}(\text{CN})(\text{CO})_5]$  in the carbonyl region (25 °C).

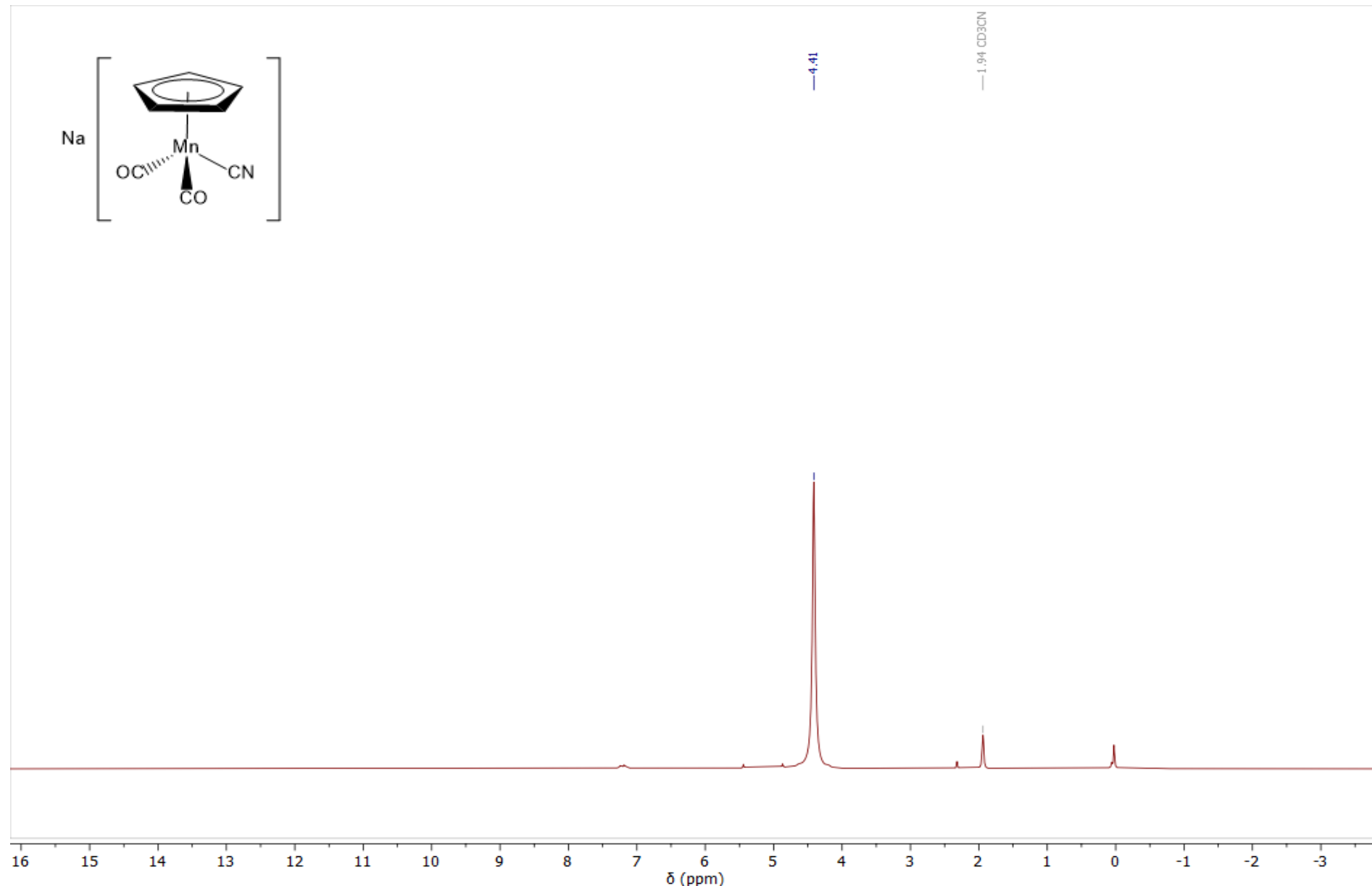


**Figure S26:** The  $^1\text{H}$  NMR spectrum of  $\text{Na}[\text{Mn}(\text{CN})(\text{CO})_2\text{Cp}]$  ( $\text{CD}_3\text{CN}$ , 400 MHz, 25 °C).

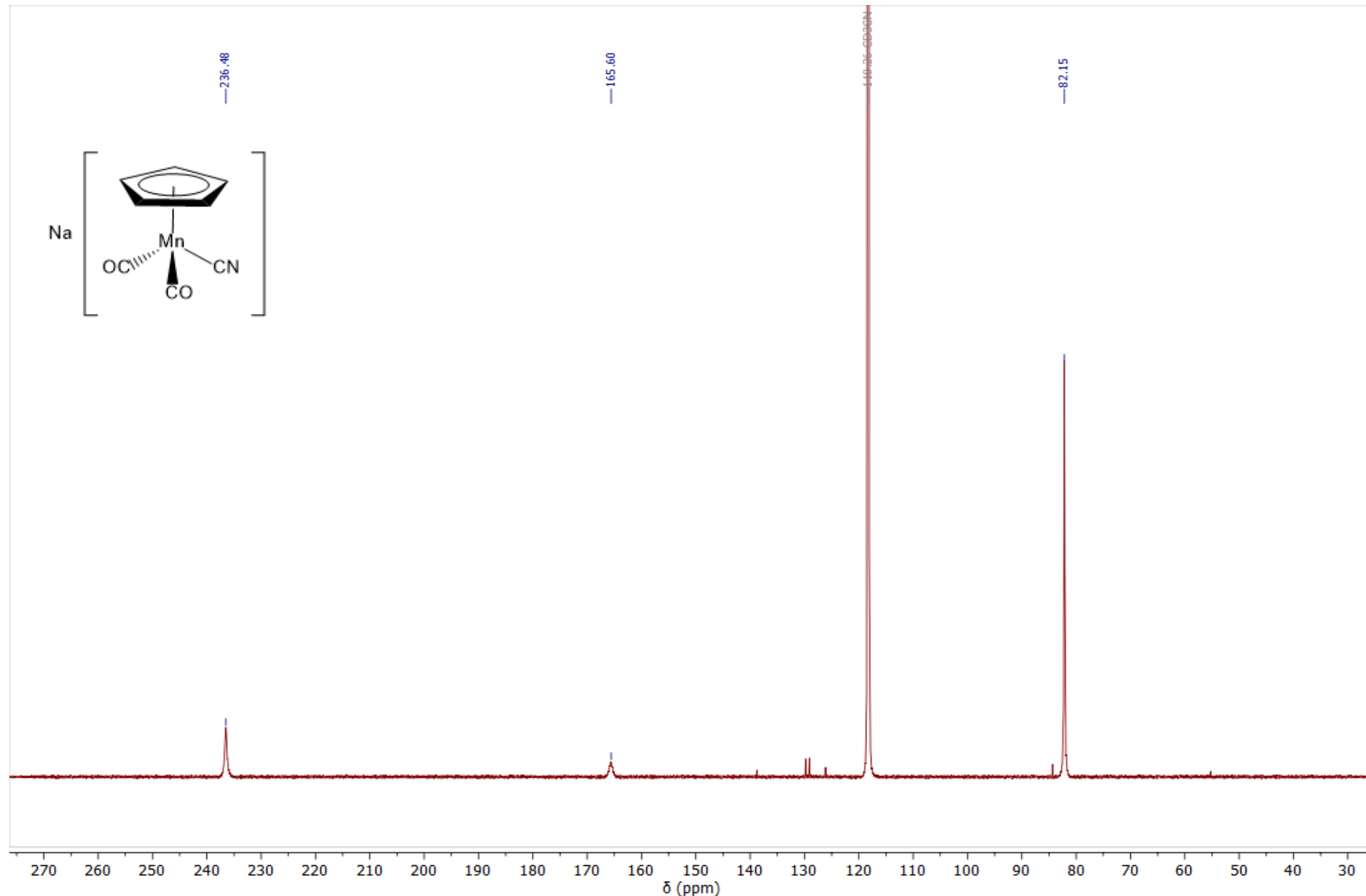


**Figure S27:** The  $^{13}\text{C}\{^1\text{H}\}$  NMR spectrum of  $\text{Na}[\text{Mn}(\text{CN})(\text{CO})_2\text{Cp}]$  ( $\text{CD}_3\text{CN}$ , 201 MHz, 25 °C).

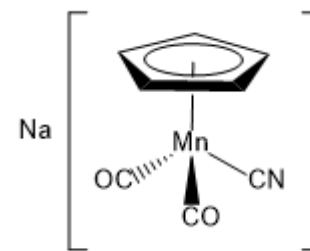
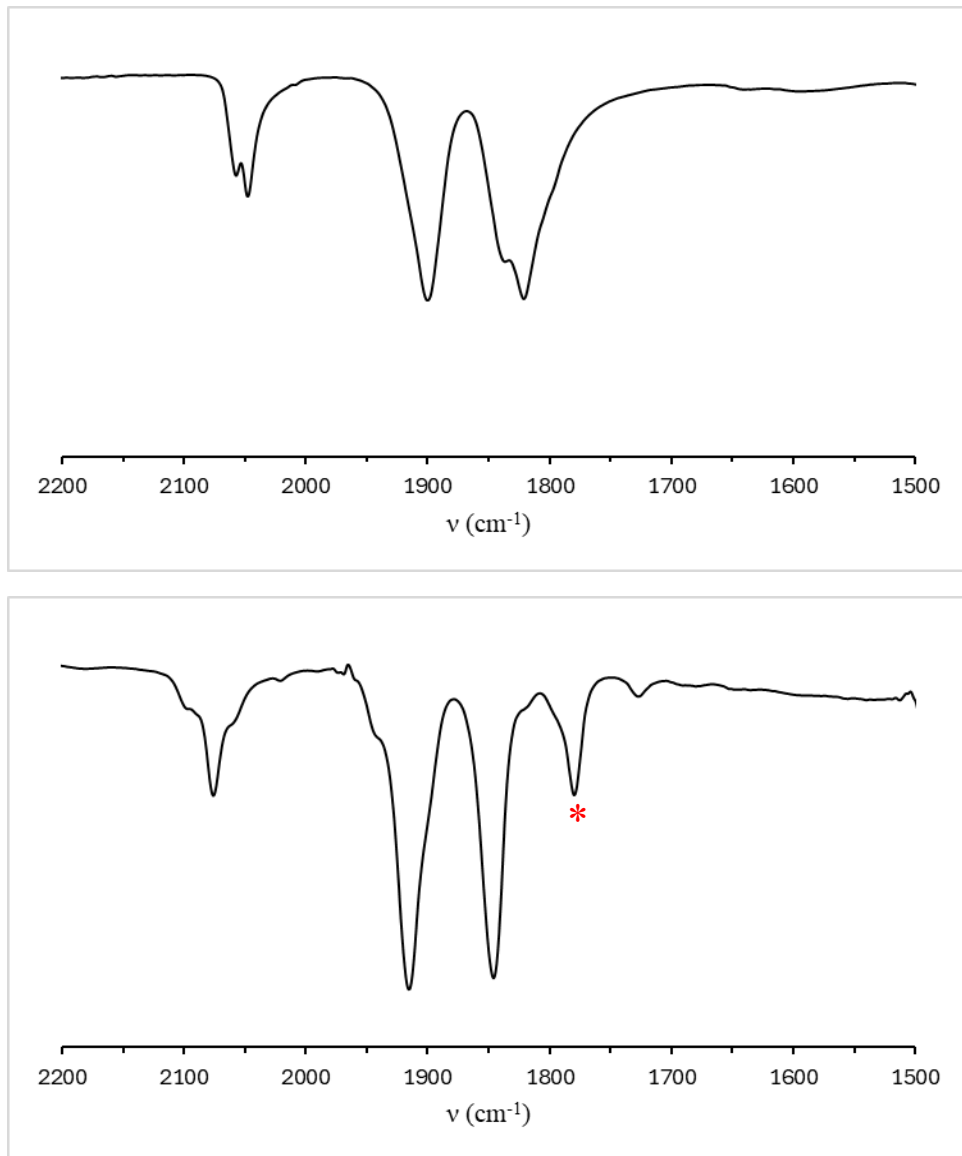


**Figure S28:** The solid state ATR-IR (top) and solution FT-IR (THF; bottom) spectra of  $\text{Na}[\text{Mn}(\text{CN})(\text{CO})_2\text{Cp}]$  in the carbonyl region ( $25^\circ\text{C}$ ). \* = oxidation impurity.

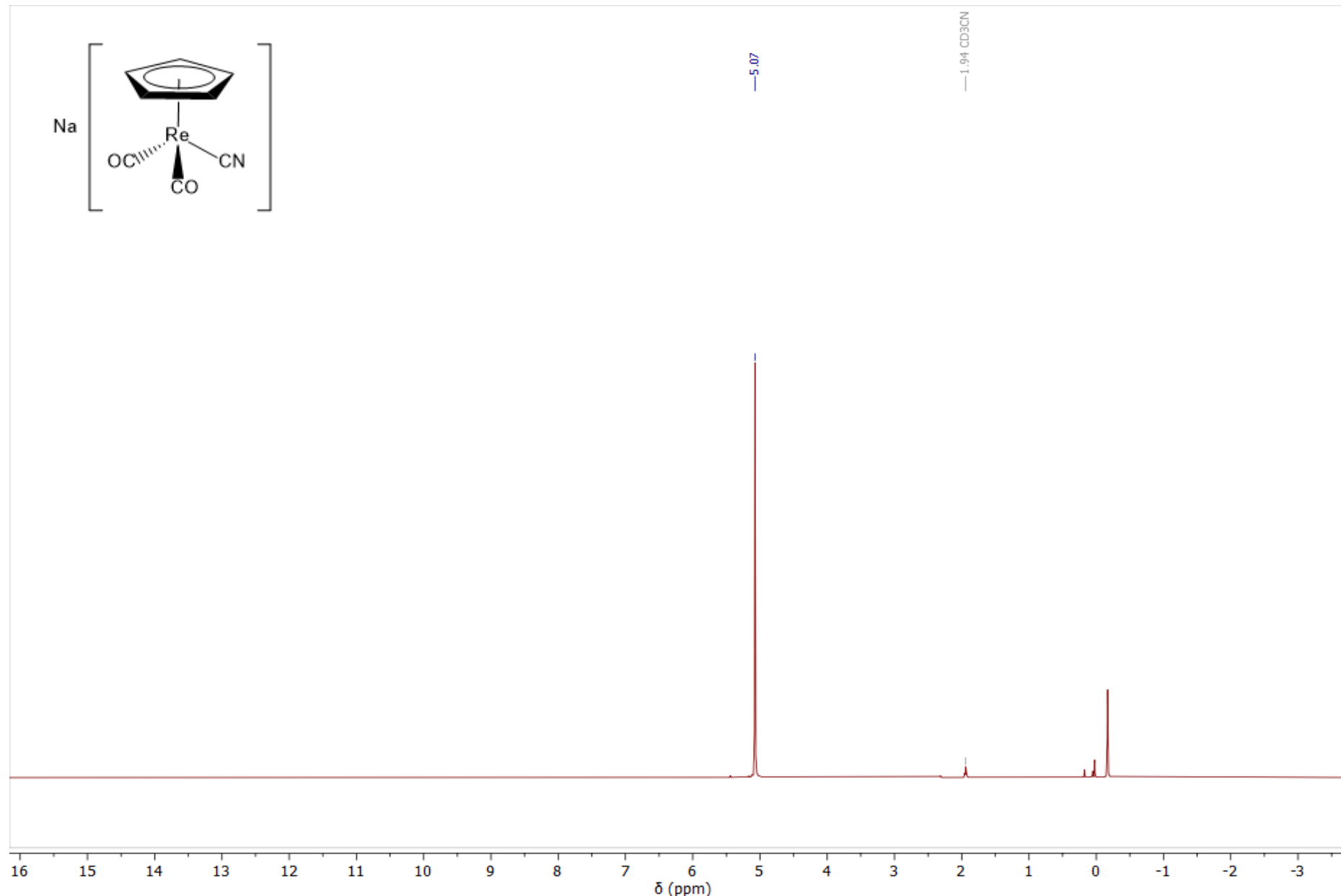


**Figure S29:** The  $^1\text{H}$  NMR spectrum of  $\text{Na}[\text{Re}(\text{CN})(\text{CO})_2\text{Cp}]$  ( $\text{CD}_3\text{CN}$ , 400 MHz, 25 °C).

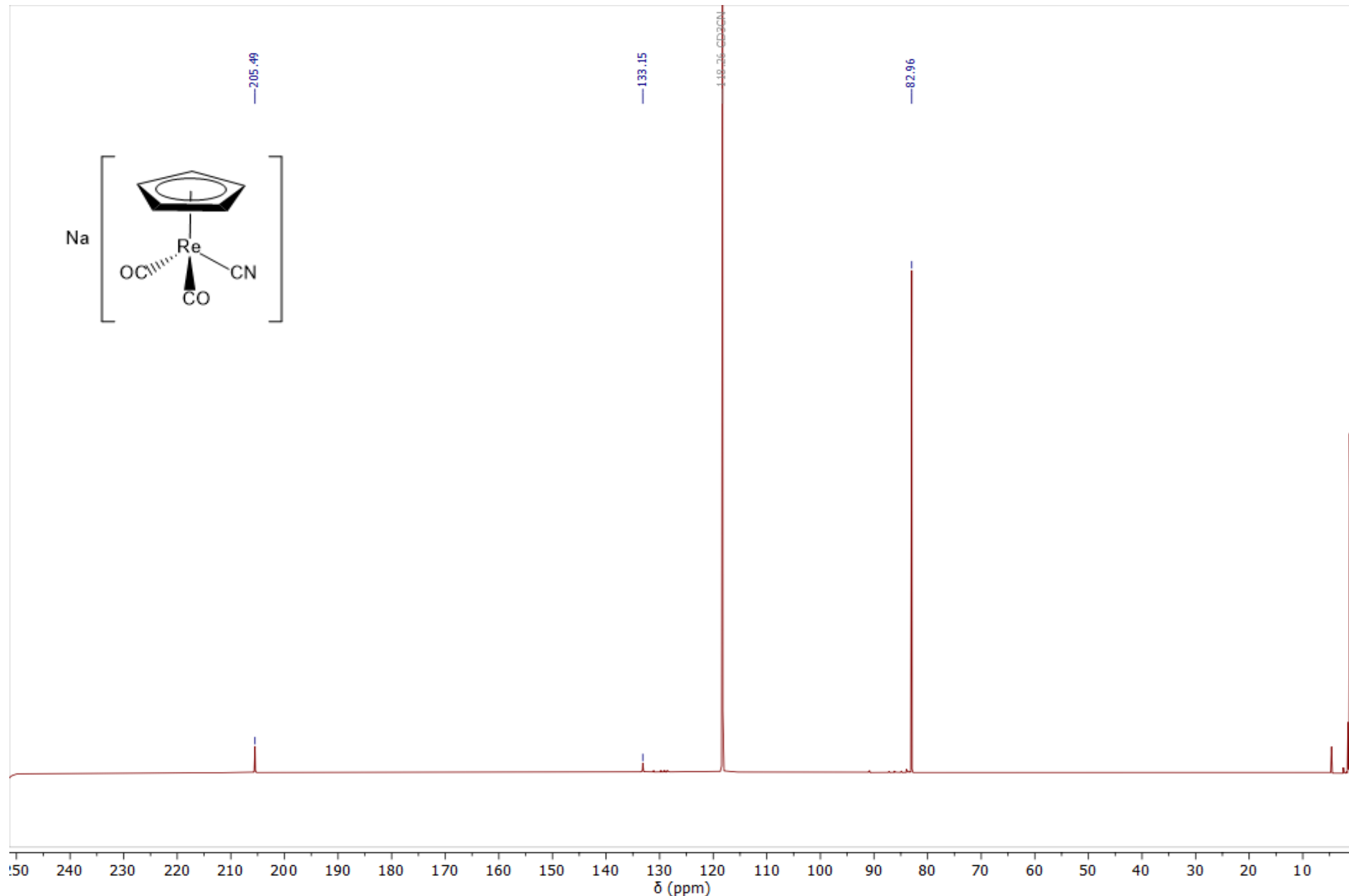


**Figure S30:** The  $^{13}\text{C}\{^1\text{H}\}$  NMR spectrum of  $\text{Na}[\text{Re}(\text{CN})(\text{CO})_2\text{Cp}]$  ( $\text{CD}_3\text{CN}$ , 201 MHz, 25 °C).

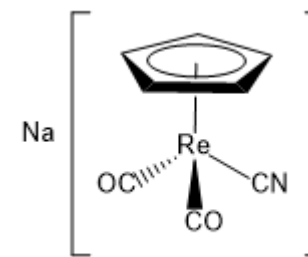
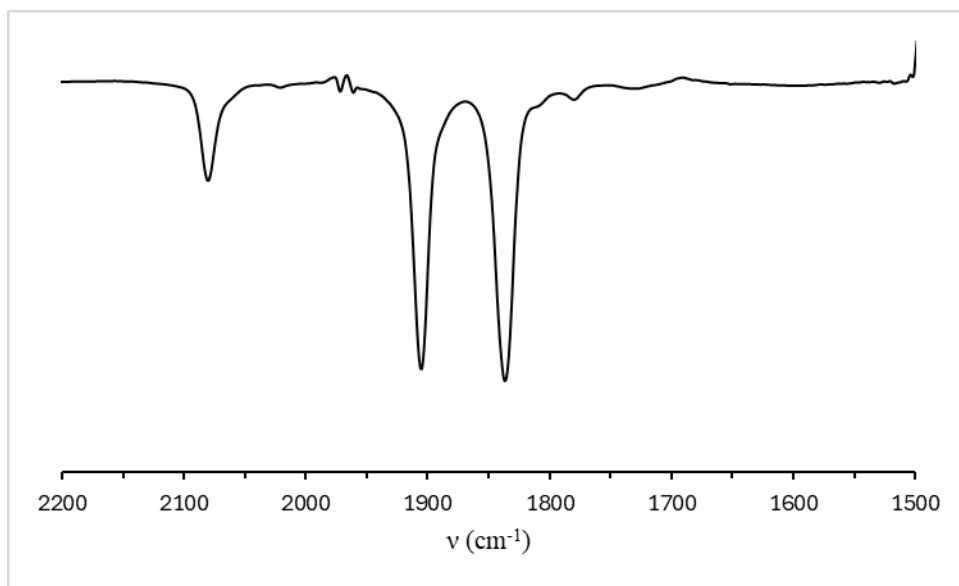
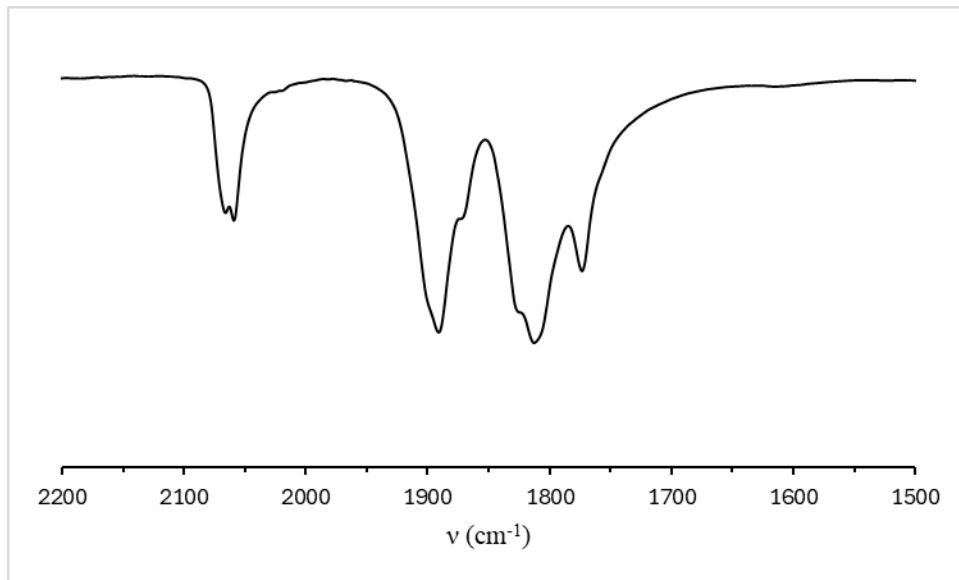


**Figure S31:** The solid state ATR-IR (top) and solution FT-IR (THF; bottom) spectra of  $\text{Na}[\text{Re}(\text{CN})(\text{CO})_2\text{Cp}]$  in the carbonyl region (25 °C).

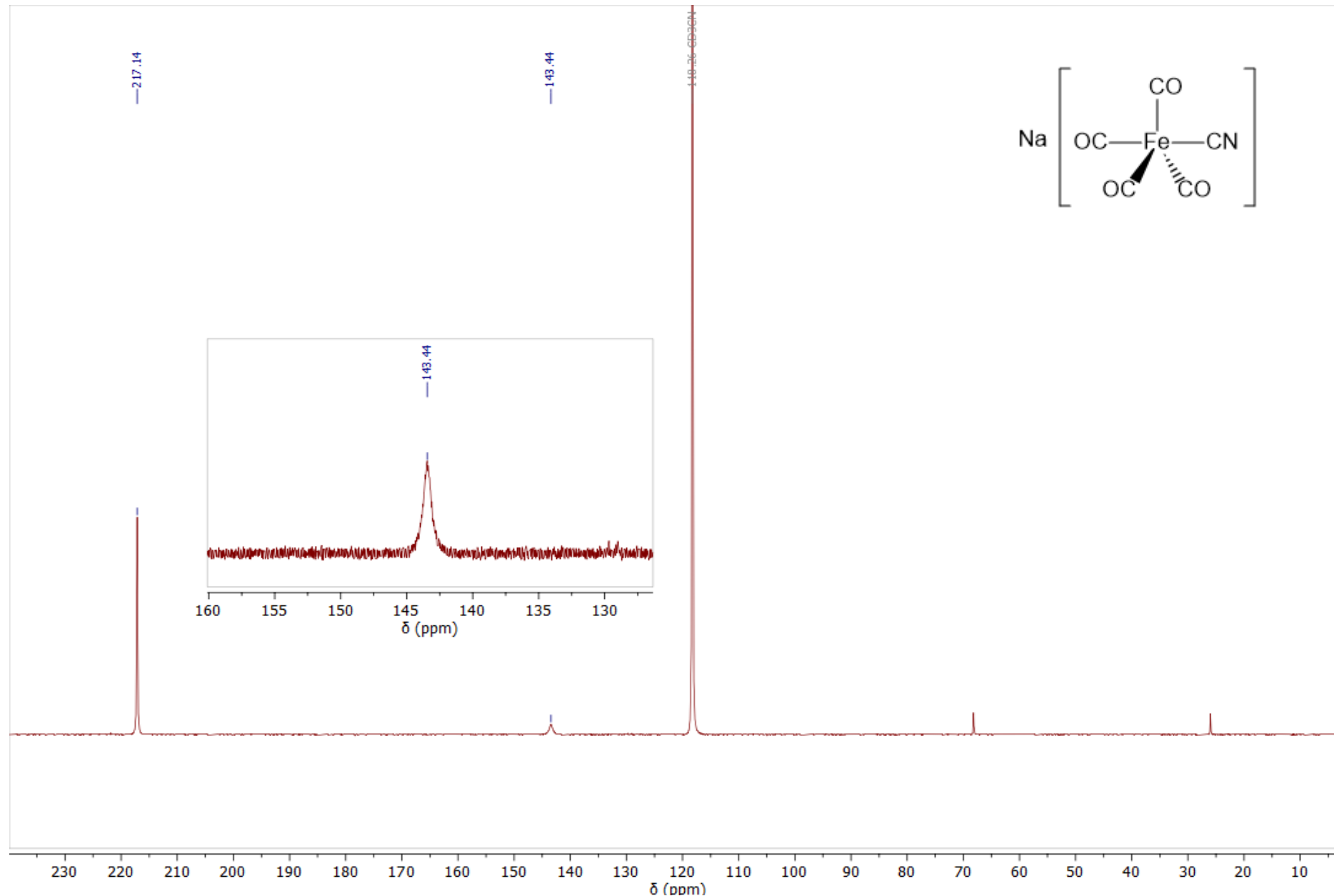
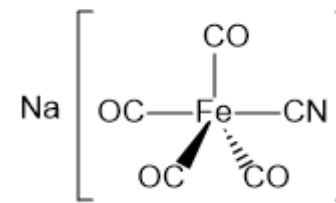
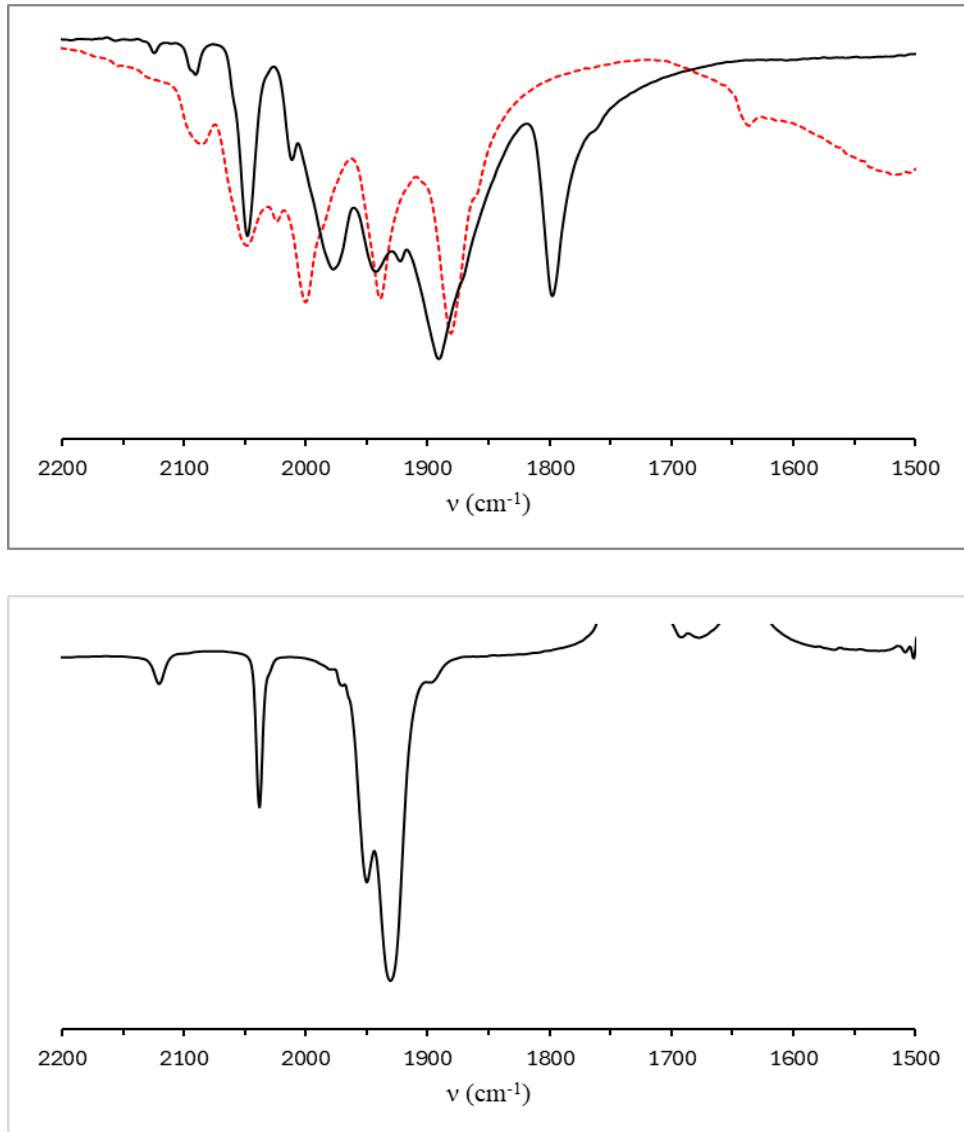
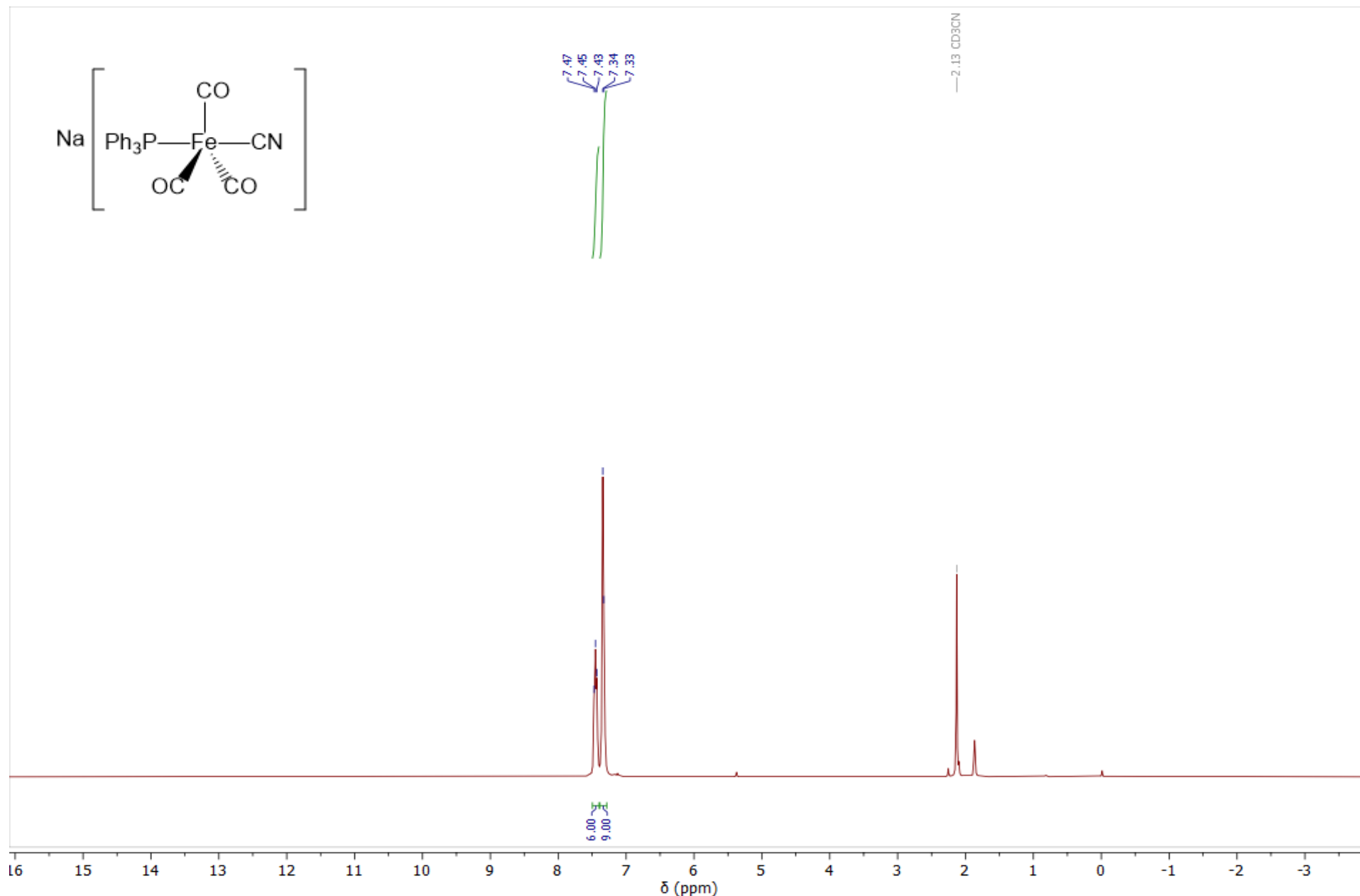


Figure S32: The  $^{13}\text{C}\{^1\text{H}\}$  NMR spectrum of  $\text{Na}[\text{Fe}(\text{CO})_4(\text{CN})]$  ( $\text{CD}_3\text{CN}$ , 201 MHz, 25 °C).



**Figure S33:** The solid state ATR-IR (top) and solution FT-IR (THF; bottom) spectra of  $\text{Na}[\text{Fe}(\text{CN})(\text{CO})_4]$  in the carbonyl region ( $25^\circ\text{C}$ ). A totally clean ATR spectrum could not be acquired due to rapid sample oxidation (hashed red trace:  $\sim 5$  min air exposure).



**Figure S34:** The  $^1\text{H}$  NMR spectrum of  $\text{Na}[\text{Fe}(\text{CN})(\text{CO})_3(\text{PPh}_3)]$  ( $\text{CD}_3\text{CN}$ , 400 MHz, 25 °C).

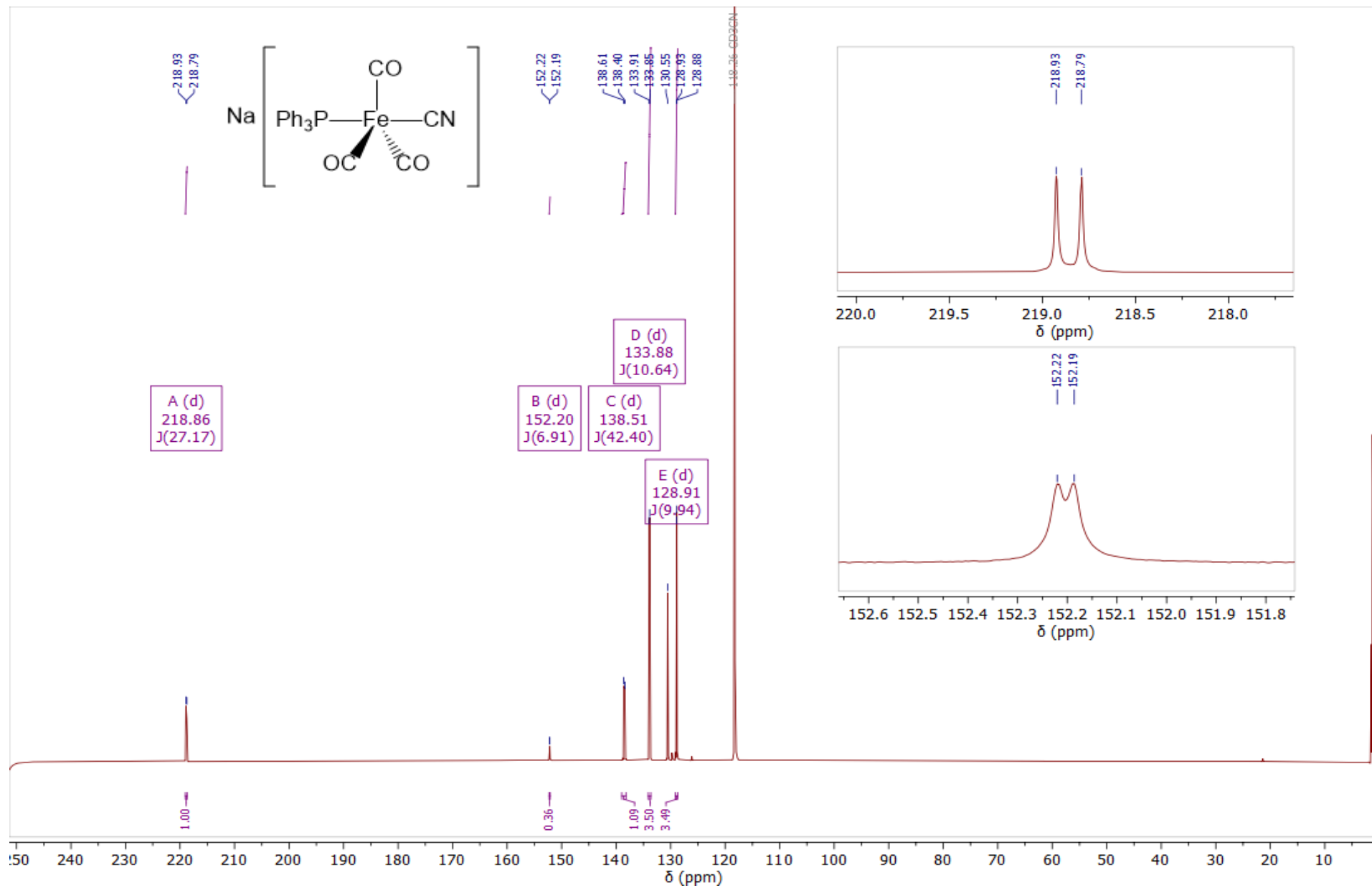


**Figure S35:** The  $^{13}\text{C}\{^1\text{H}\}$  NMR spectrum of  $\text{Na}[\text{Fe}(\text{CN})(\text{CO})_3(\text{PPh}_3)]$  ( $\text{CD}_3\text{CN}$ , 201 MHz, 25 °C).

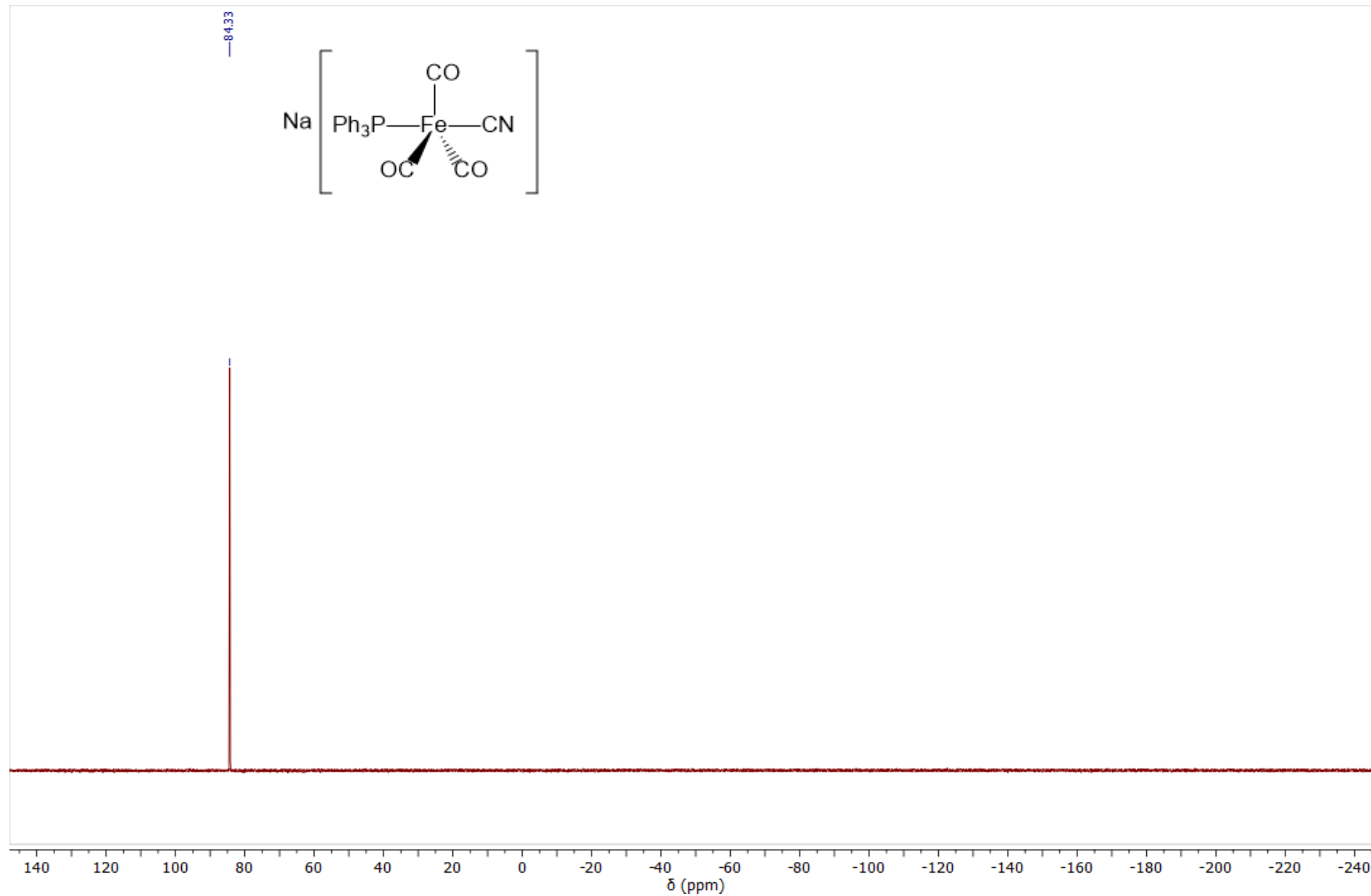


**Figure S36:** The  $^{31}\text{P}\{^1\text{H}\}$  NMR spectrum of  $\text{Na}[\text{Fe}(\text{CN})(\text{CO})_3(\text{PPh}_3)]$  ( $\text{CD}_3\text{CN}$ , 162 MHz, 25 °C).

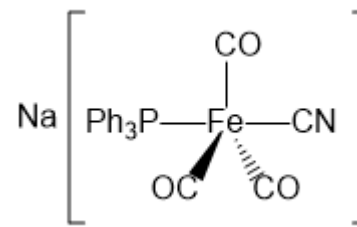
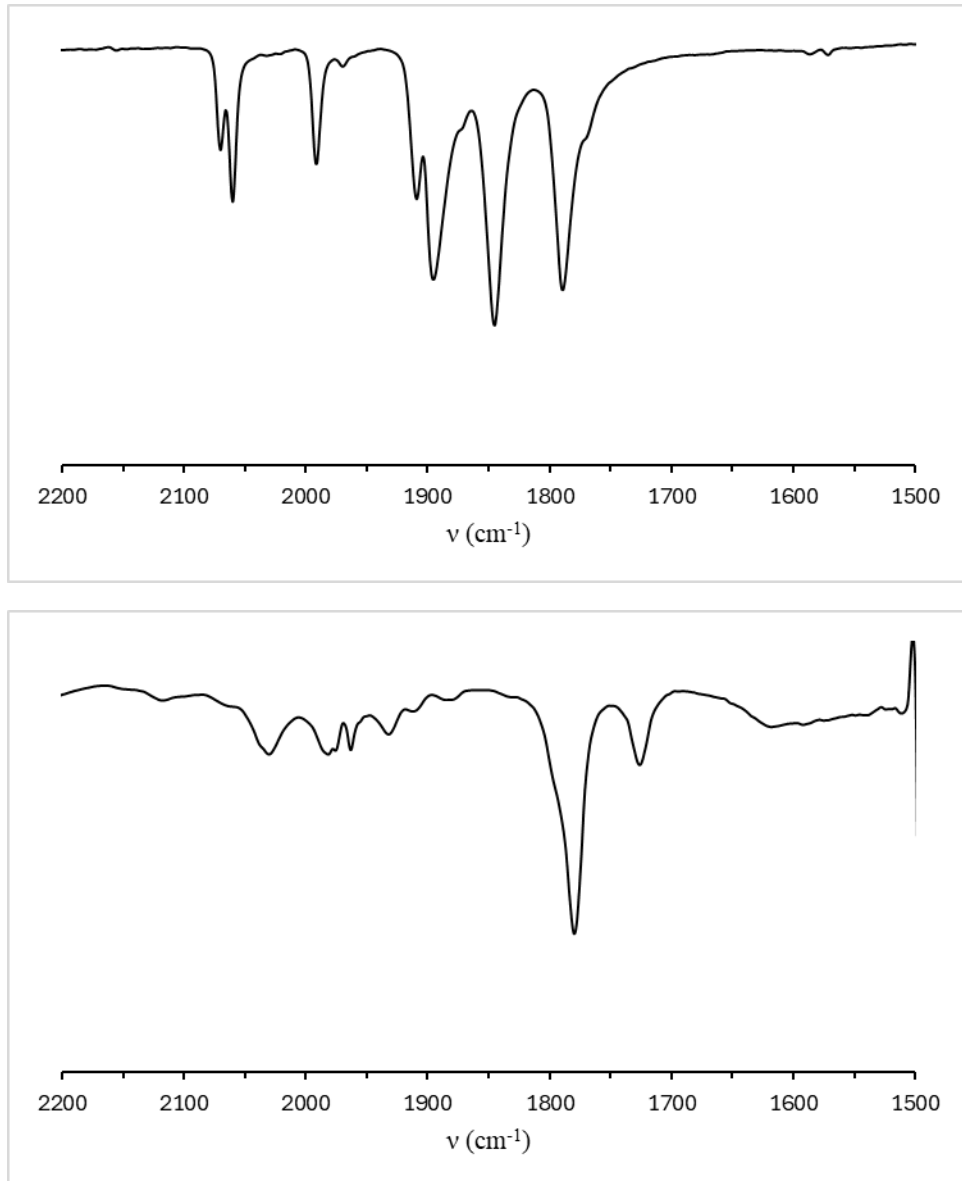


**Figure S37:** The solid state ATR-IR (top) and solution FT-IR (THF; bottom) spectra of  $\text{Na}[\text{Fe}(\text{CN})(\text{CO})_3(\text{PPh}_3)]$  in the carbonyl region ( $25^\circ\text{C}$ ).

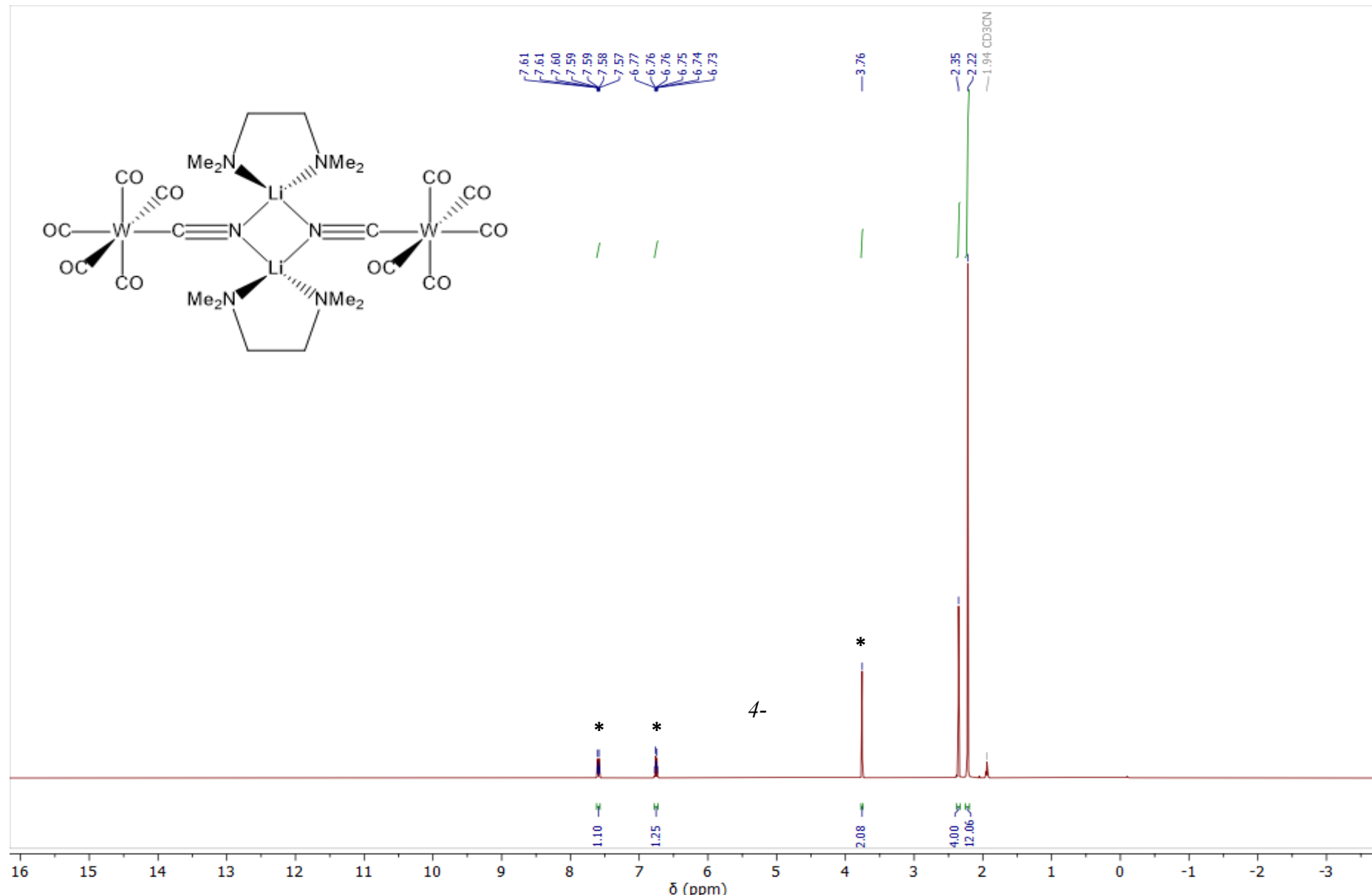


**Figure S38:** The  $^1\text{H}$  NMR spectrum of  $[\text{LiW}(\text{CN})(\text{CO})_5 \cdot \text{TMEDA}]_2$  containing 4-iodoanisole internal standard ( $\text{CD}_3\text{CN}$ , 400 MHz, 25 °C).

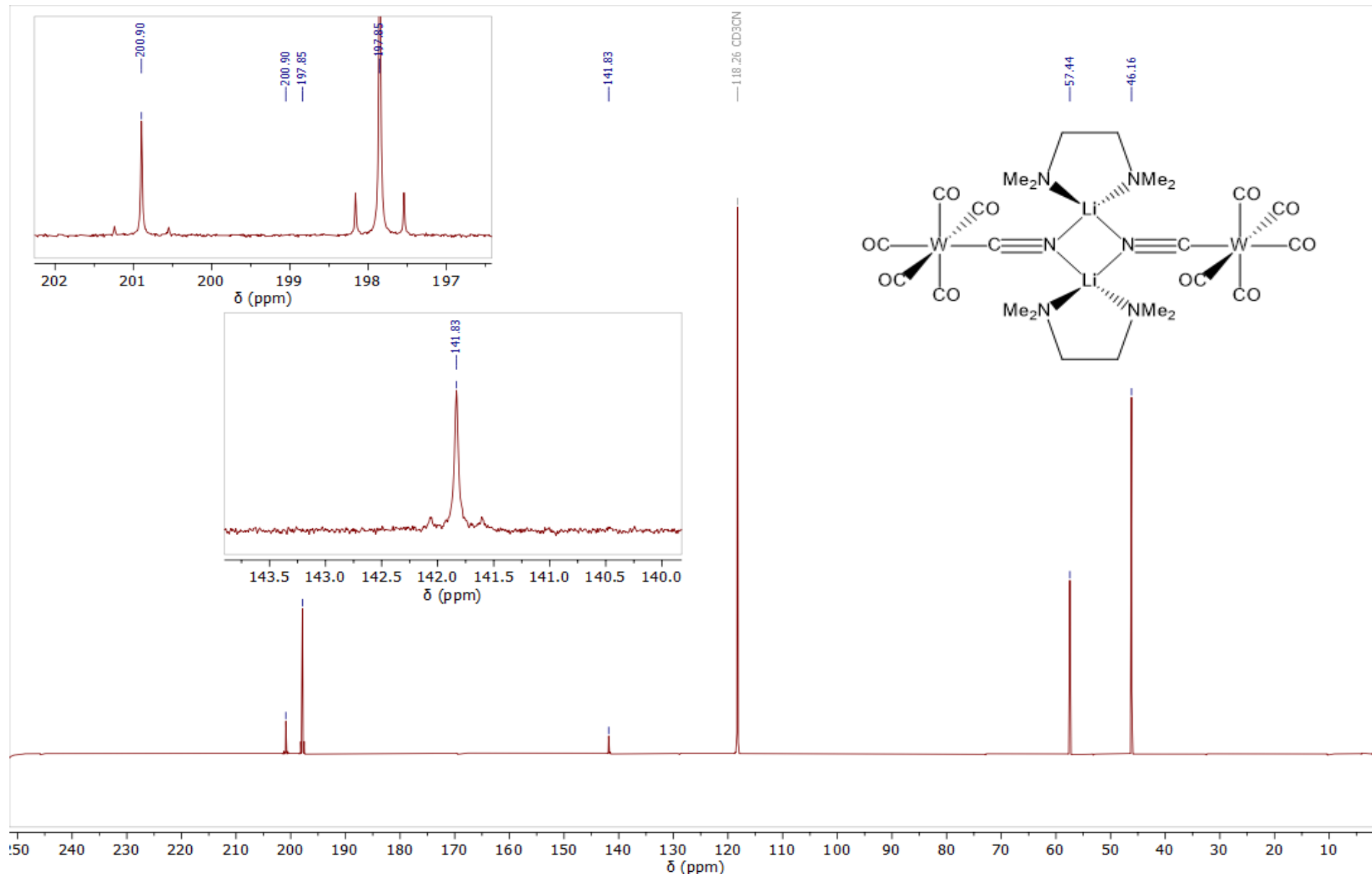


**Figure S39:** The  $^{13}\text{C}\{^1\text{H}\}$  NMR spectrum of  $[\text{LiW}(\text{CN})(\text{CO})_5 \cdot \text{TMEDA}]_2$  ( $\text{CD}_3\text{CN}$ , 201 MHz, 25 °C).

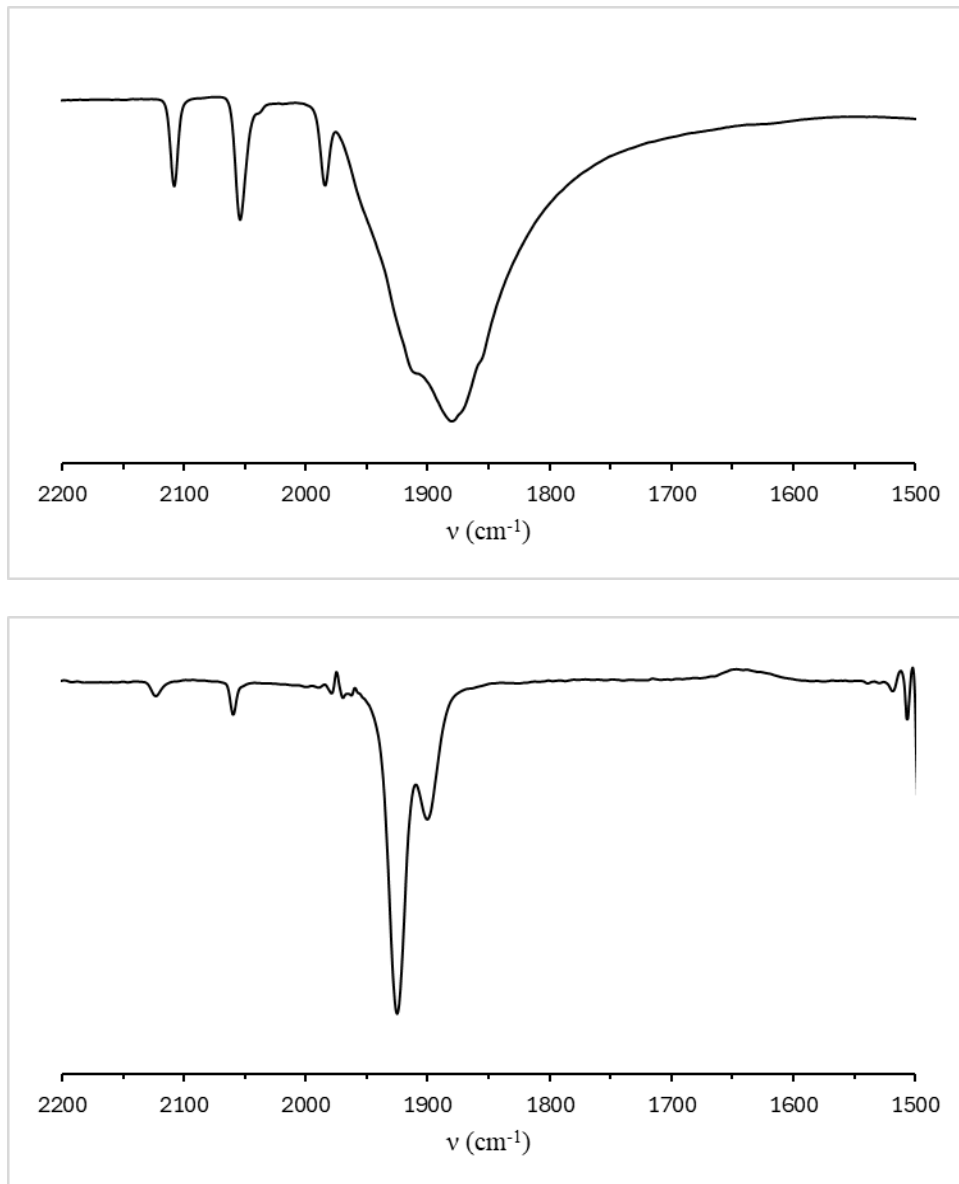


**Figure S40:** The solid state ATR-IR (top) and solution FT-IR (THF; bottom) spectra of  $[\text{LiW}(\text{CN})(\text{CO})_5\text{-TMEDA}]_2$  in the carbonyl region ( $25^\circ\text{C}$ ).

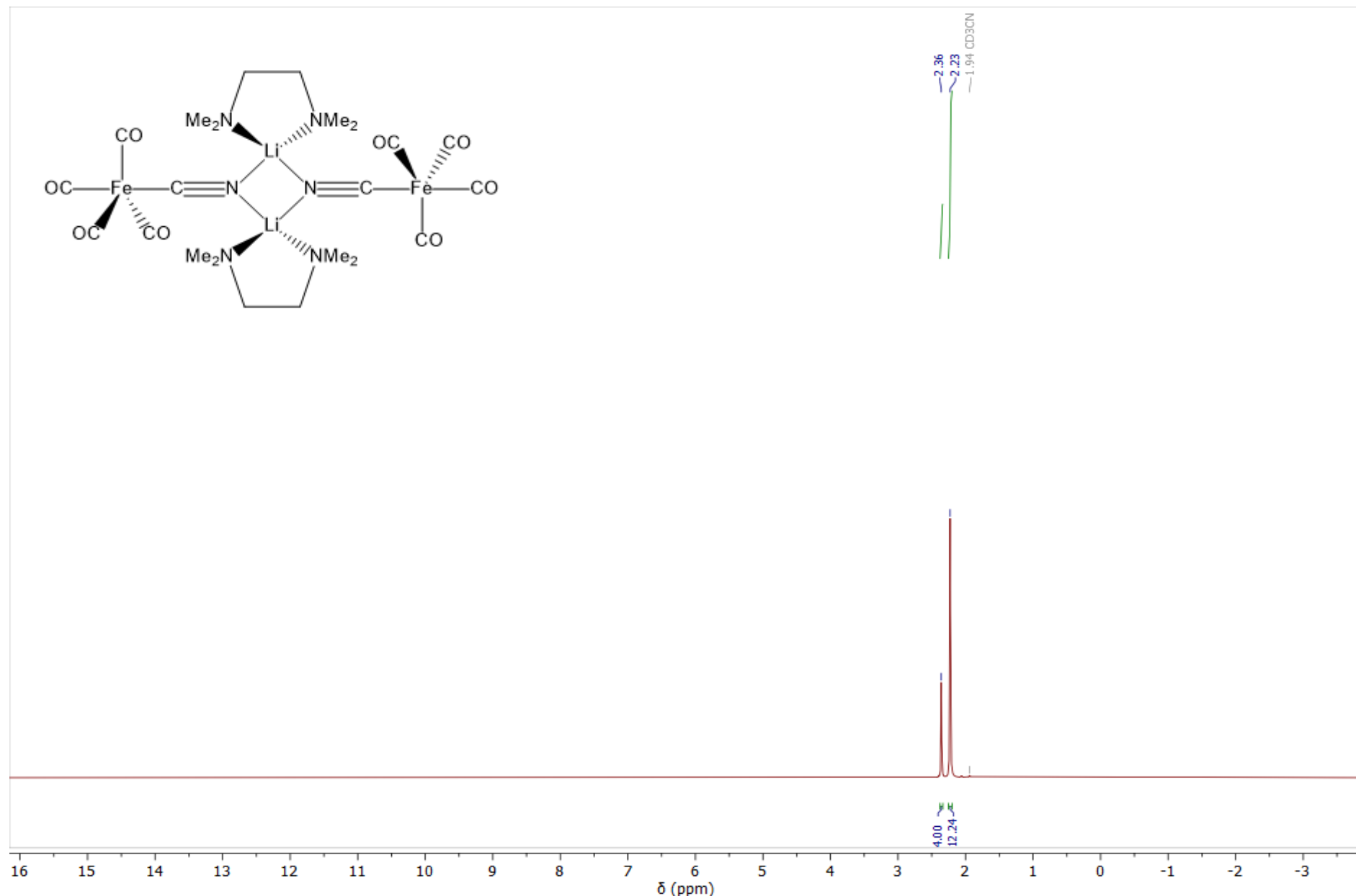


**Figure S41:** The  $^1\text{H}$  NMR spectrum of  $[\text{LiFe}(\text{CN})(\text{CO})_4 \cdot \text{TMEDA}]_2$  ( $\text{CD}_3\text{CN}$ , 400 MHz, 25 °C).

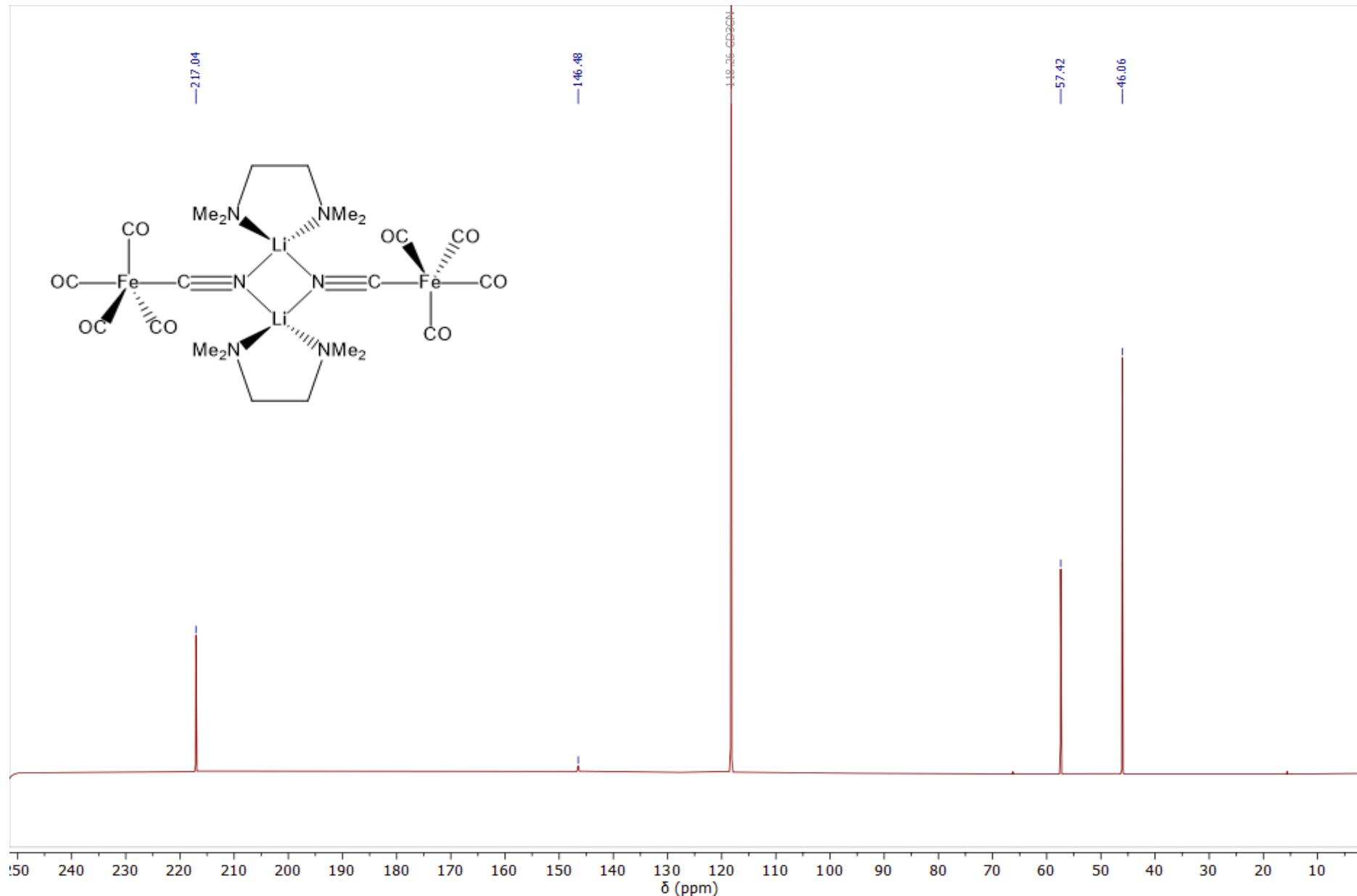
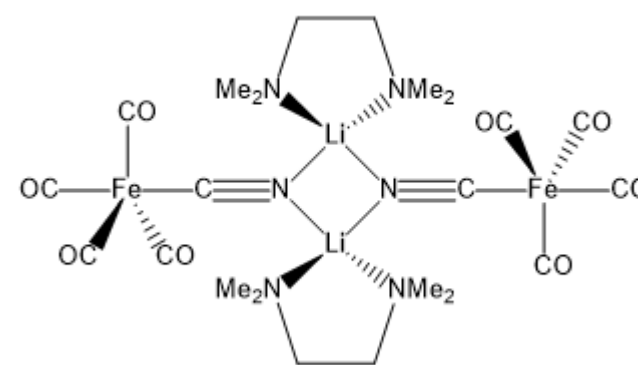
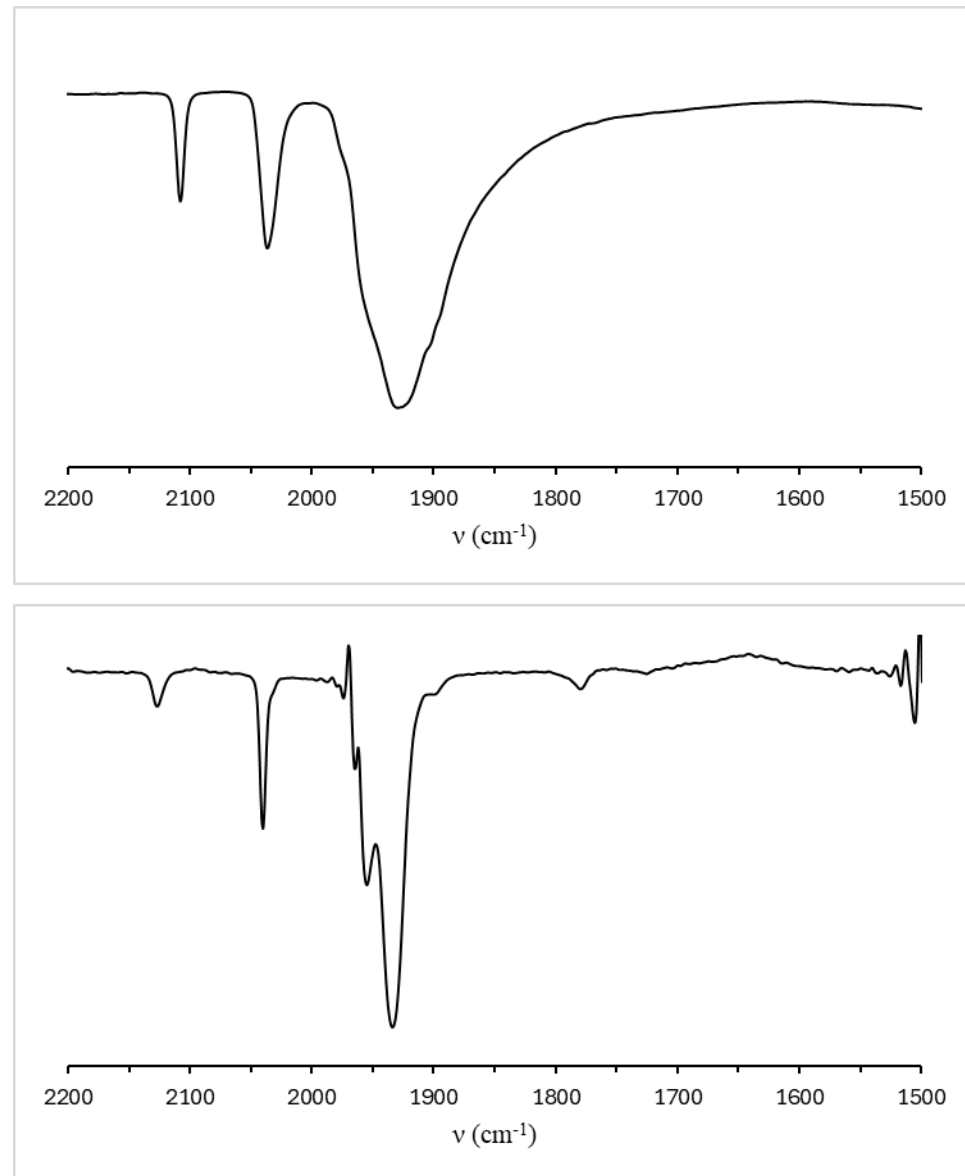


Figure S42: The  $^{13}\text{C}\{^1\text{H}\}$  NMR spectrum of  $[\text{LiFe}(\text{CN})(\text{CO})_4 \cdot \text{TMEDA}]_2$  (CD<sub>3</sub>CN, 201 MHz, 25 °C).



**Figure S43:** The solid state ATR-IR (top) and solution FT-IR (THF; bottom) spectra of  $[\text{LiFe}(\text{CN})(\text{CO})_4]\cdot\text{TMEDA}$  in the carbonyl region (25 °C).

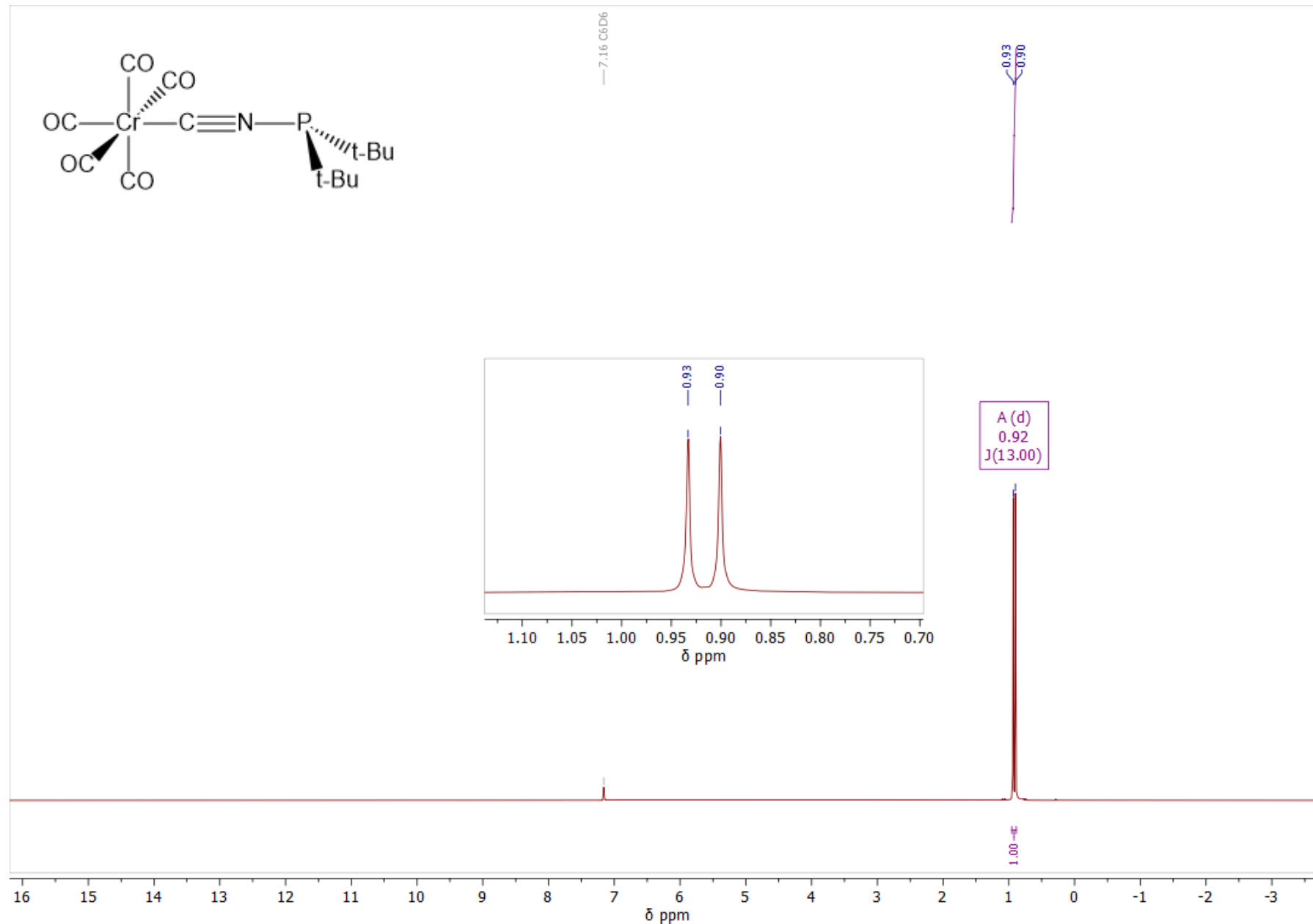
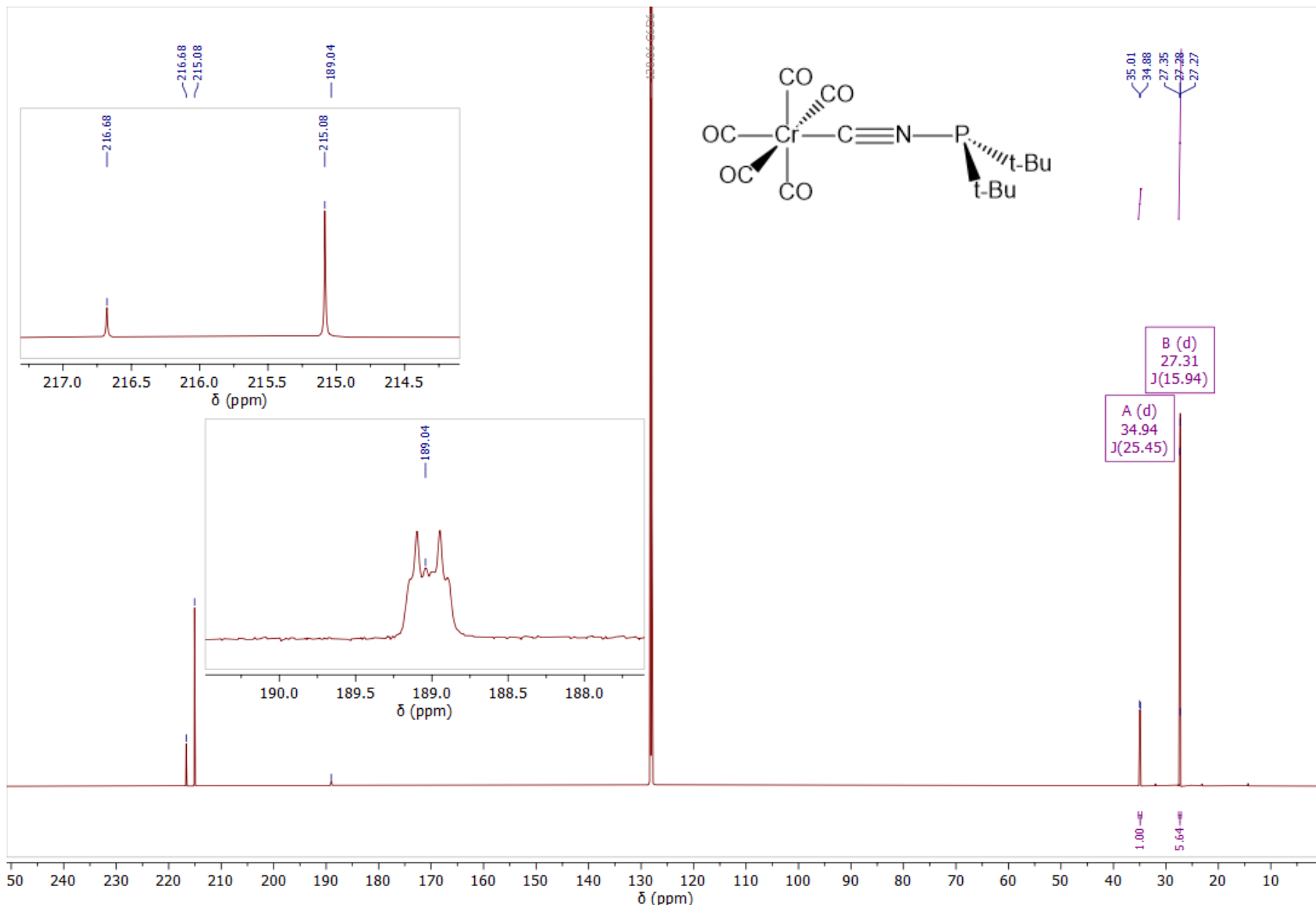


Figure S44: The  $^1\text{H}$  NMR spectrum of  $[\text{Cr}(\text{CNP}^{\text{t}}\text{Bu}_2)(\text{CO})_5]$  ( $\text{C}_6\text{D}_6$ , 400 MHz, 25 °C).

## ELECTRONIC SUPPORTING INFORMATION



**Figure S45:** The  $^{13}\text{C}\{^1\text{H}\}$  NMR spectrum of  $[\text{Cr}(\text{CN}^{\text{t}}\text{Bu}_2)(\text{CO})_5]$  ( $\text{C}_6\text{D}_6$ , 201 MHz, 25 °C).

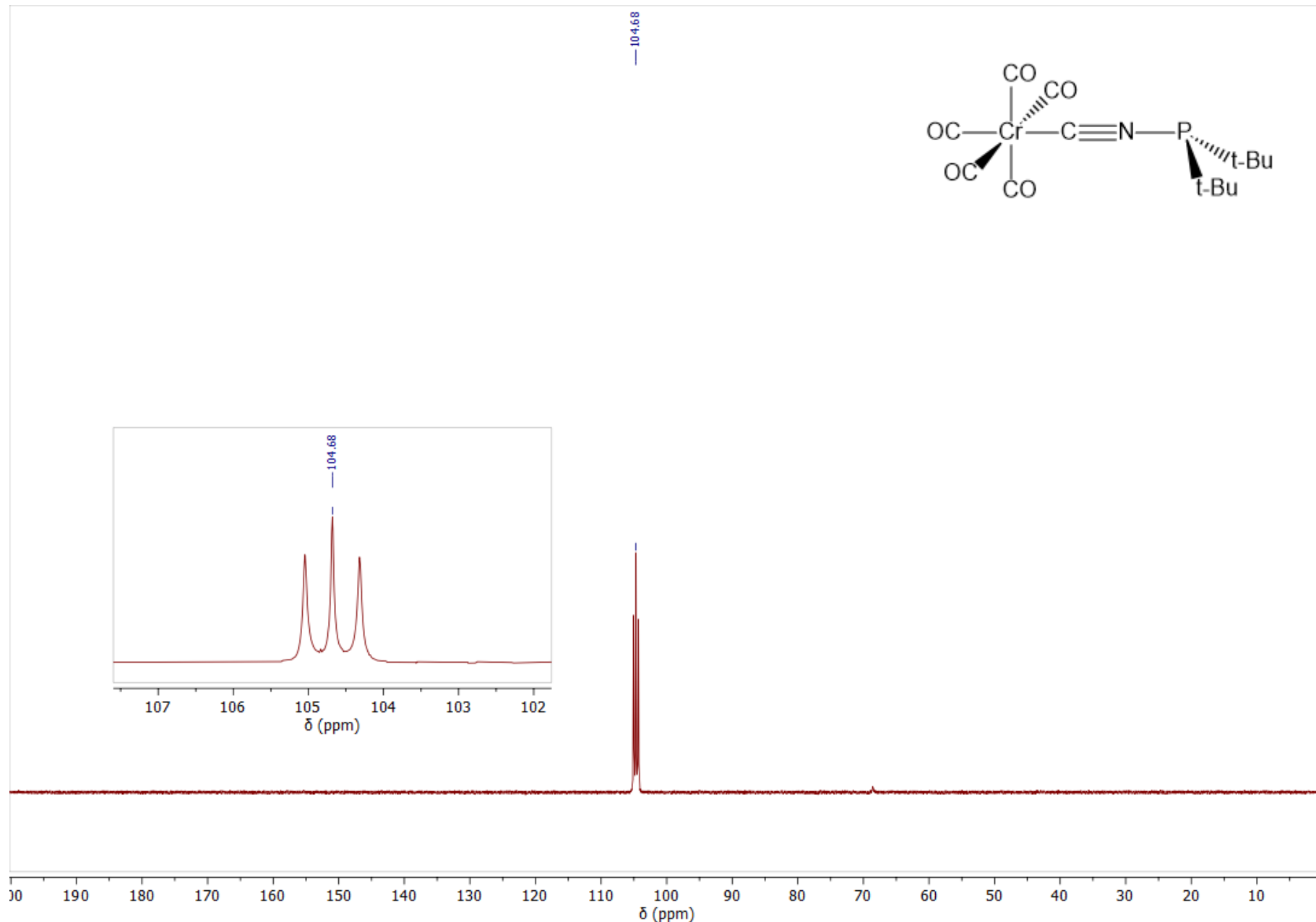
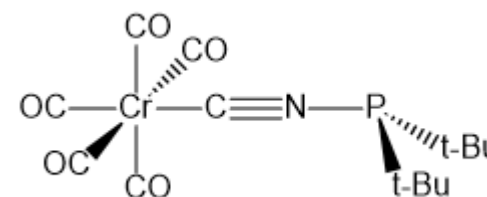
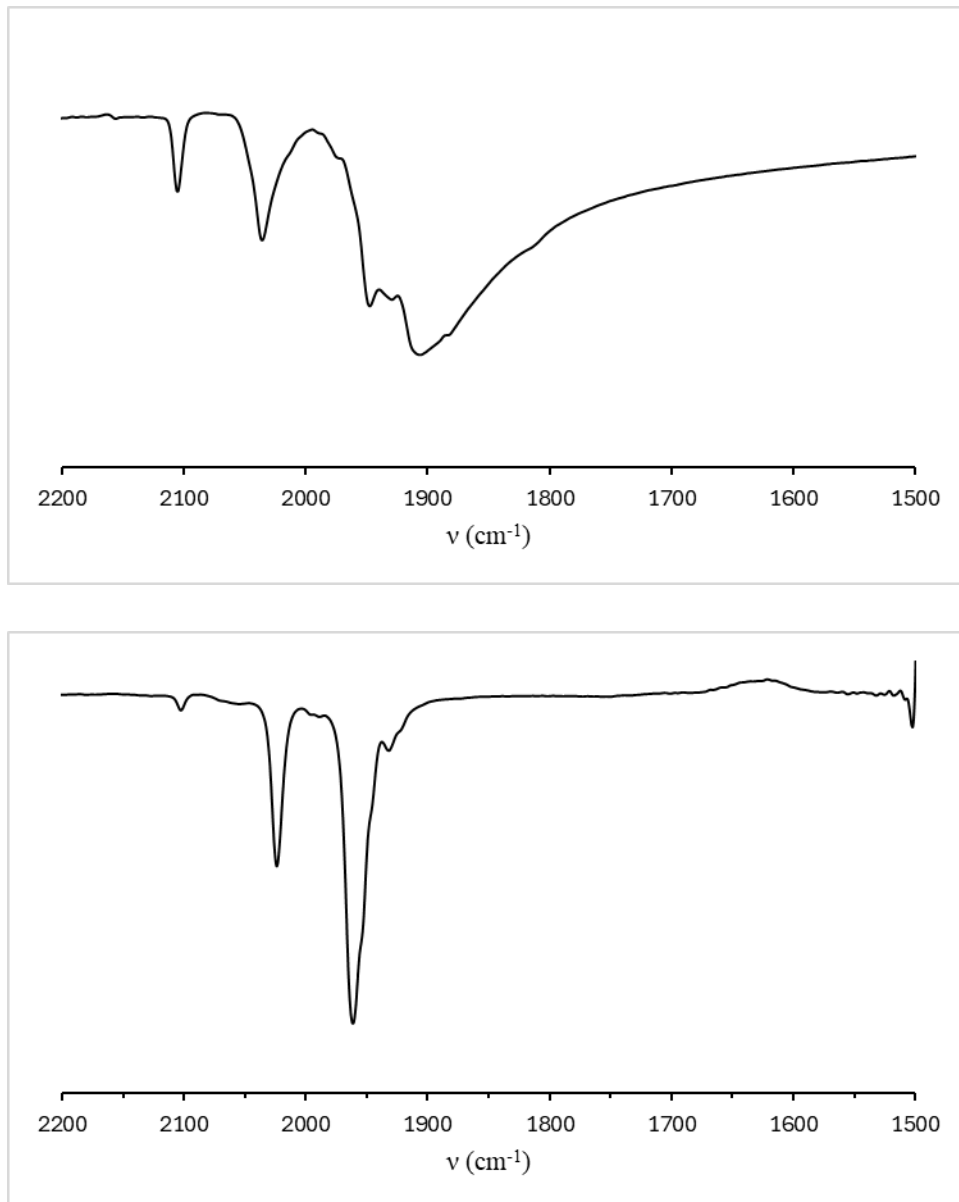
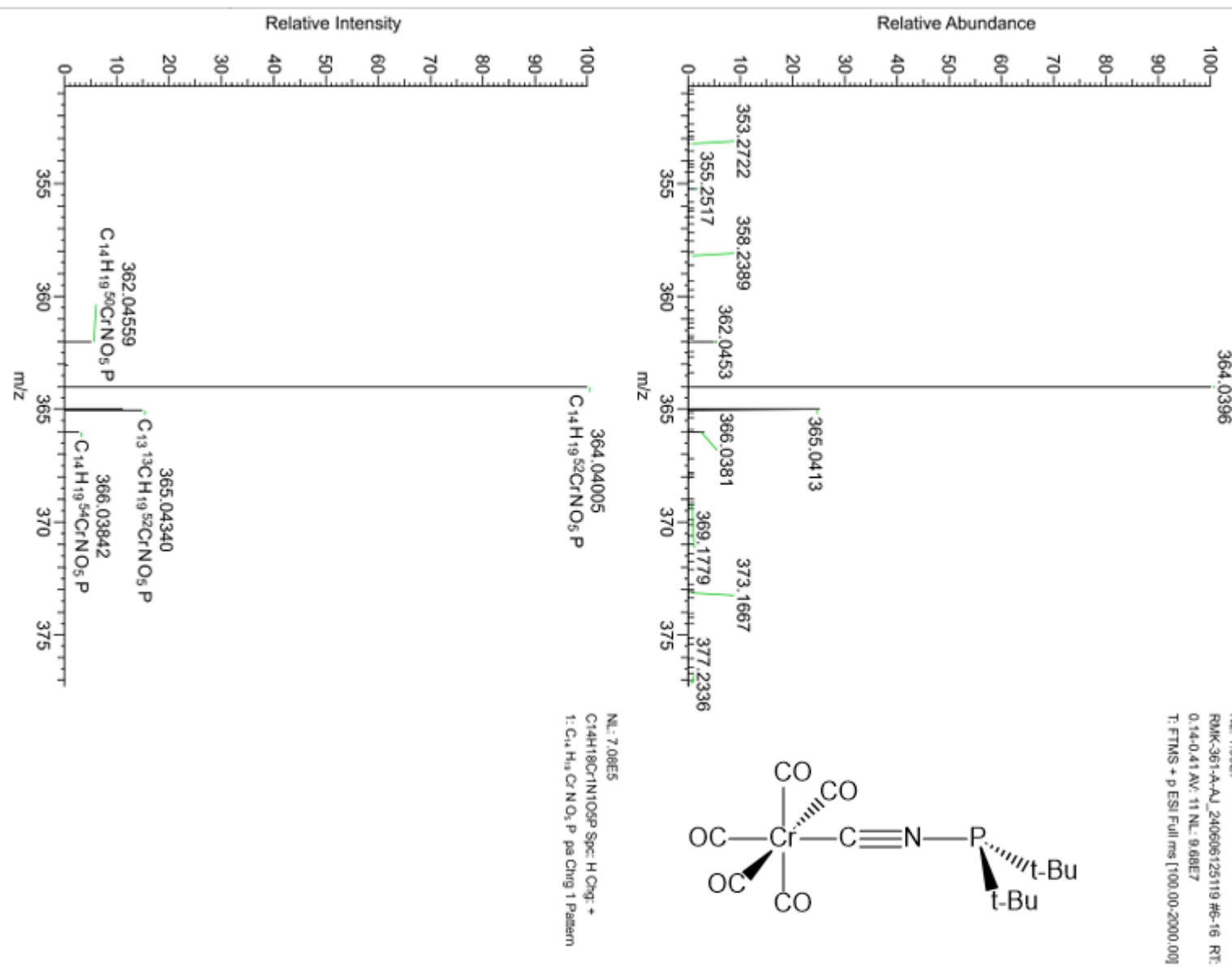


Figure S46: The  $^{31}\text{P}\{^1\text{H}\}$  NMR spectrum of  $[\text{Cr}(\text{CNP}^{\text{t}}\text{Bu}_2)(\text{CO})_5]$  ( $\text{C}_6\text{D}_6$ , 162 MHz, 25 °C).



**Figure S47:** The solid state ATR-IR (top) and solution FT-IR (*n*-hexane; bottom) spectra of  $[\text{Cr}(\text{CNP}^{\text{t}}\text{Bu}_2)(\text{CO})_5]$  in the carbonyl region (25 °C).



**Figure S48:** The HR-MS of  $[\text{Cr}(\text{CNP}^t\text{Bu}_2)(\text{CO})_5]$  (ESI, positive ion mode, MeCN).

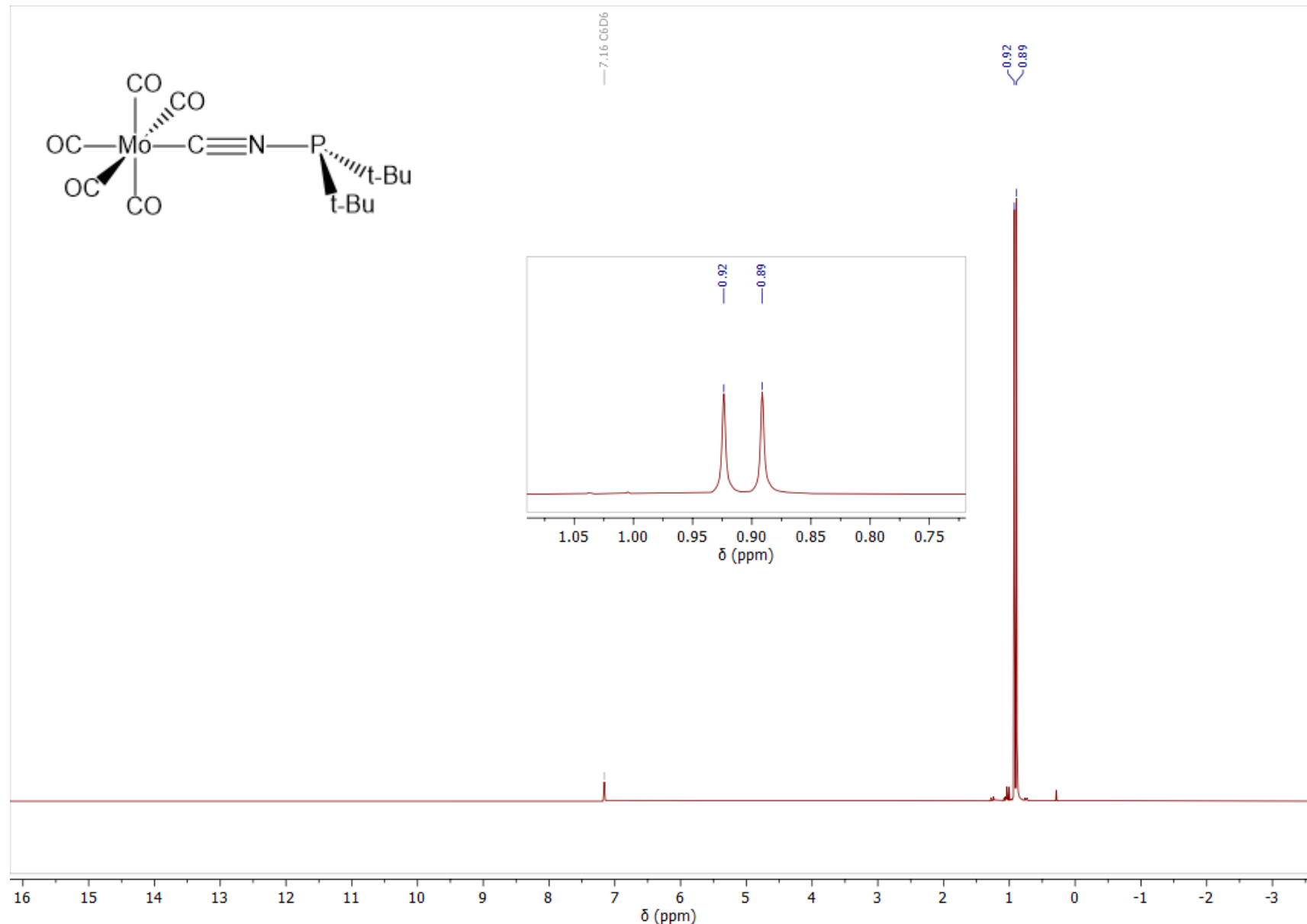


**Figure S49:** The <sup>1</sup>H NMR spectrum of  $[\text{Mo}(\text{CNP}^{\text{t-Bu}}_2)(\text{CO})_5]$  ( $\text{C}_6\text{D}_6$ , 400 MHz, 25 °C).

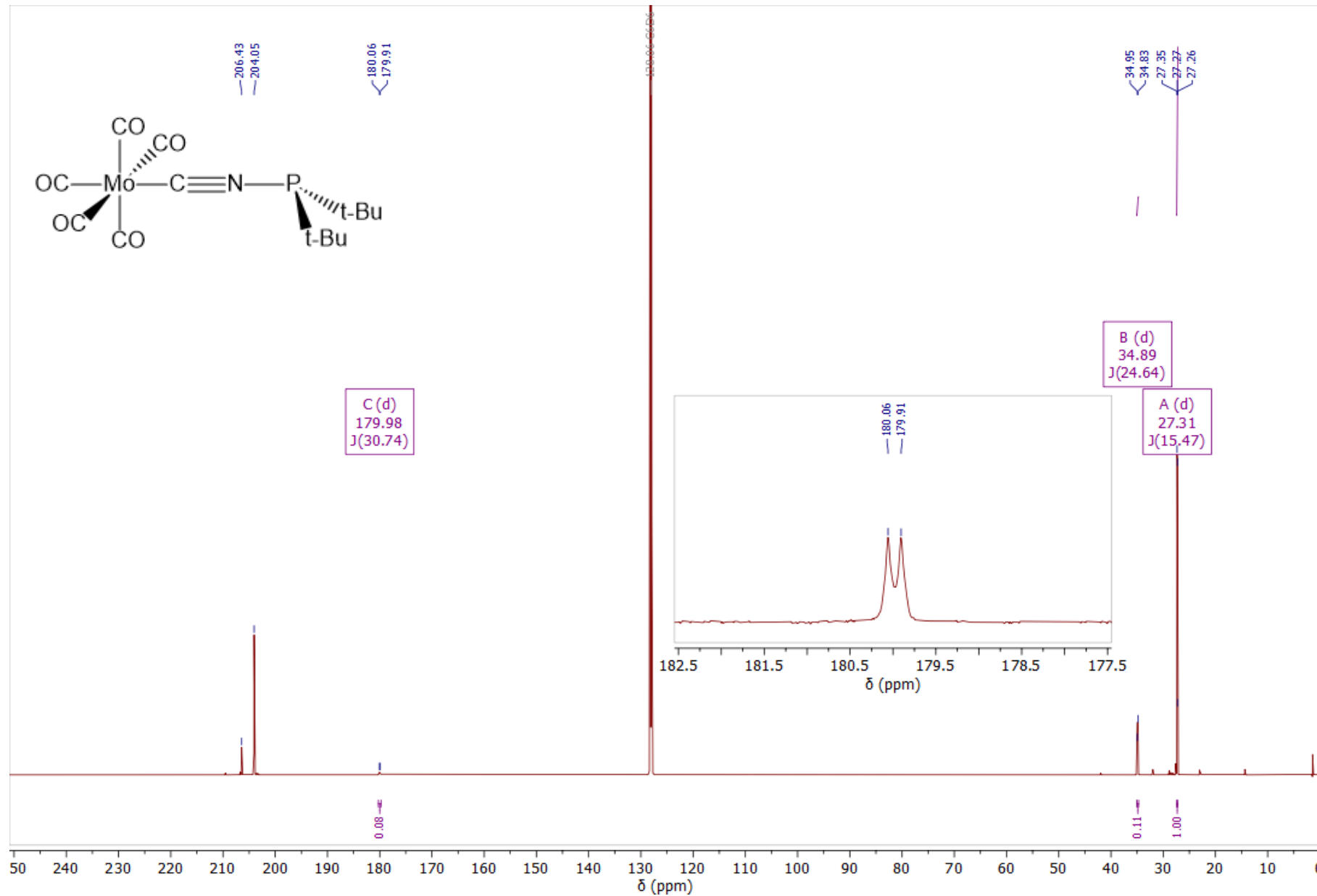
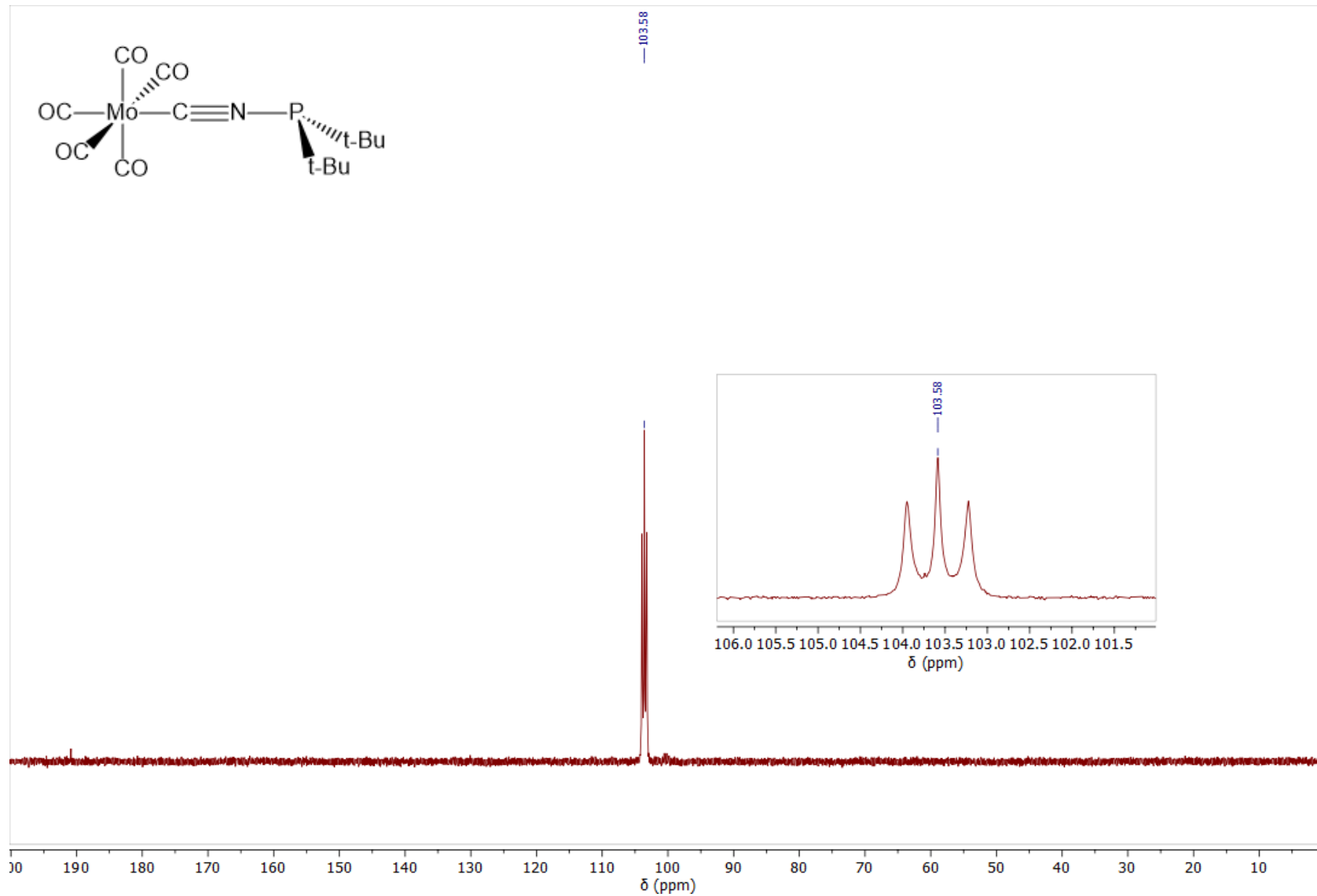
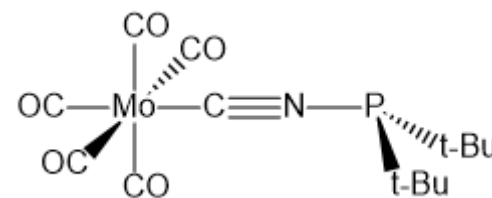
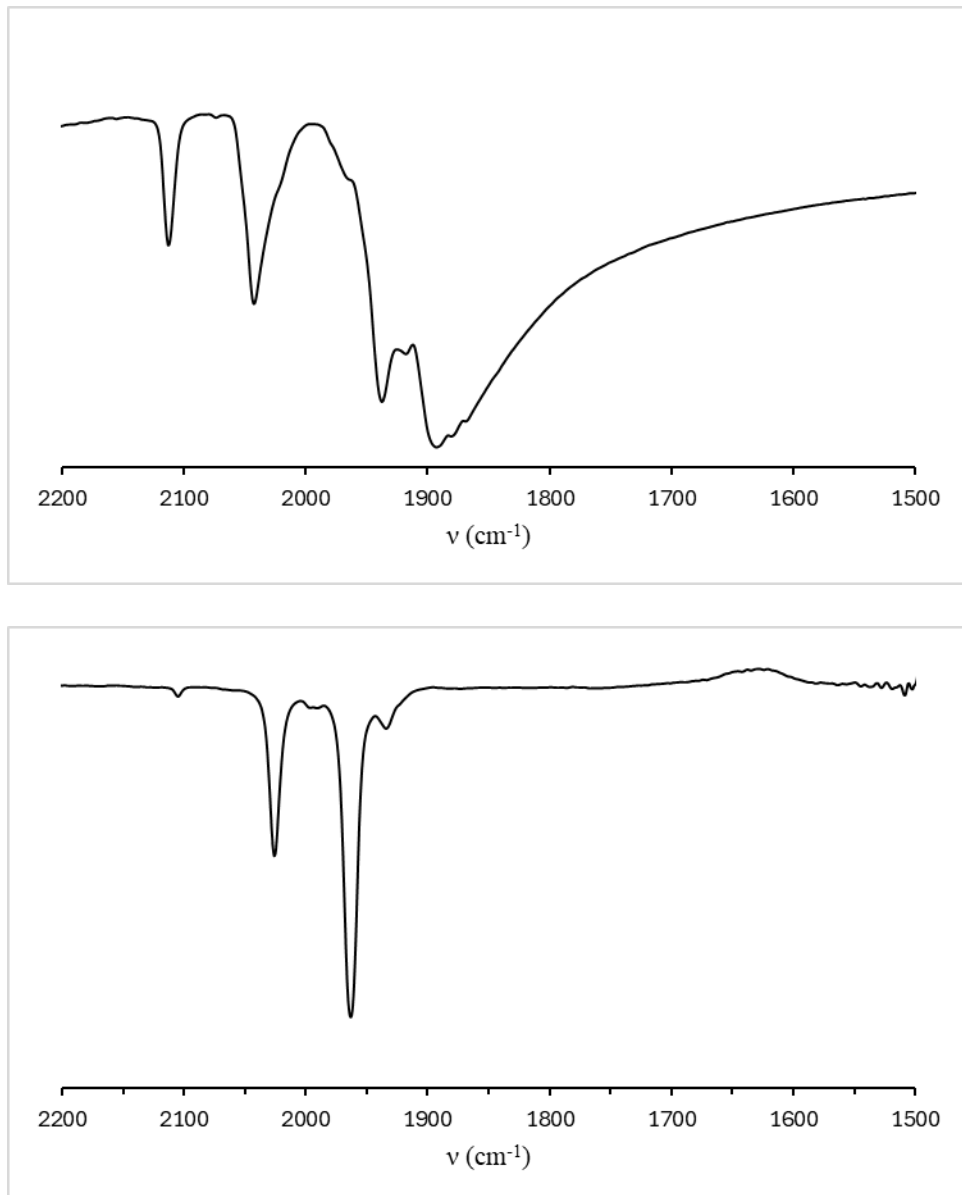


Figure S50: The  $^{13}\text{C}\{^1\text{H}\}$  NMR spectrum of  $[\text{Mo}(\text{CNP}^{\text{t}}\text{Bu}_2)(\text{CO})_5]$  ( $\text{C}_6\text{D}_6$ , 201 MHz, 25 °C).



**Figure S51:** The  $^{31}\text{P}\{^1\text{H}\}$  NMR spectrum of  $[\text{Mo}(\text{CNP}^{\text{t-Bu}}_2)(\text{CO})_5]$  ( $\text{C}_6\text{D}_6$ , 162 MHz, 25 °C).



**Figure S52:** The solid state ATR-IR (top) and solution FT-IR (*n*-hexane; bottom) spectra of  $[\text{Mo}(\text{CNP}^{\text{t-Bu}}_2)(\text{CO})_5]$  in the carbonyl region (25 °C).

# ELECTRONIC SUPPORTING INFORMATION

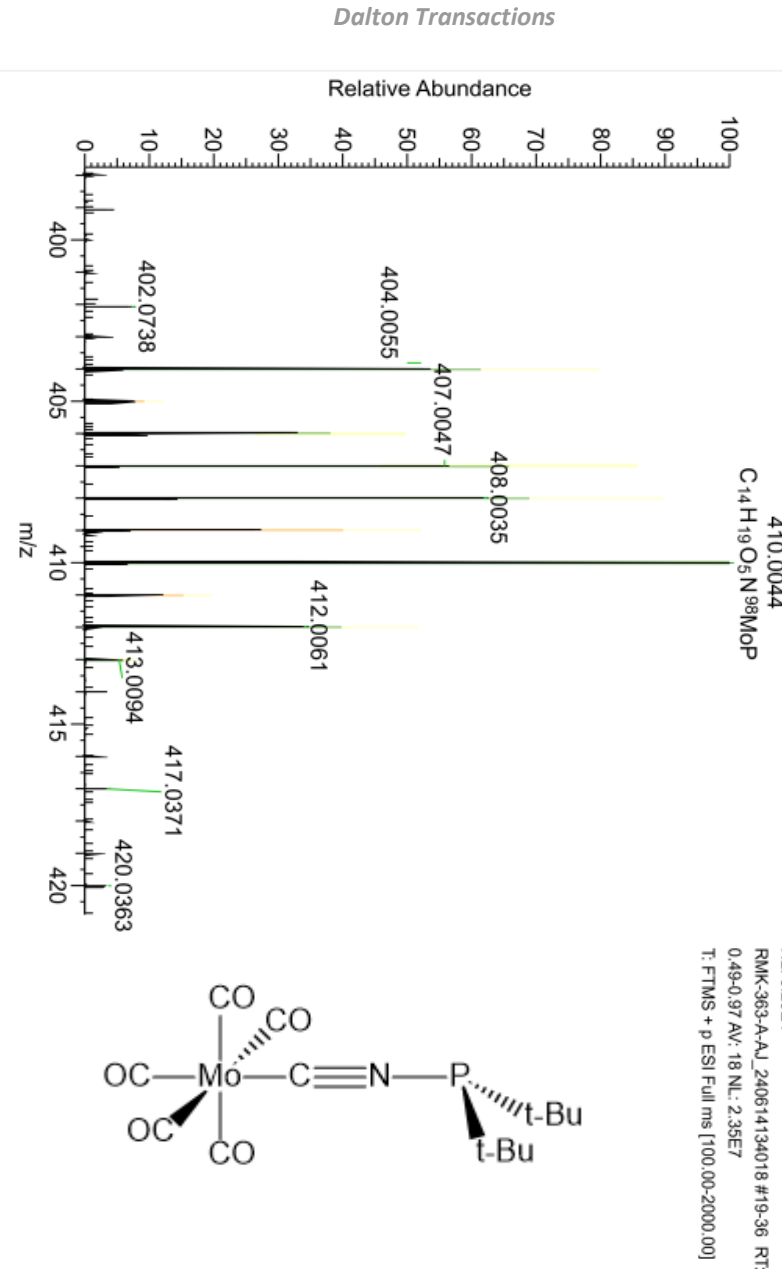
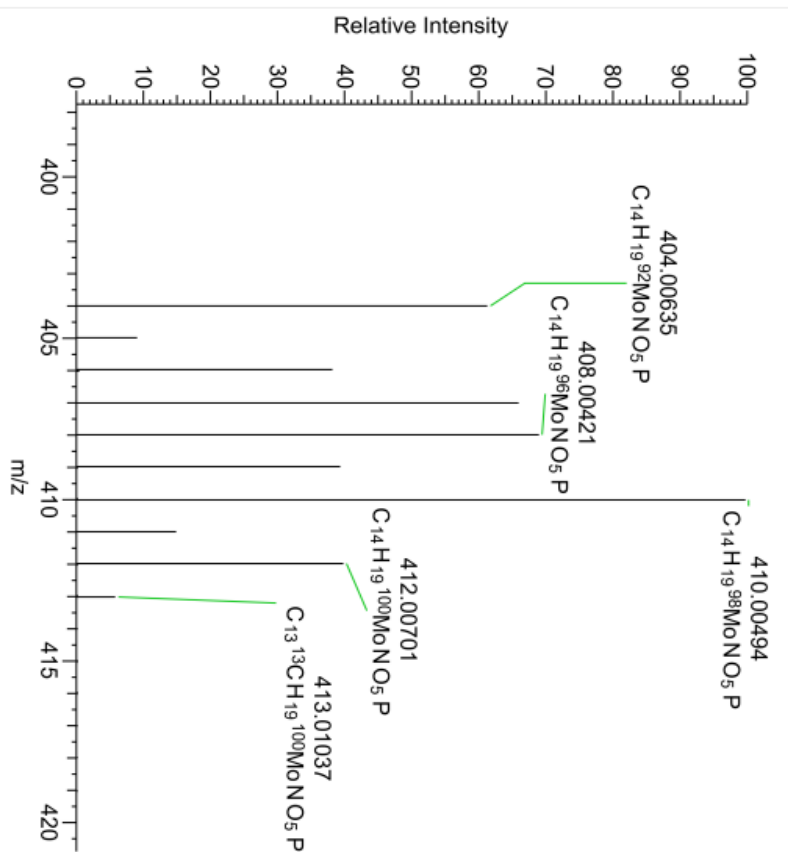


**Figure S53:** The HR-MS of  $[\text{Mo}(\text{CNP}^t\text{Bu}_2)(\text{CO})_5]$  (ESI, positive ion mode, MeCN).

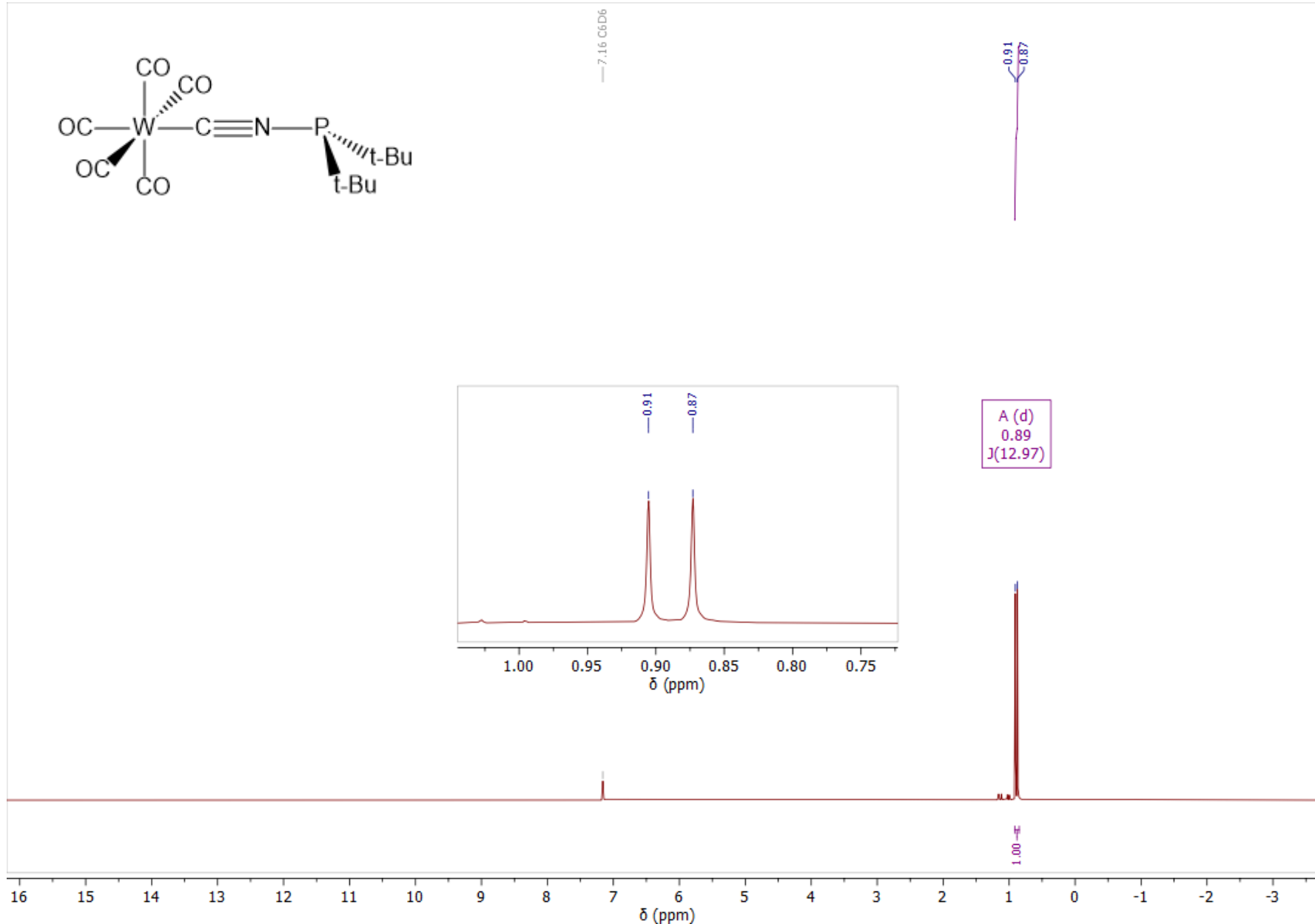


**Figure S54:** The  $^1\text{H}$  NMR spectrum of  $[W(CNPr^tBu_2)(CO)_5]$  ( $\text{C}_6\text{D}_6$ , 400 MHz, 25 °C).

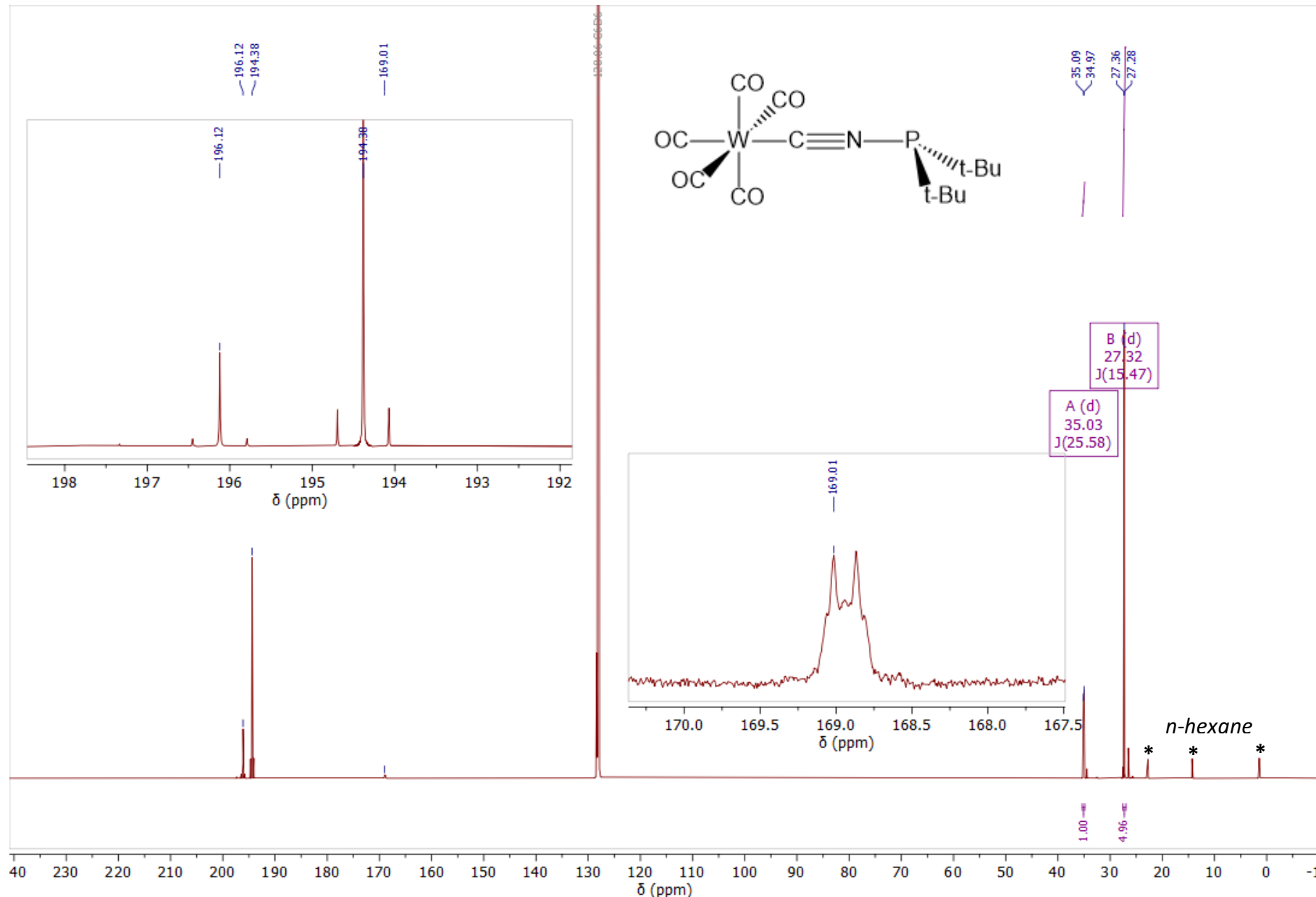


**Figure S55:** The  $^{13}\text{C}\{^1\text{H}\}$  NMR spectrum of  $[\text{W}(\text{CNP}^t\text{Bu}_2)(\text{CO})_5]$  ( $\text{C}_6\text{D}_6$ , 201 MHz, 25 °C).

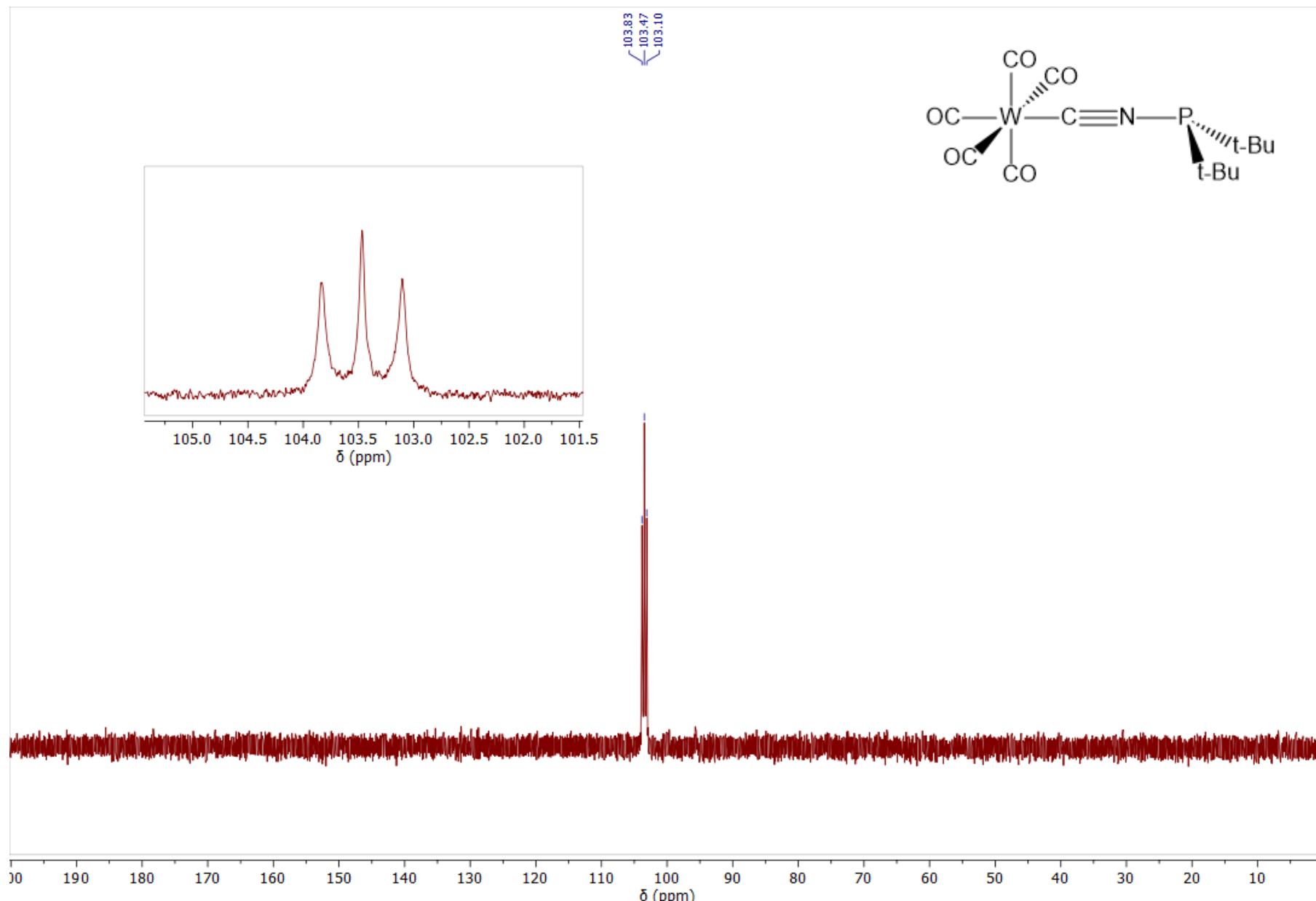


**Figure S56:** The  $^{31}\text{P}\{^1\text{H}\}$  NMR spectrum of  $[\text{W}(\text{CNPr}_2)(\text{CO})_5]$  ( $\text{C}_6\text{D}_6$ , 162 MHz, 25 °C).

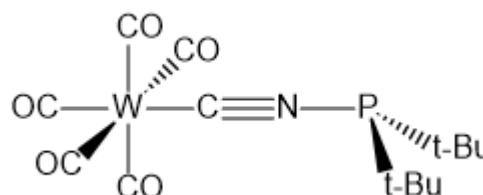
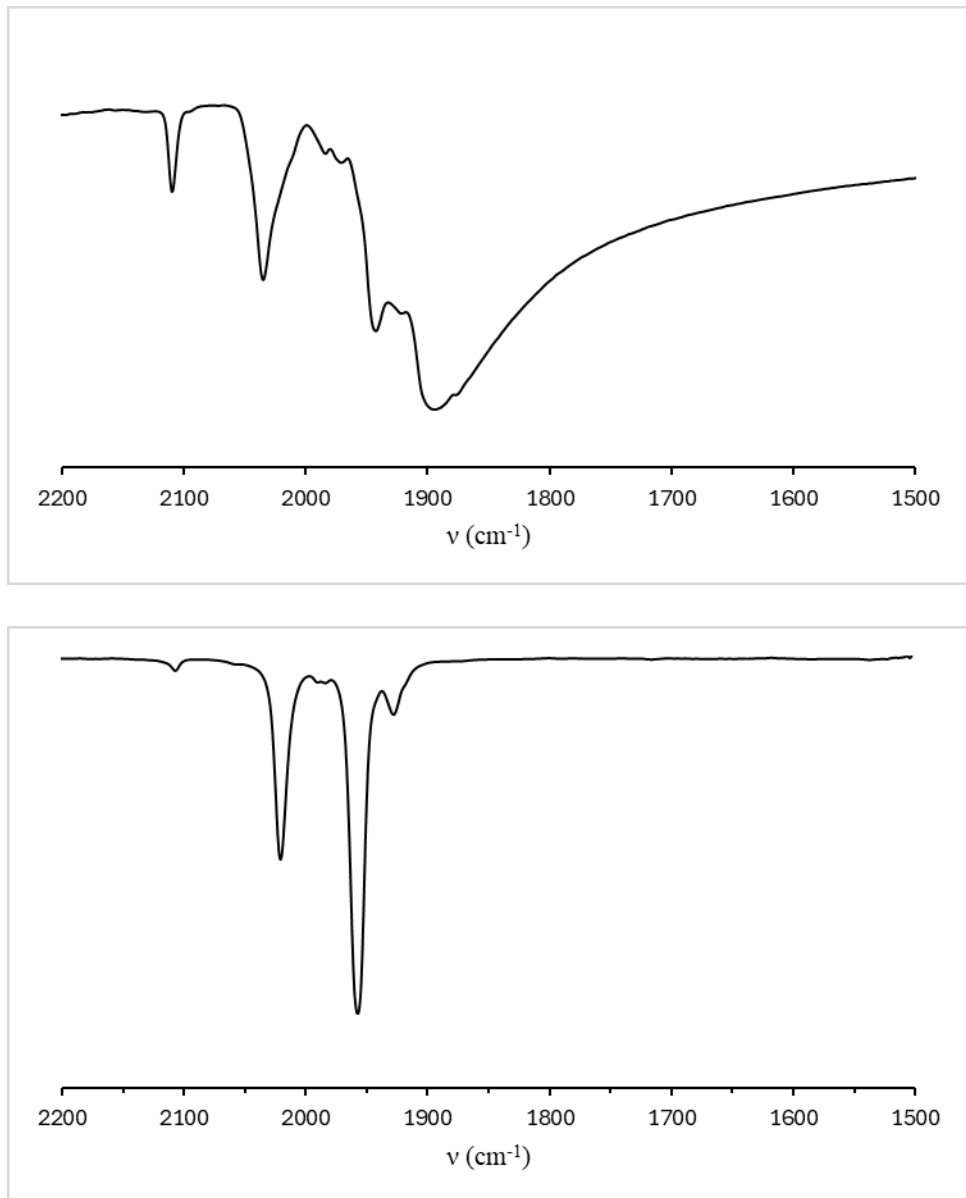


**Figure S57:** The solid state ATR-IR (top) and solution FT-IR (*n*-hexane; bottom) spectra of  $[W(CN{P}^t{B}u_2)(CO)_5]$  in the carbonyl region (25 °C).

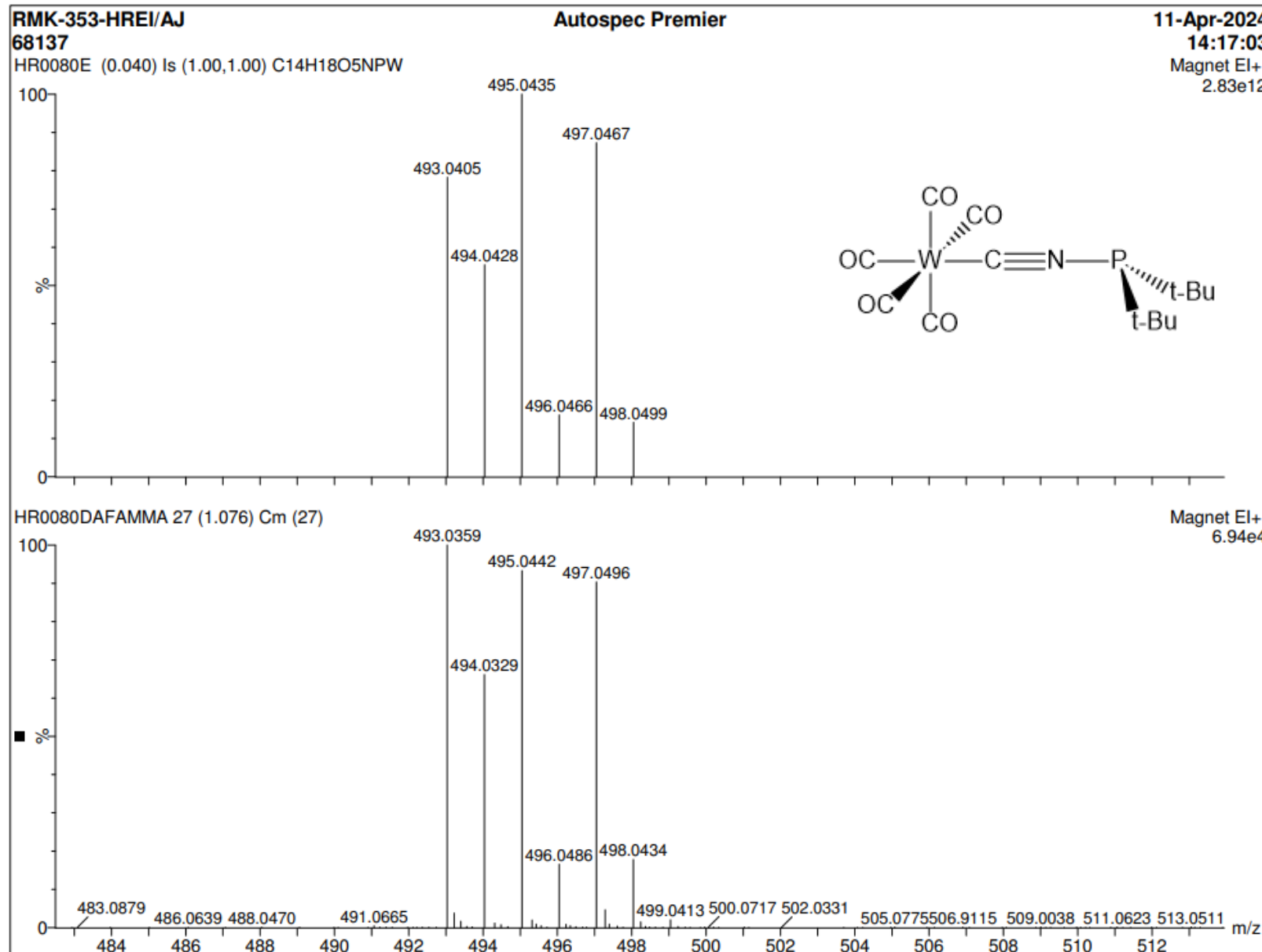


**Figure S58:** The HR-MS of  $[W(CNPr_2)(CO)_5]$  (EI, positive ion mode, MeCN).

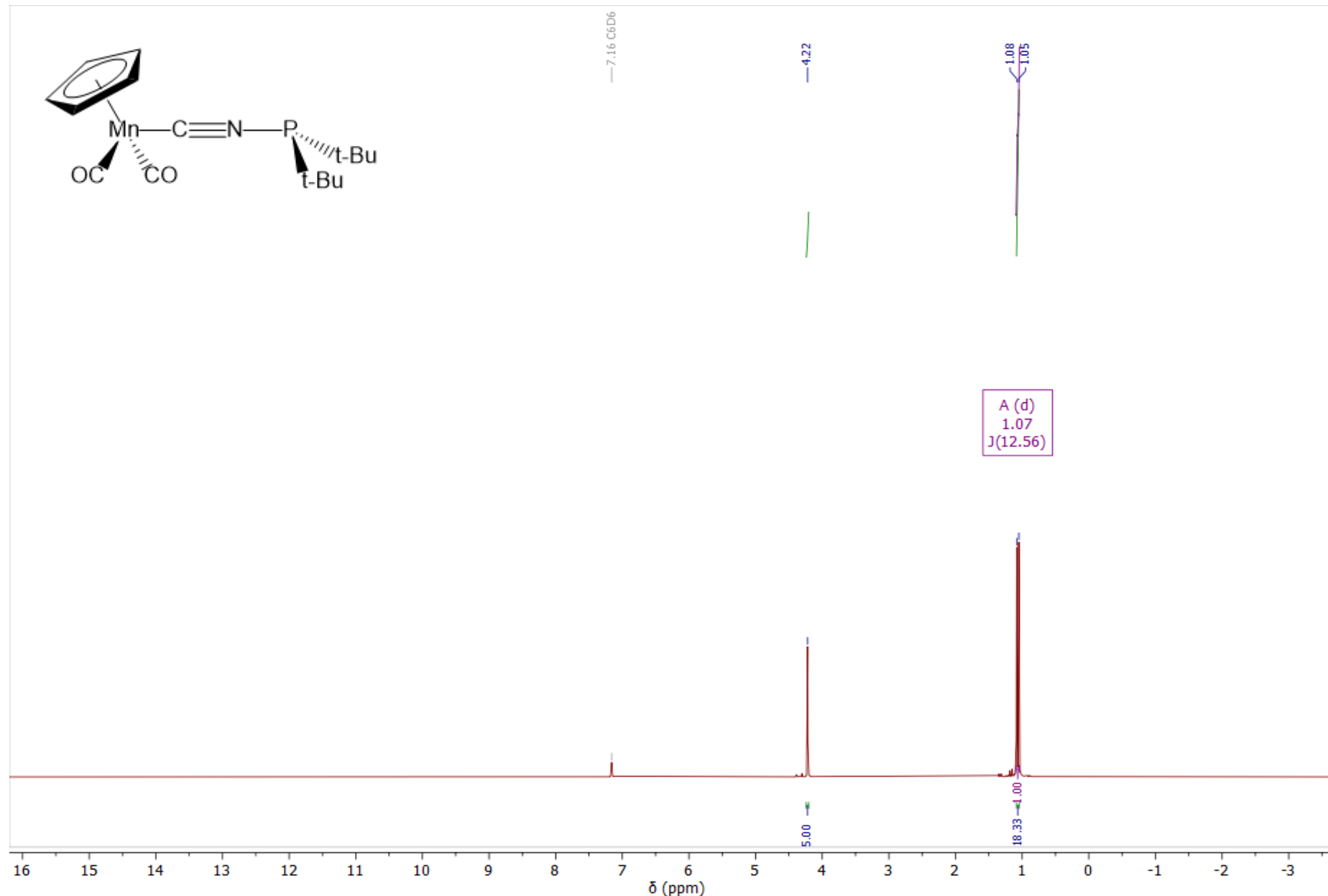
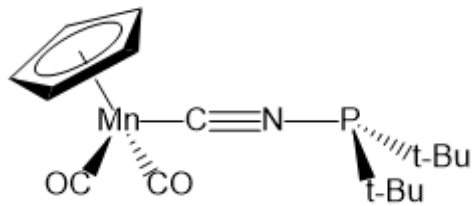


**Figure S59:** The  $^1\text{H}$  NMR spectrum of  $[\text{Mn}(\text{CNP}^t\text{Bu}_2)(\text{CO})_2\text{Cp}]$  ( $\text{C}_6\text{D}_6$ , 400 MHz, 25 °C).

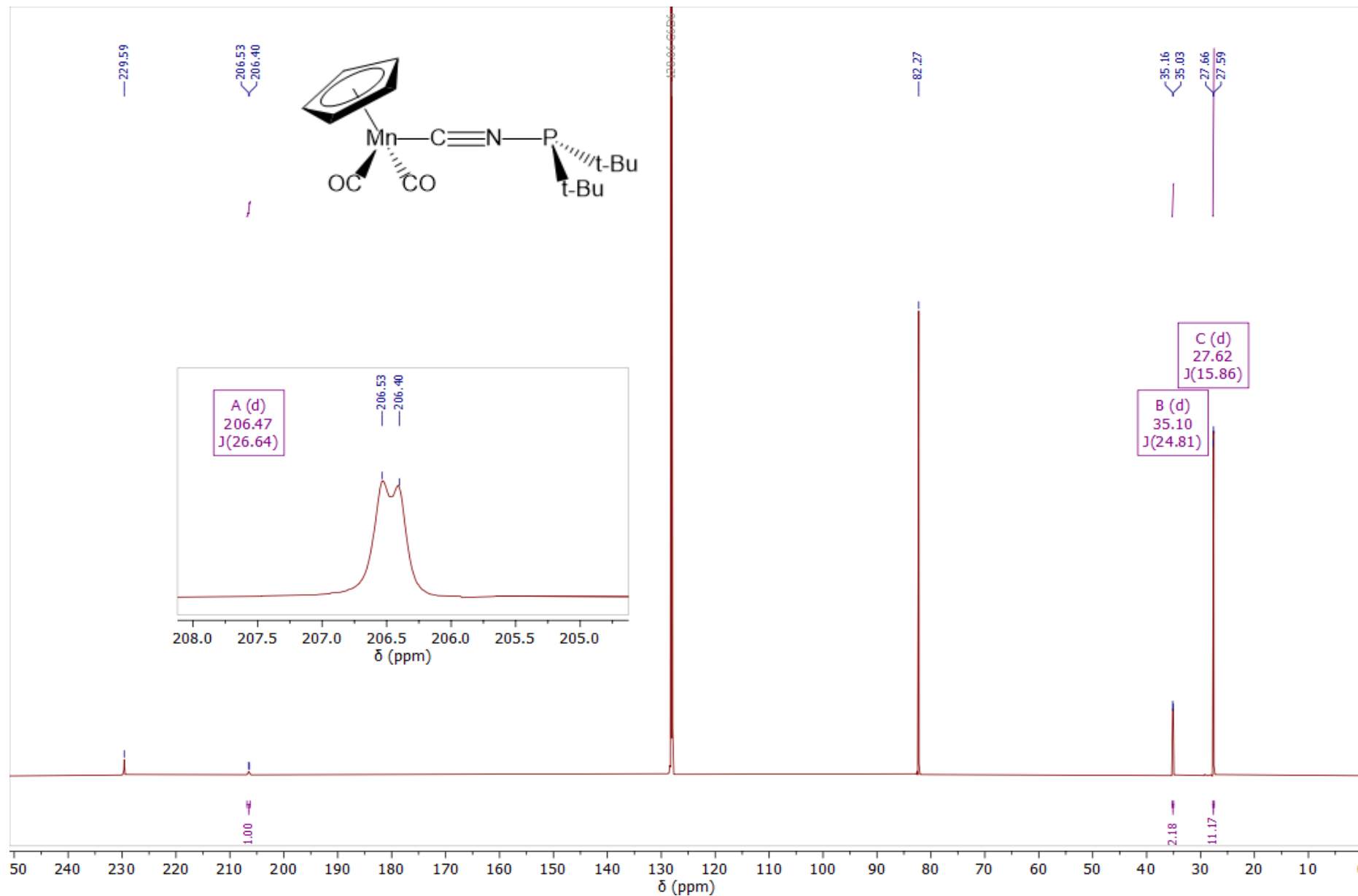
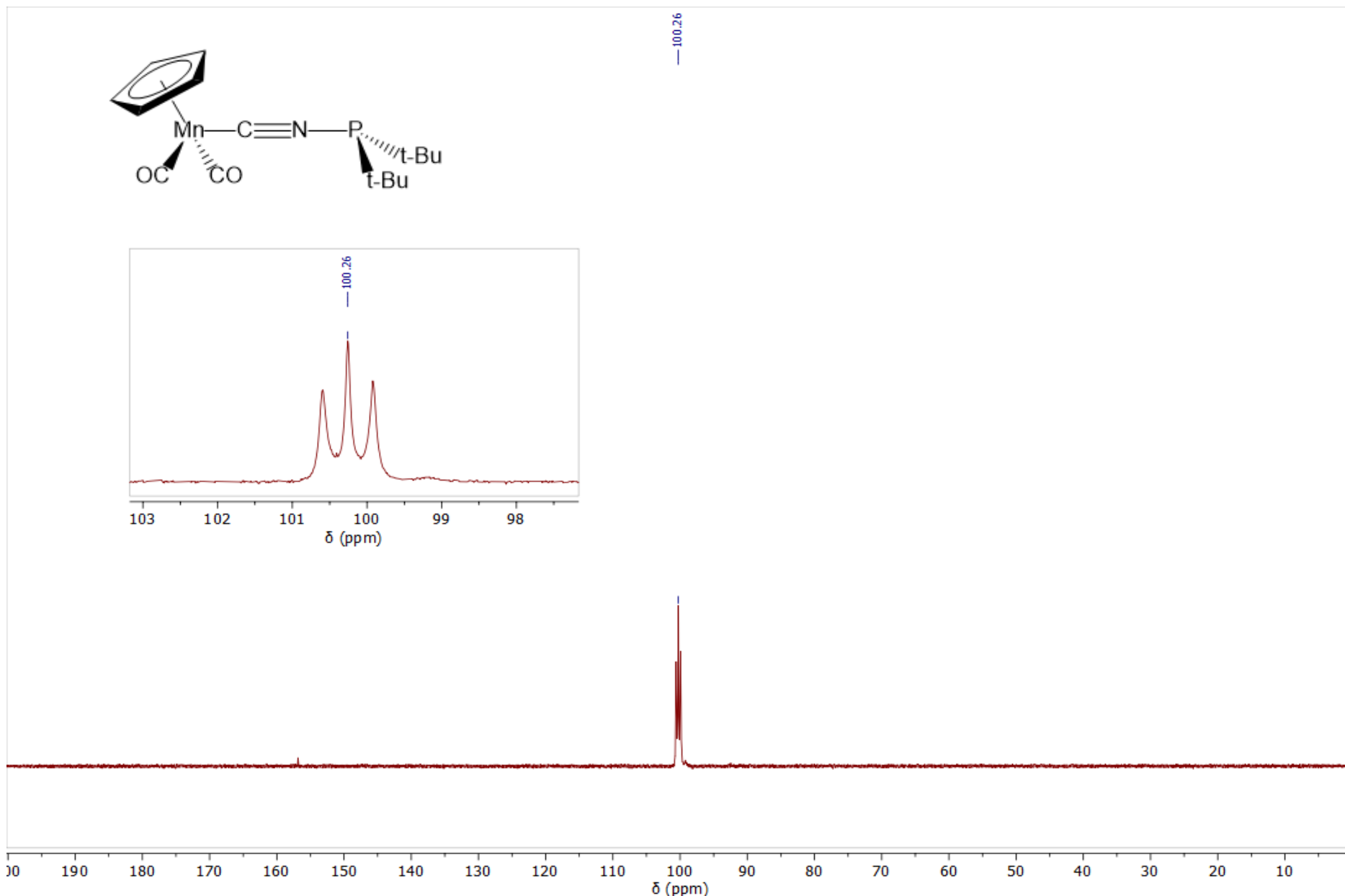
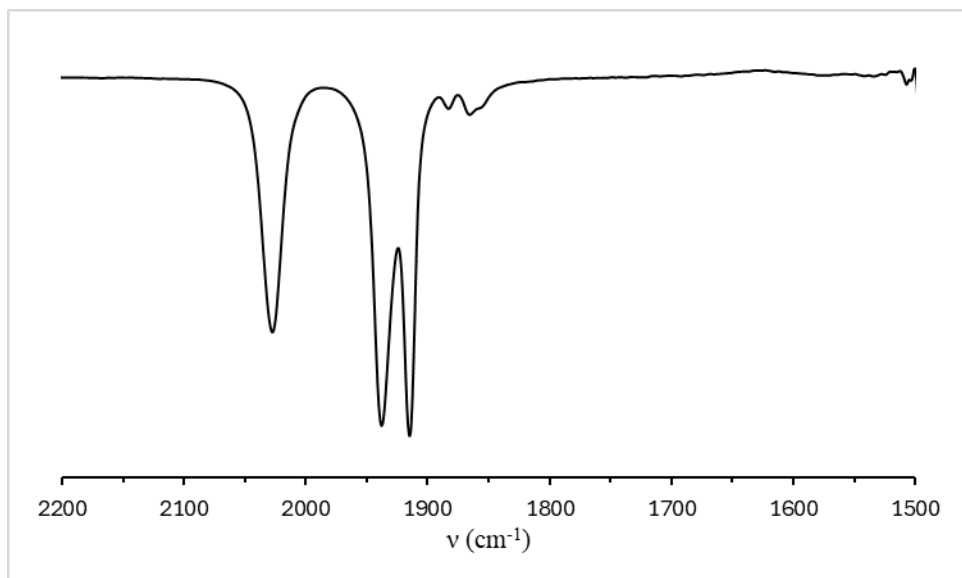
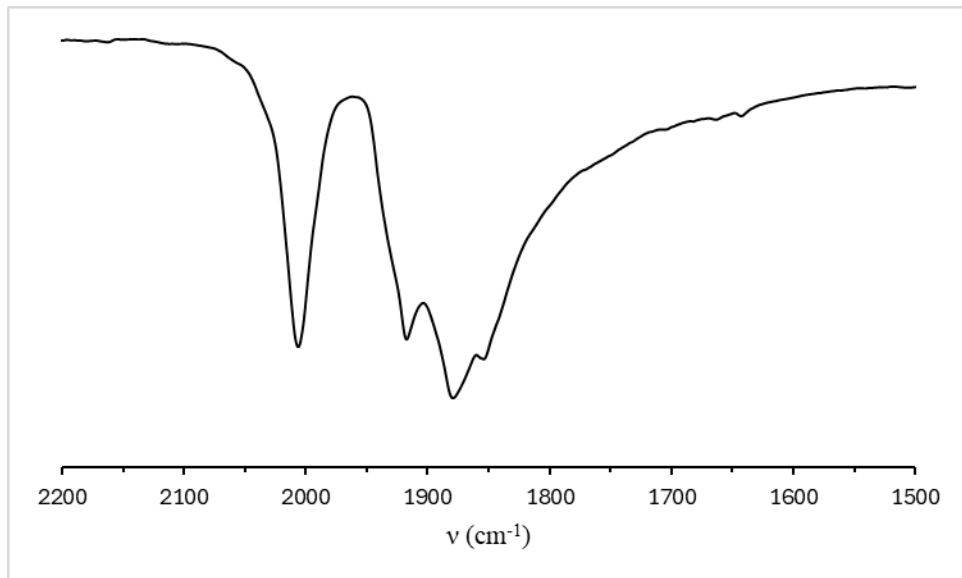


Figure S60: The  $^{13}\text{C}\{^1\text{H}\}$  NMR spectrum of  $[\text{Mn}(\text{CNP}^t\text{Bu}_2)(\text{CO})_2\text{Cp}]$  ( $\text{C}_6\text{D}_6$ , 201 MHz, 25 °C).

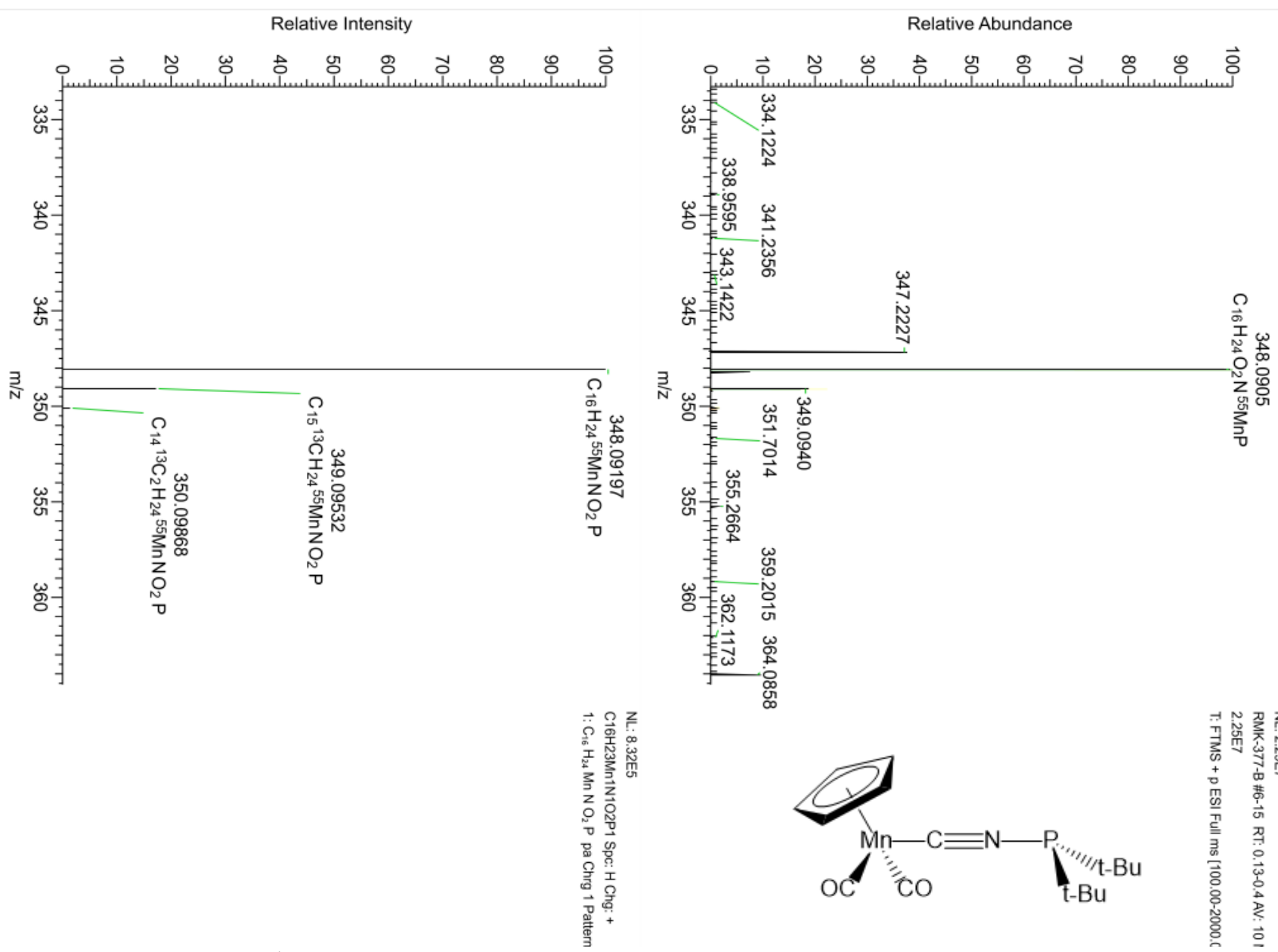


**Figure S61:** The  $^{31}\text{P}\{^1\text{H}\}$  NMR spectrum of  $[\text{Mn}(\text{CNPr}^t\text{Bu}_2)(\text{CO})_2\text{Cp}]$  ( $\text{C}_6\text{D}_6$ , 162 MHz, 25 °C).



**Figure S62:** The solid state ATR-IR (top) and solution FT-IR (*n*-hexane; bottom) spectra of  $[\text{Mn}(\text{CNP}^{\text{t}}\text{Bu}_2)(\text{CO})_2\text{Cp}]$  in the carbonyl region (25 °C).

## ELECTRONIC SUPPORTING INFORMATION

**Figure S63:** The HR-MS of [Mn(CNPrBu<sub>2</sub>)(CO)<sub>2</sub>Cp]<sup>2+</sup> (ESI, positive ion mode, MeCN).

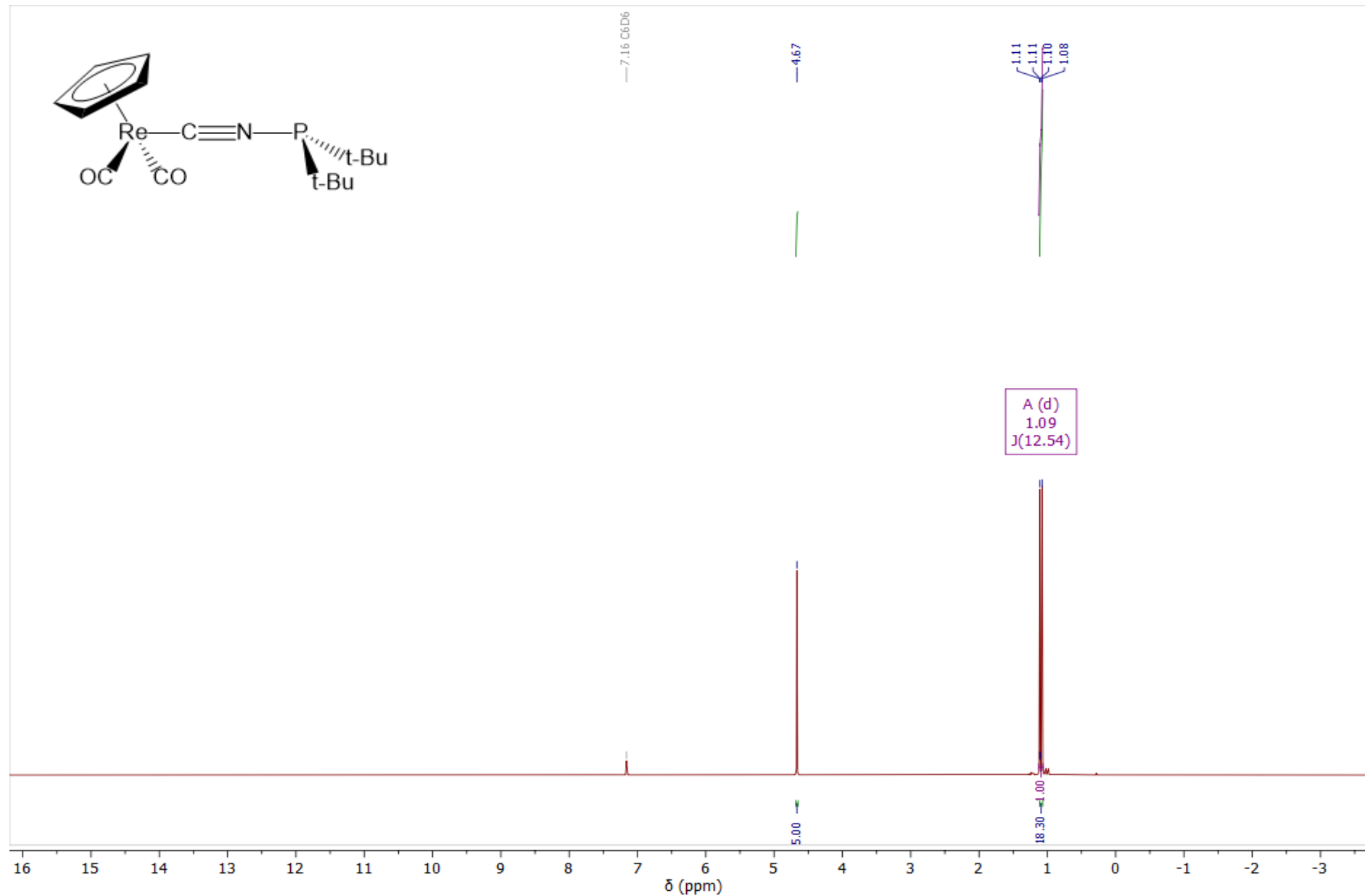
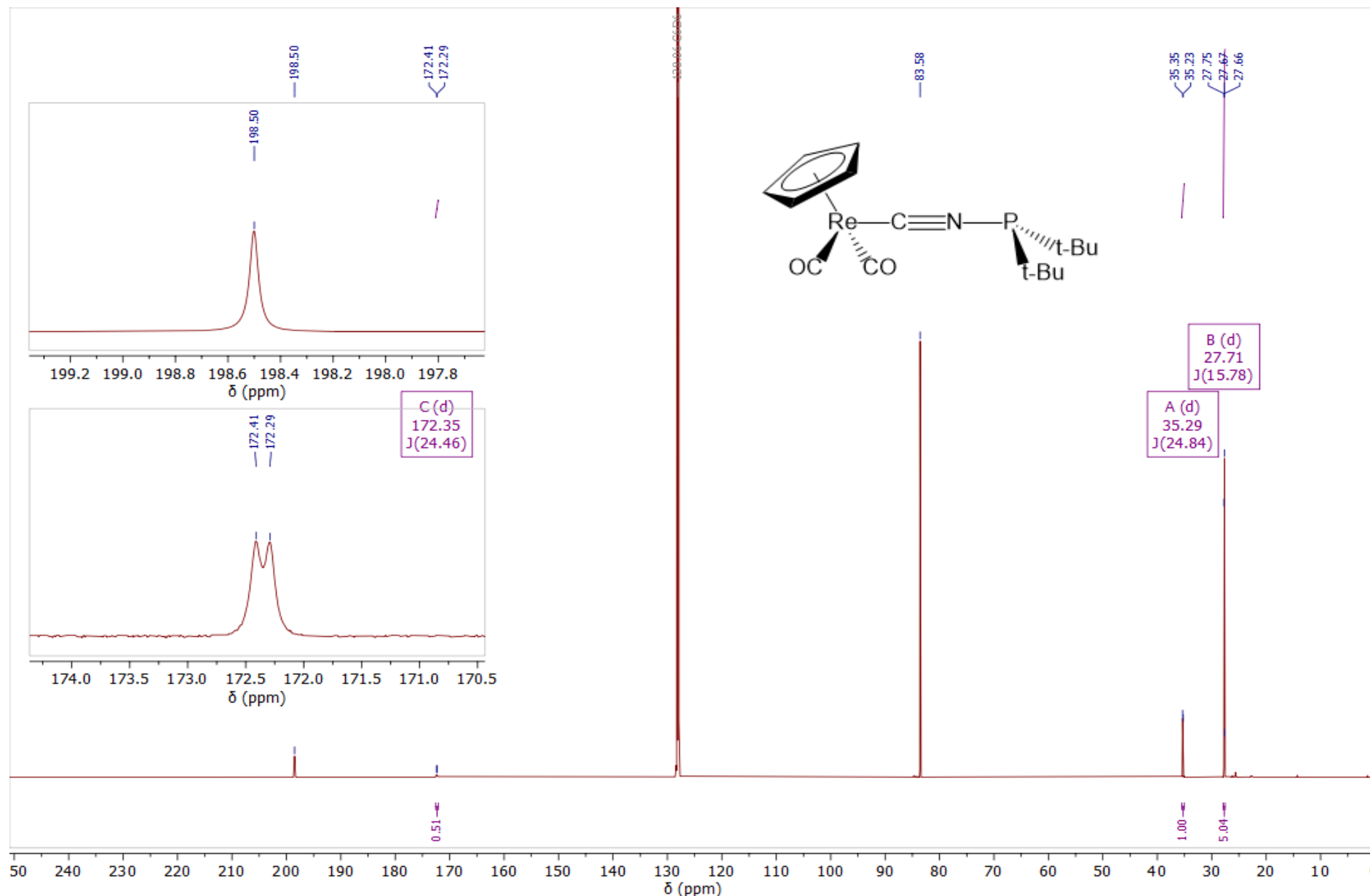
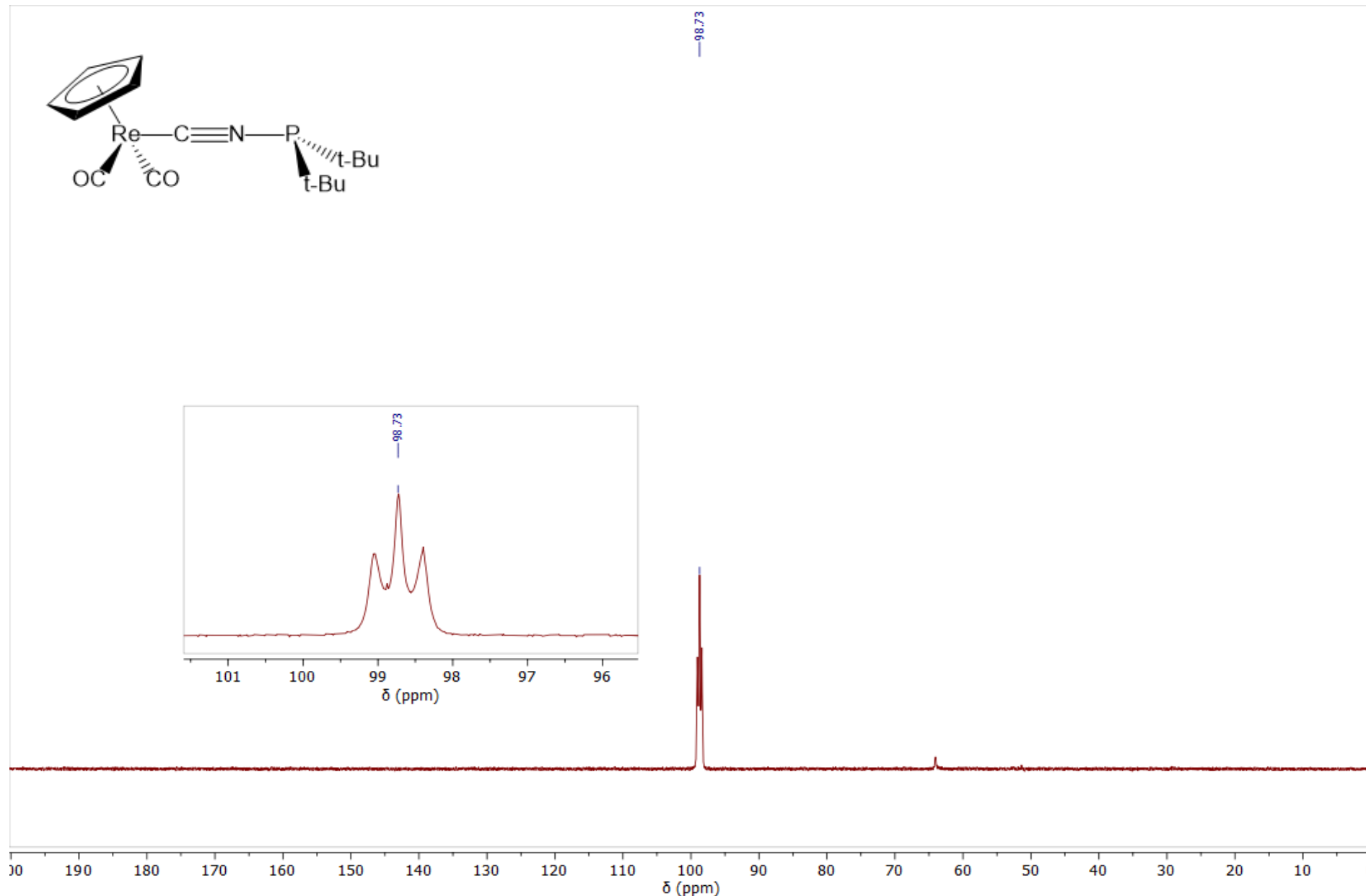


Figure S64: The  $^1\text{H}$  NMR spectrum of  $[\text{Re}(\text{CNP}^{\text{t}}\text{Bu}_2)(\text{CO})_2\text{Cp}]$  ( $\text{C}_6\text{D}_6$ , 400 MHz, 25 °C).



**Figure S65:** The  $^{13}\text{C}\{^1\text{H}\}$  NMR spectrum of  $[\text{Re}(\text{CNP}^t\text{Bu}_2)(\text{CO})_2\text{Cp}]$  ( $\text{C}_6\text{D}_6$ , 201 MHz, 25 °C).



**Figure S66:** The  $^{31}\text{P}\{^1\text{H}\}$  NMR spectrum of  $[\text{Re}(\text{CNP}^t\text{Bu}_2)(\text{CO})_2\text{Cp}]$  ( $\text{C}_6\text{D}_6$ , 162 MHz, 25 °C).

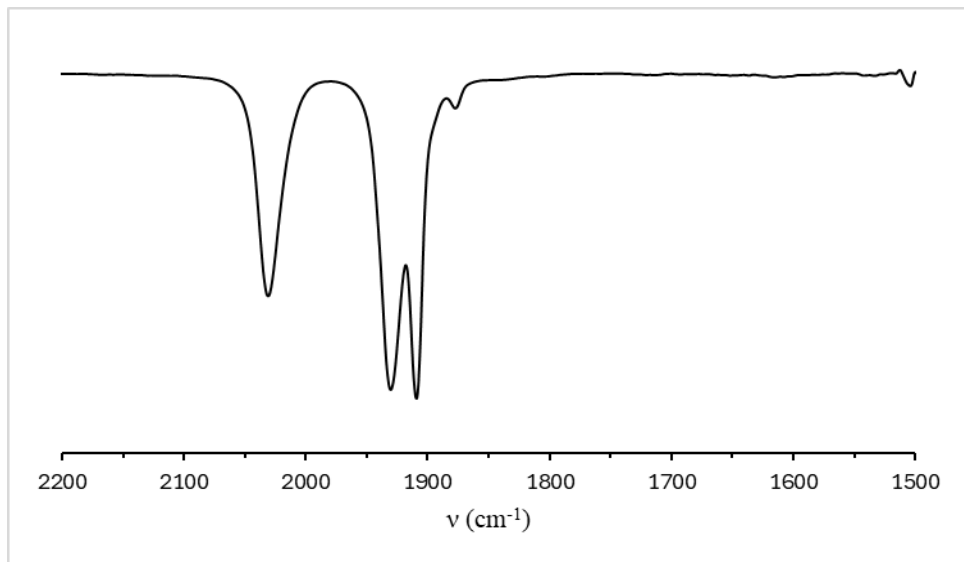
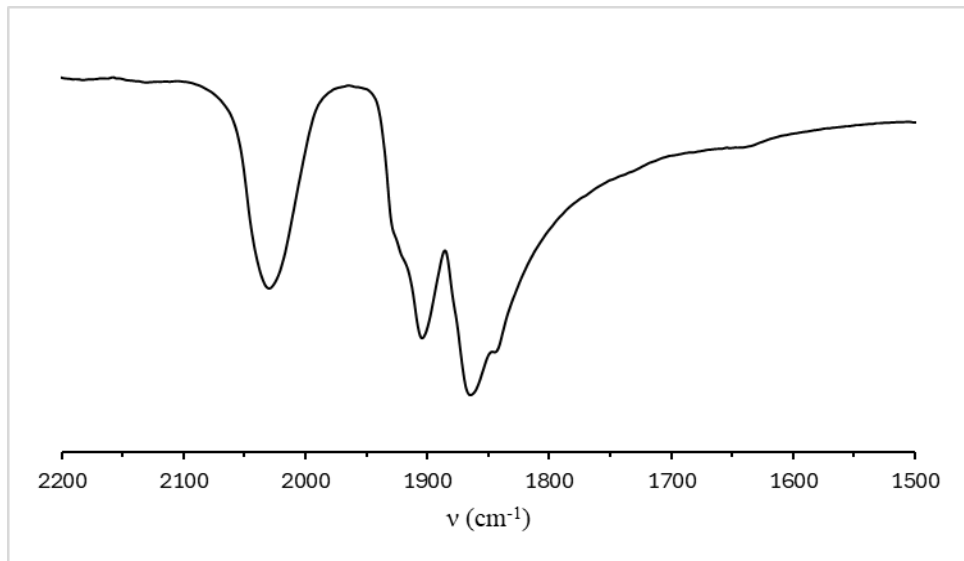


**Figure S67:** The solid state ATR-IR (top) and solution FT-IR (*n*-hexane; bottom) spectra of  $[\text{Re}(\text{CNP}^{\text{t-Bu}}_2)(\text{CO})_2\text{Cp}]$  in the carbonyl region (25 °C).

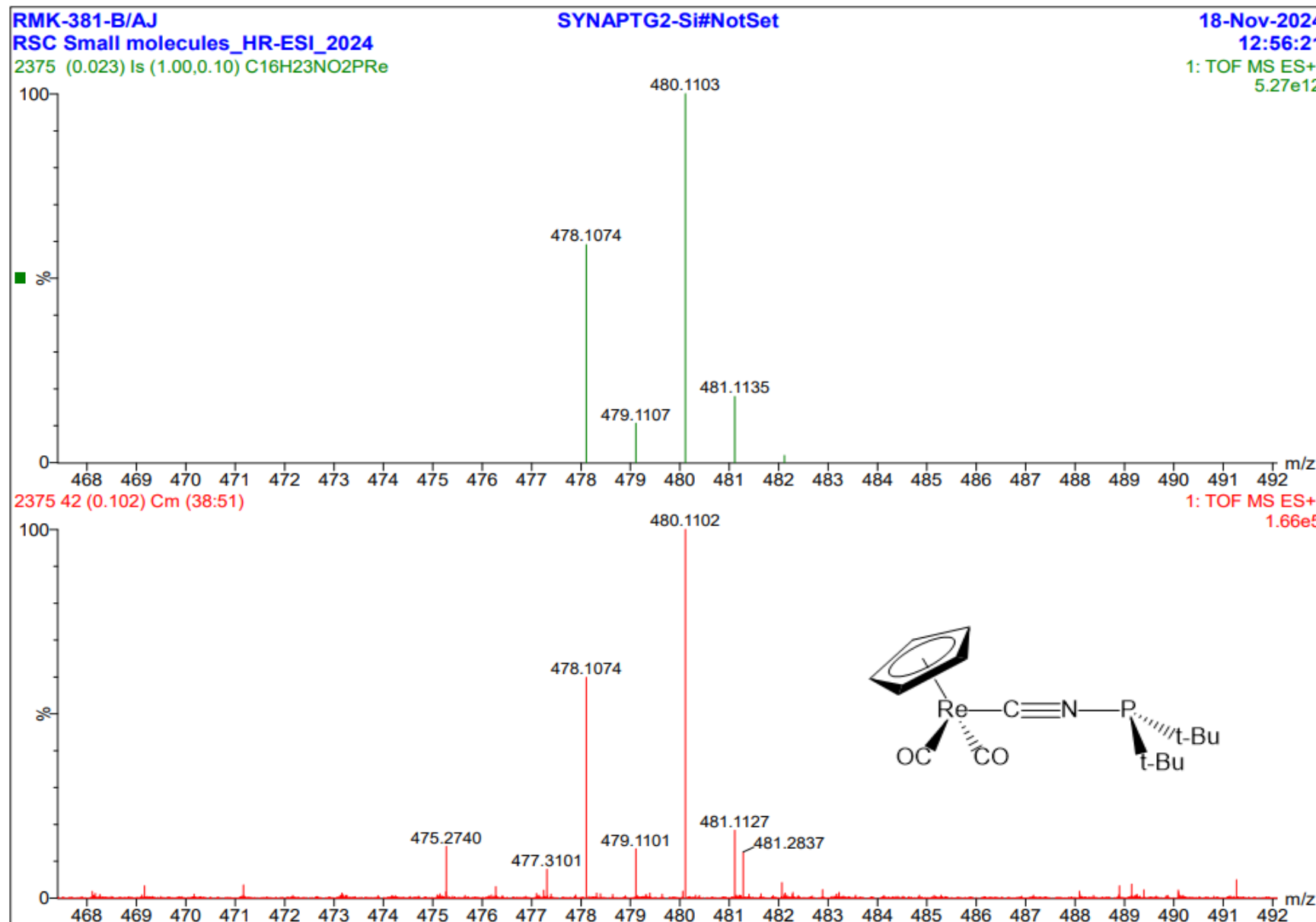


**Figure S68:** The HR-MS of  $[\text{Re}(\text{CNP}^t\text{Bu}_2)(\text{CO})_2\text{Cp}]$  (ESI, positive ion mode, MeCN).

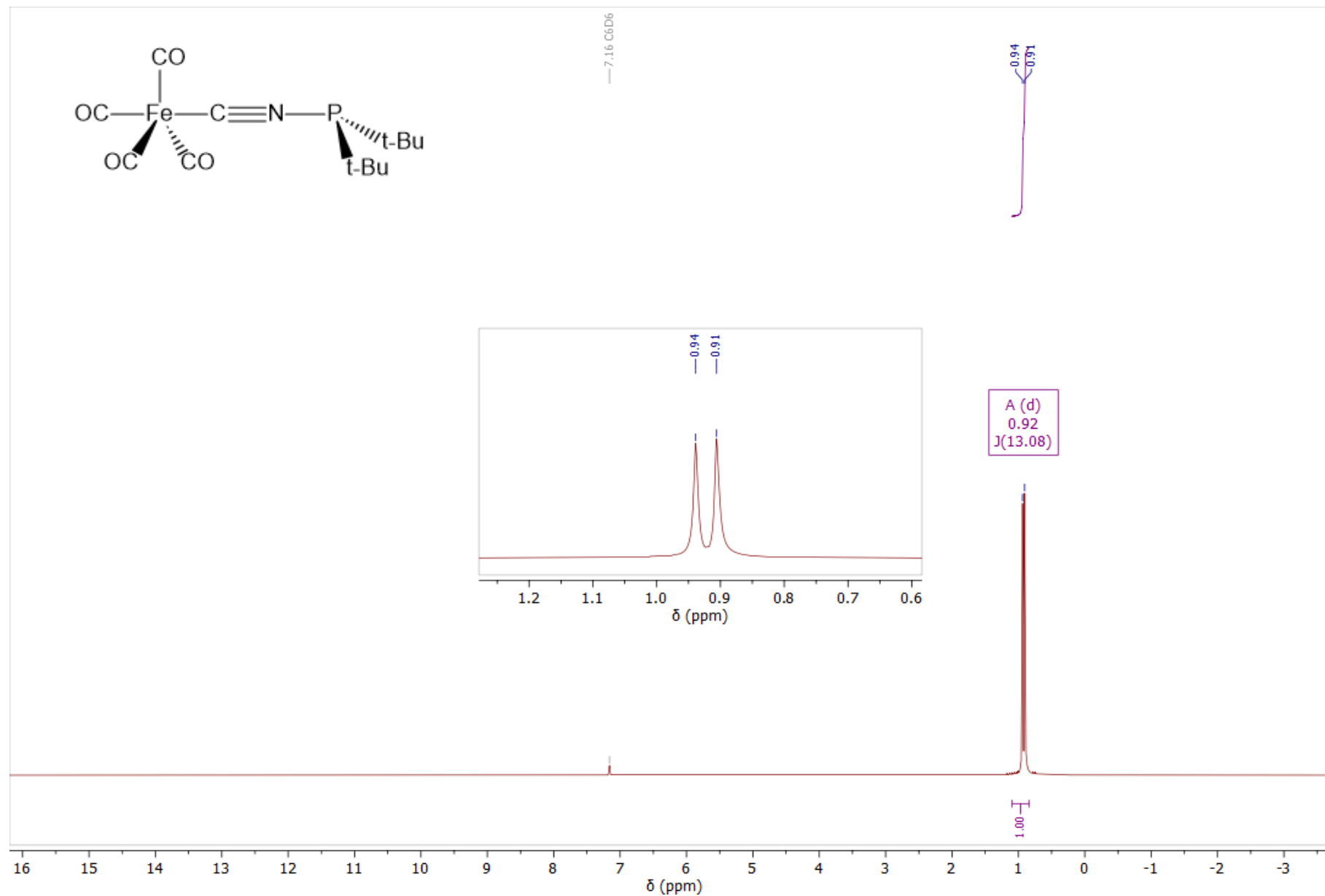


**Figure S69:** The <sup>1</sup>H NMR spectrum of  $[\text{Fe}(\text{CNP}^t\text{Bu}_2)(\text{CO})_4]$  ( $\text{C}_6\text{D}_6$ , 400 MHz, 25 °C).

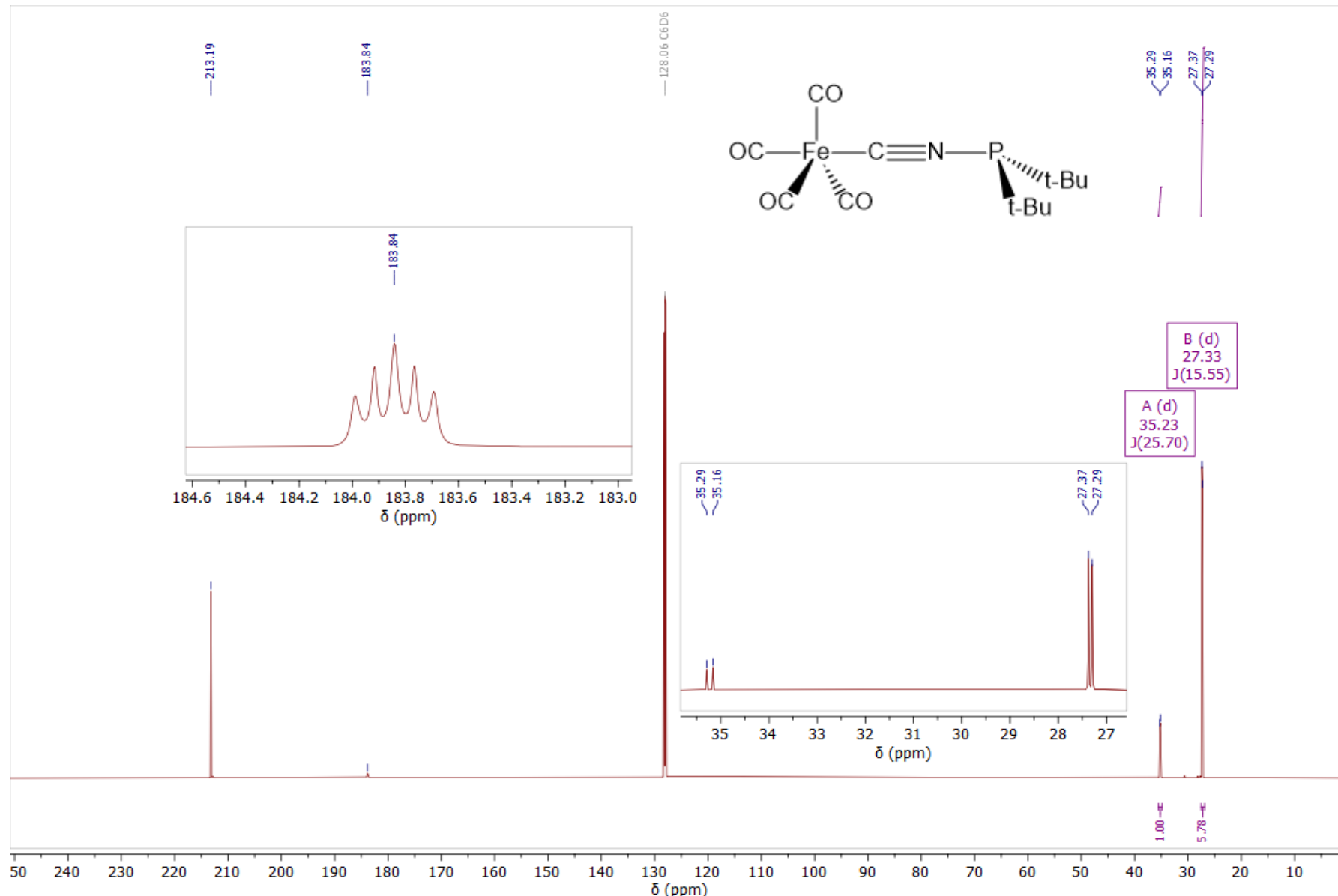


**Figure S70:** The  $^{13}\text{C}\{^1\text{H}\}$  NMR spectrum of  $[\text{Fe}(\text{CNP}^{\text{t}}\text{Bu}_2)(\text{CO})_4]$  ( $\text{C}_6\text{D}_6$ , 201 MHz, 25 °C).

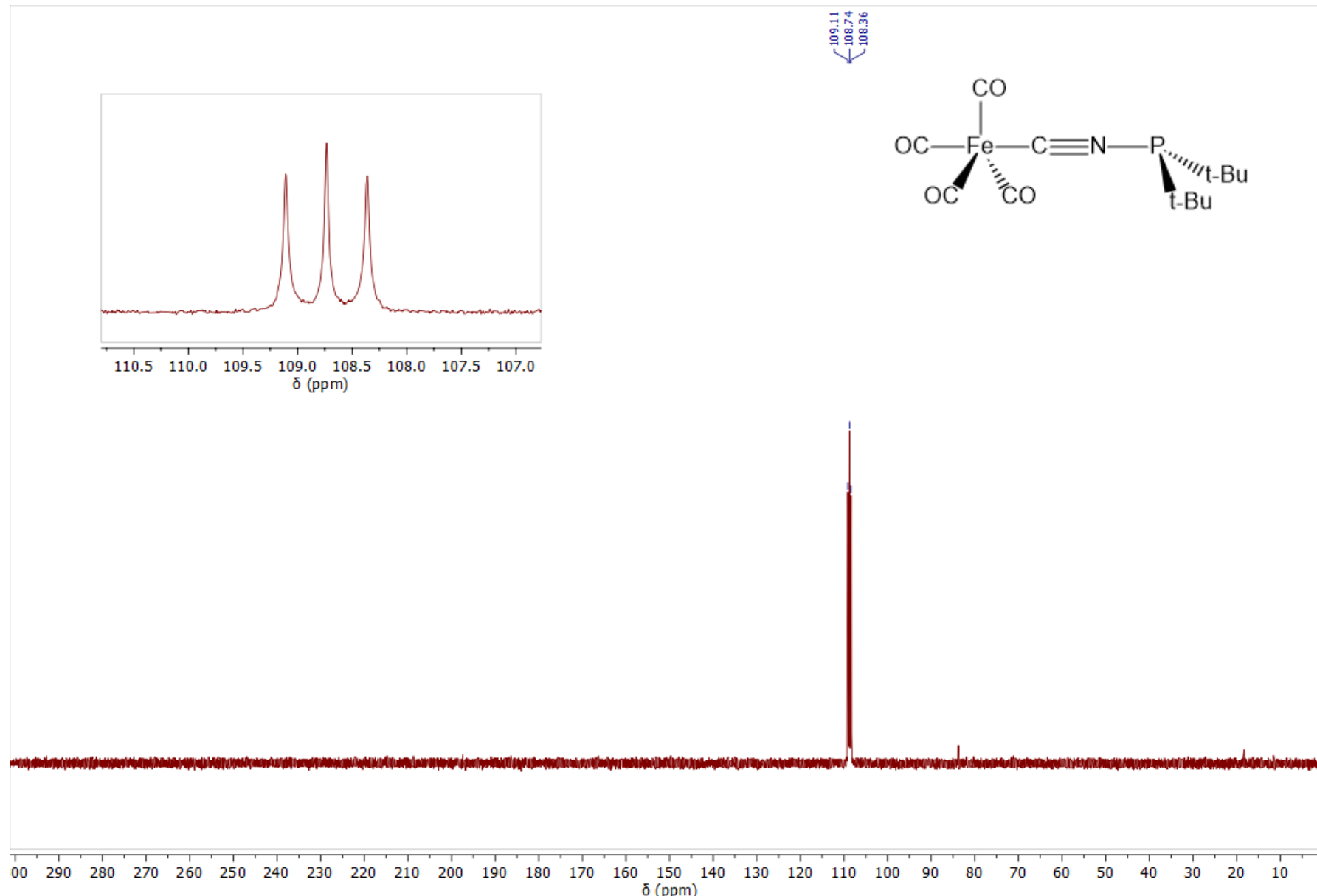


**Figure S71:** The  $^{31}\text{P}\{^1\text{H}\}$  NMR spectrum of  $[\text{Fe}(\text{CNP}^{\text{t-Bu}}_2)(\text{CO})_4]$  ( $\text{C}_6\text{D}_6$ , 162 MHz, 25 °C).

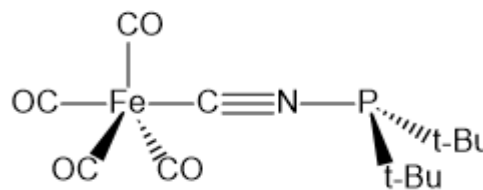
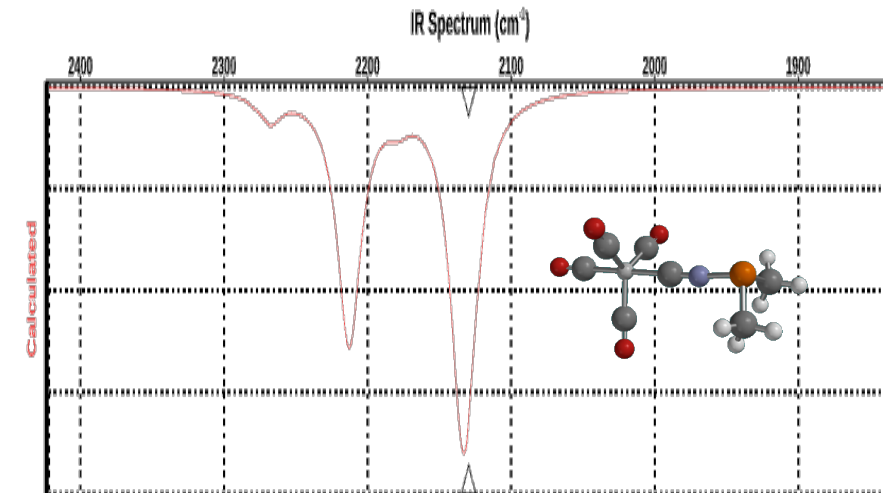
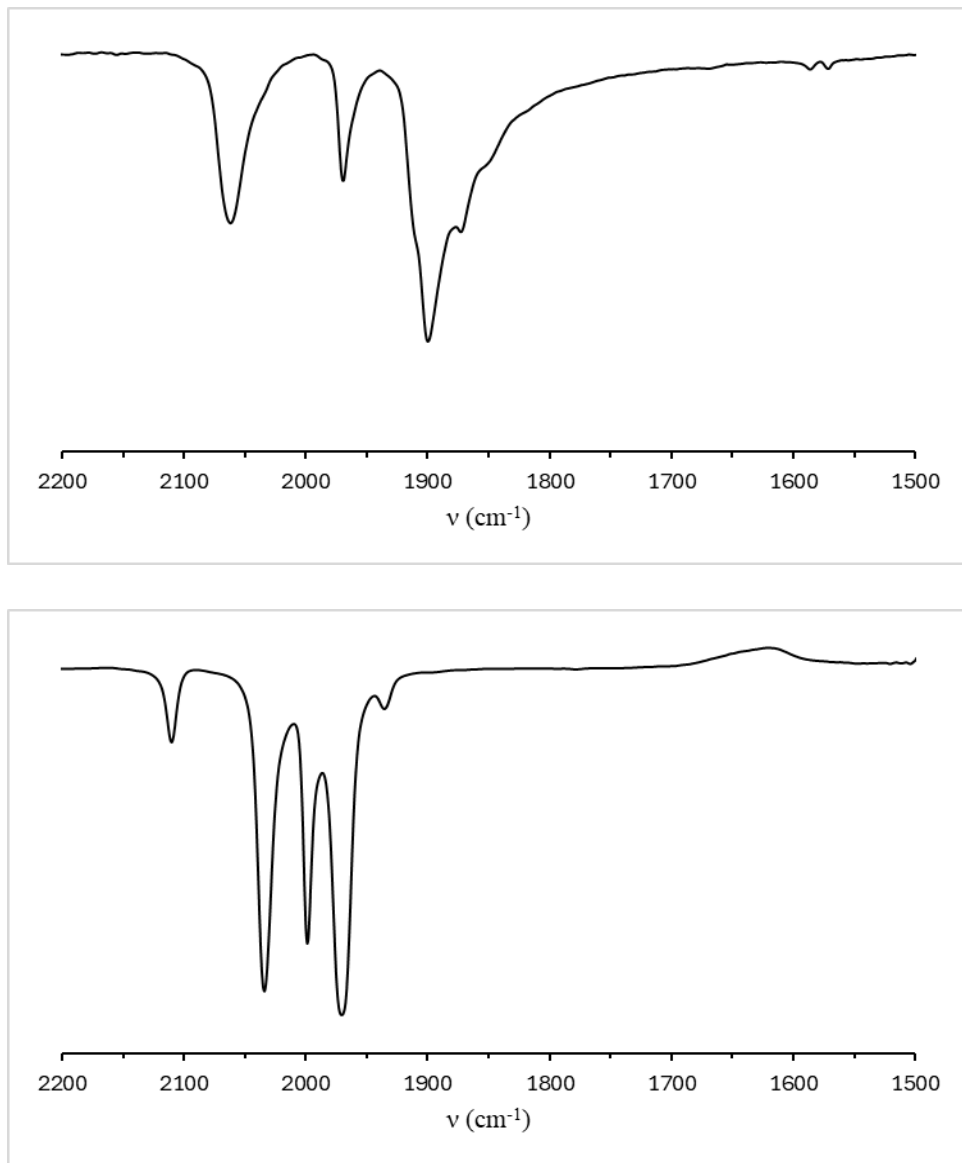


**Figure S72:** The solid state ATR-IR (top) and solution FT-IR (*n*-hexane; bottom) spectra of  $[\text{Fe}(\text{CNP}^t\text{Bu}_2)(\text{CO})_4]$  in the carbonyl region (25 °C). Calculated Infrared spectrum (Gas Phase) for *axial*- $[\text{Fe}(\text{CNPMe}_2)(\text{CO})_4]$  isomer (M06-2X/6-31G\*)

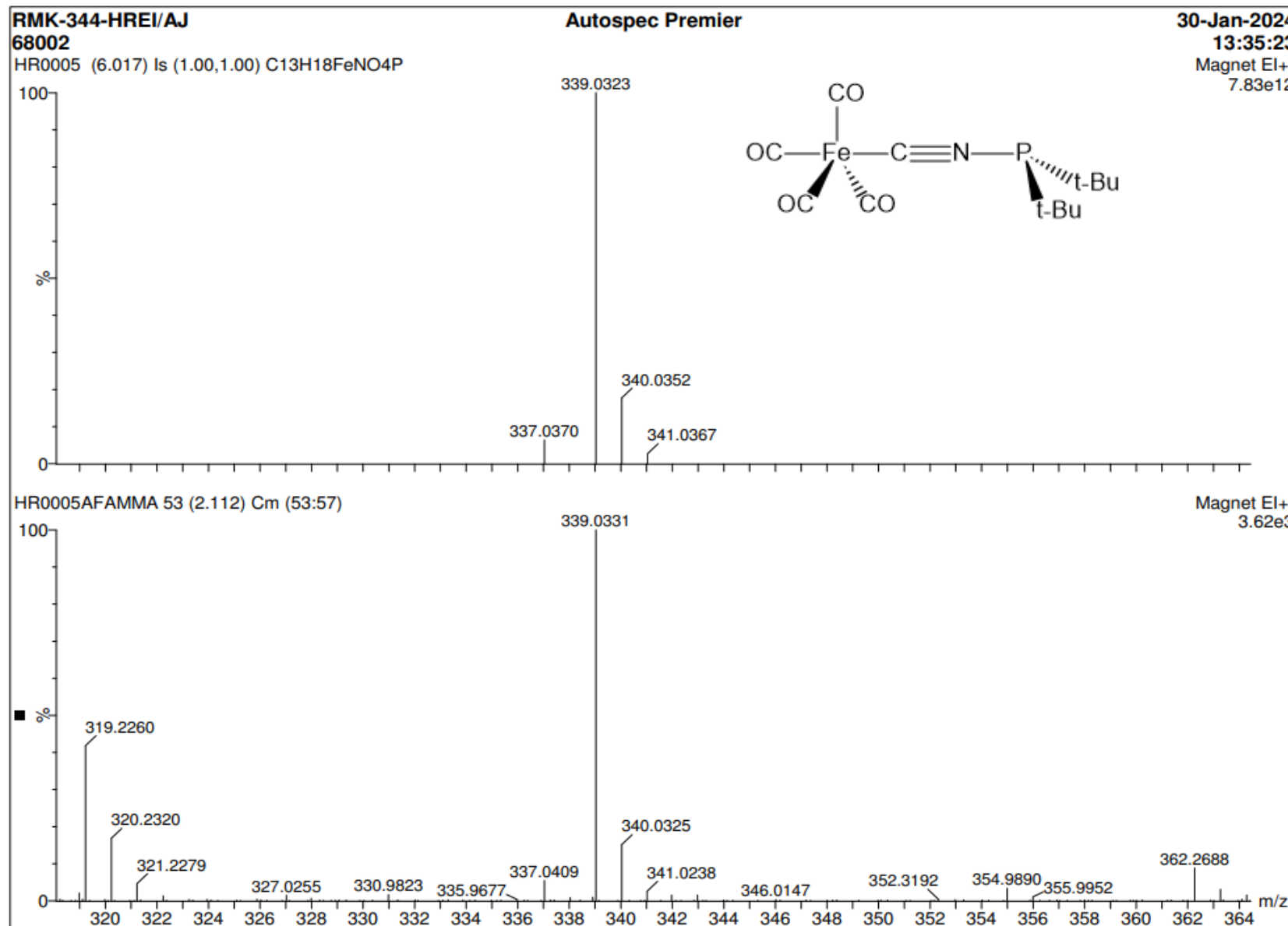


**Figure S73:** The HR-MS of  $[\text{Fe}(\text{CNP}^{\text{t}}\text{Bu}_2)(\text{CO})_4]$  (EI, positive ion mode, MeCN).

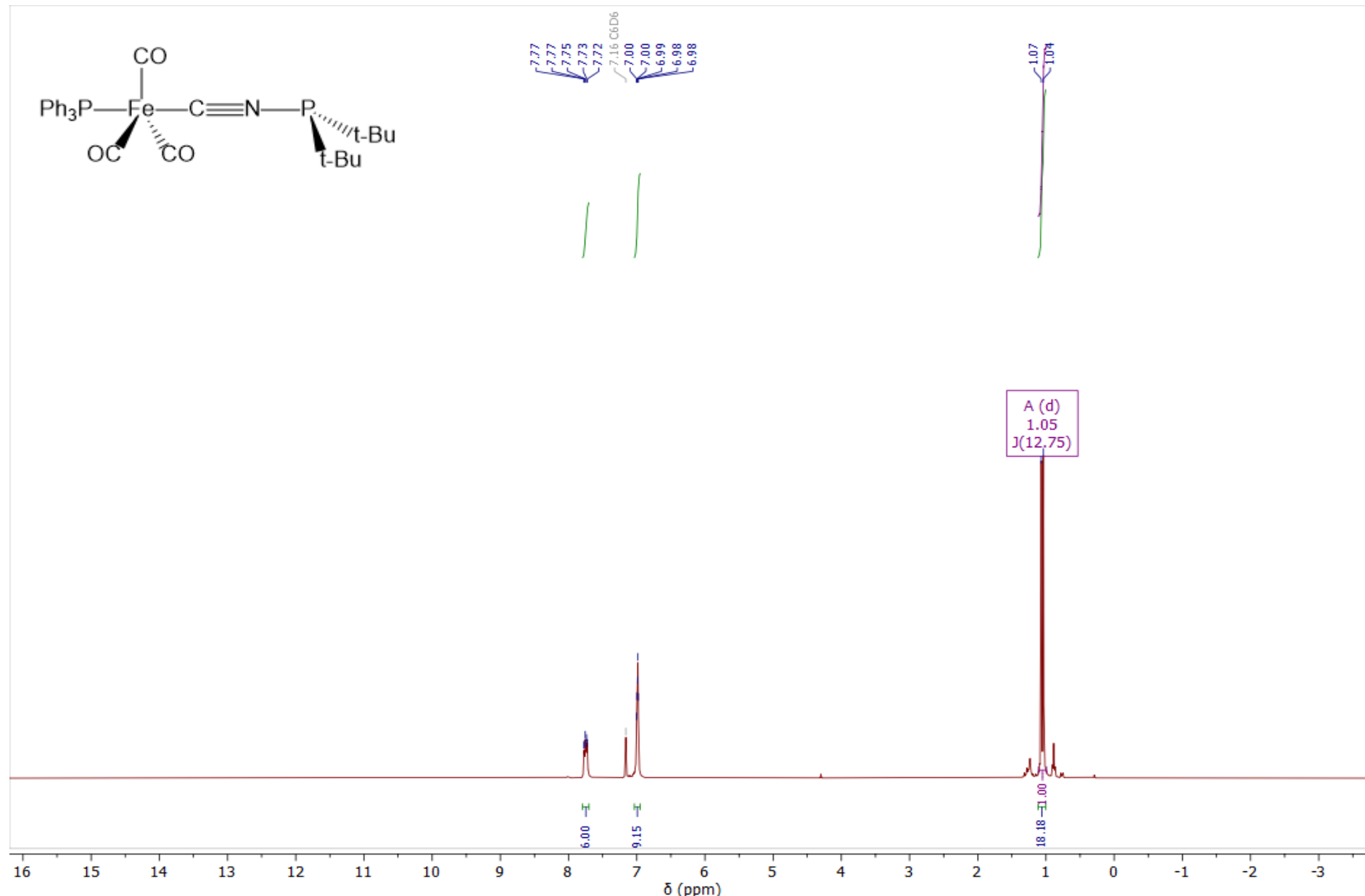


Figure S74: The <sup>1</sup>H NMR spectrum of  $[\text{Fe}(\text{CNP}^t\text{Bu}_2)(\text{CO})_3(\text{PPh}_3)]$  (C<sub>6</sub>D<sub>6</sub>, 400 MHz, 25 °C).

## ELECTRONIC SUPPORTING INFORMATION

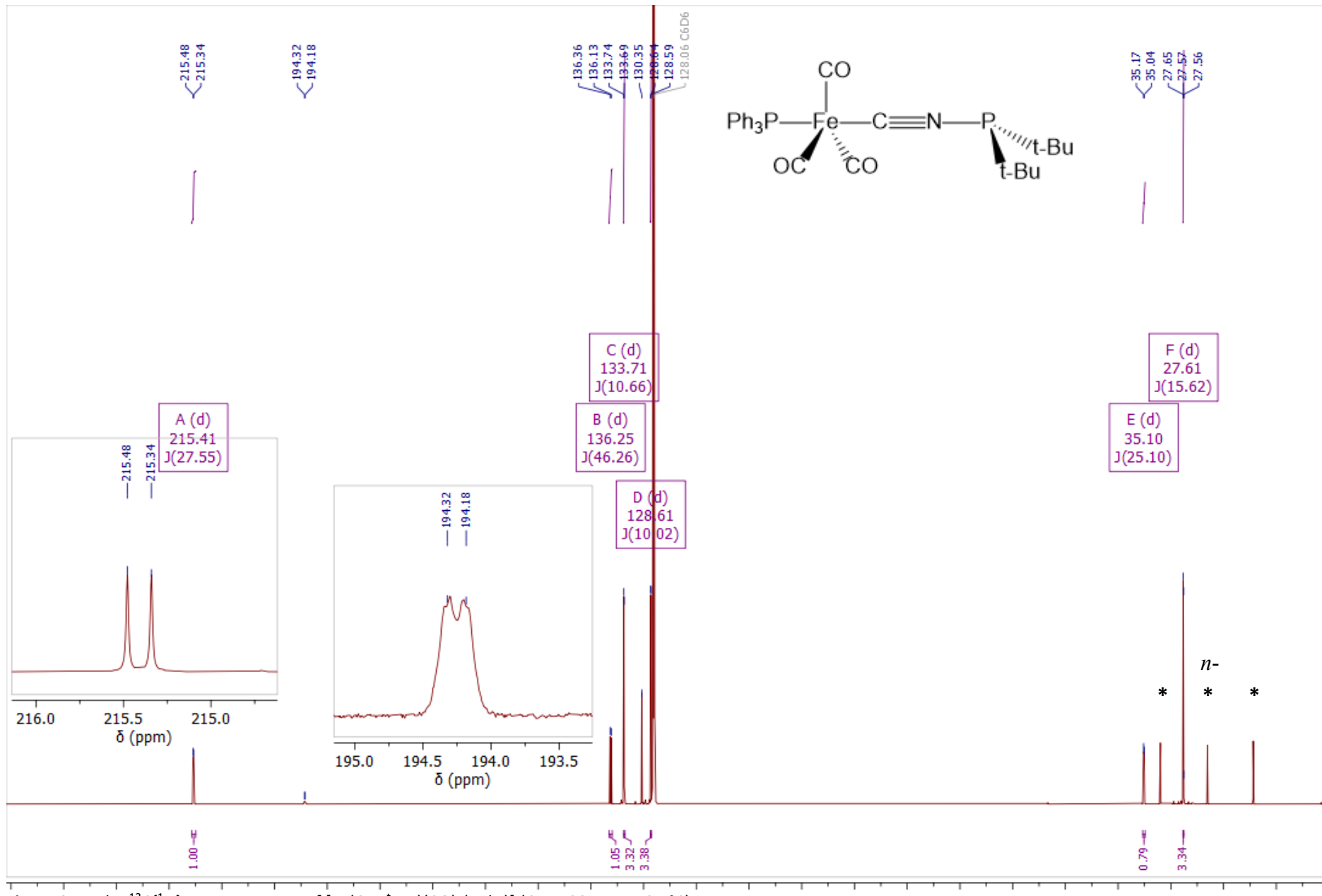


Figure S75: The  $^{13}\text{C}\{^1\text{H}\}$  NMR spectrum of  $[\text{Fe}(\text{CNP}^{\text{t}}\text{Bu}_2)(\text{CO})_3(\text{PPh}_3)]$  ( $\text{C}_6\text{D}_6$ , 201 MHz, 25 °C).

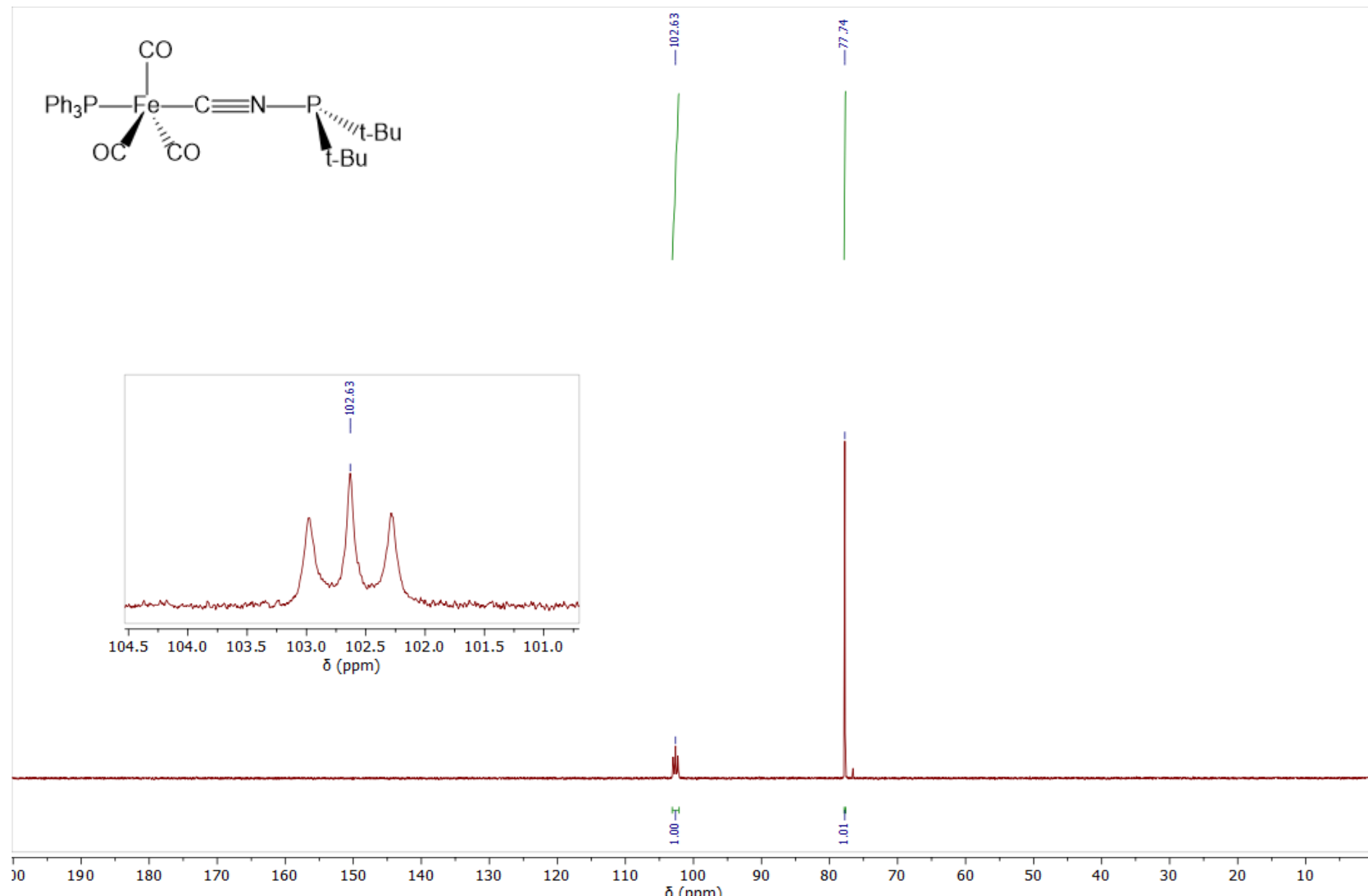
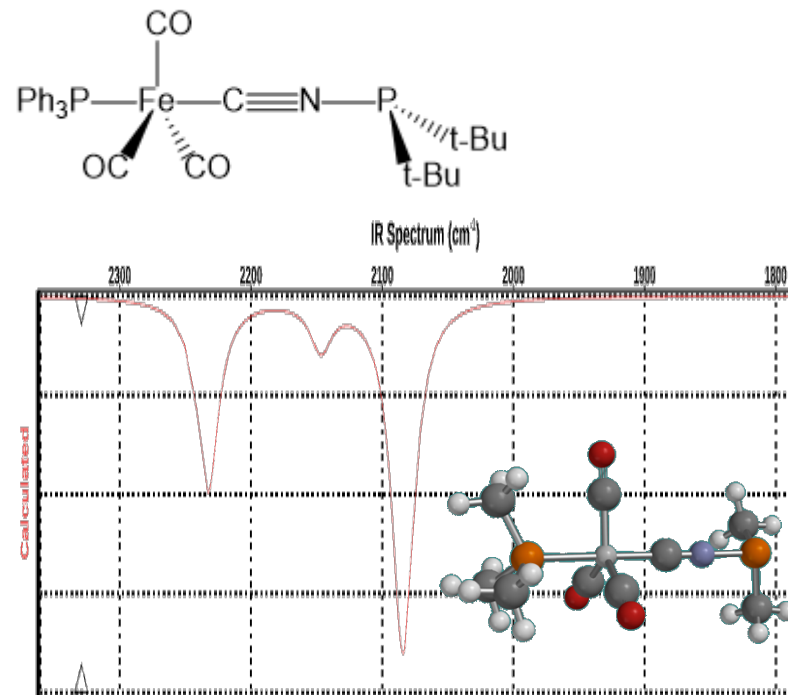
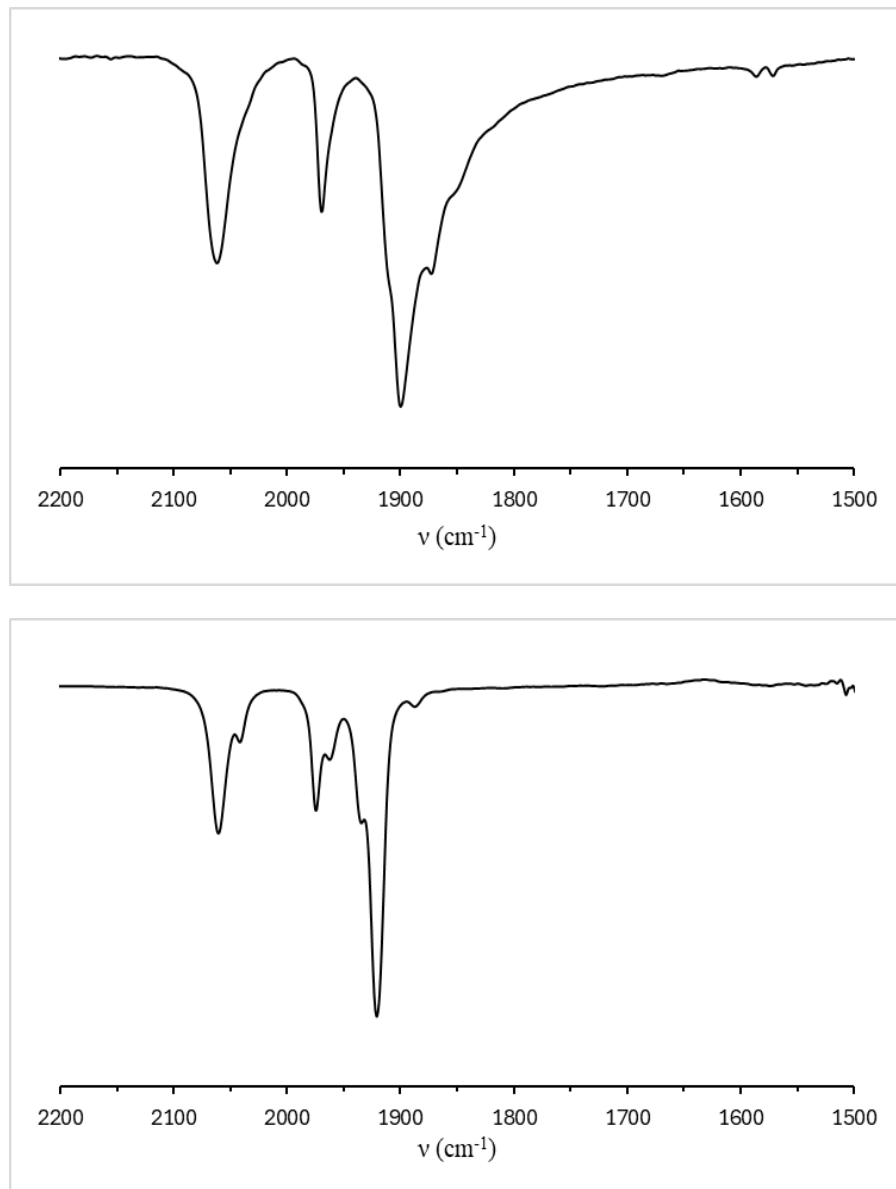


Figure S76: The  $^{31}\text{P}\{^1\text{H}\}$  NMR spectrum of  $[\text{Fe}(\text{CNP}^t\text{Bu}_2)(\text{CO})_3(\text{PPh}_3)]$  ( $\text{C}_6\text{D}_6$ , 162 MHz, 25 °C)

## ELECTRONIC SUPPORTING INFORMATION

## Dalton Transactions



**Figure S77:** The solid state ATR-IR (top) and solution FT-IR (*n*-hexane; bottom) spectra of  $[\text{Fe}(\text{CNP}^t\text{Bu}_2)(\text{CO})_3(\text{PPh}_3)]$  in the carbonyl region (25 °C). Calculated infrared spectrum for  $\text{trans-}[ \text{Fe}(\text{CNPMMe}_2)(\text{CO})_3(\text{PMe}_3) ]$  (M06-2X/6-315\*).

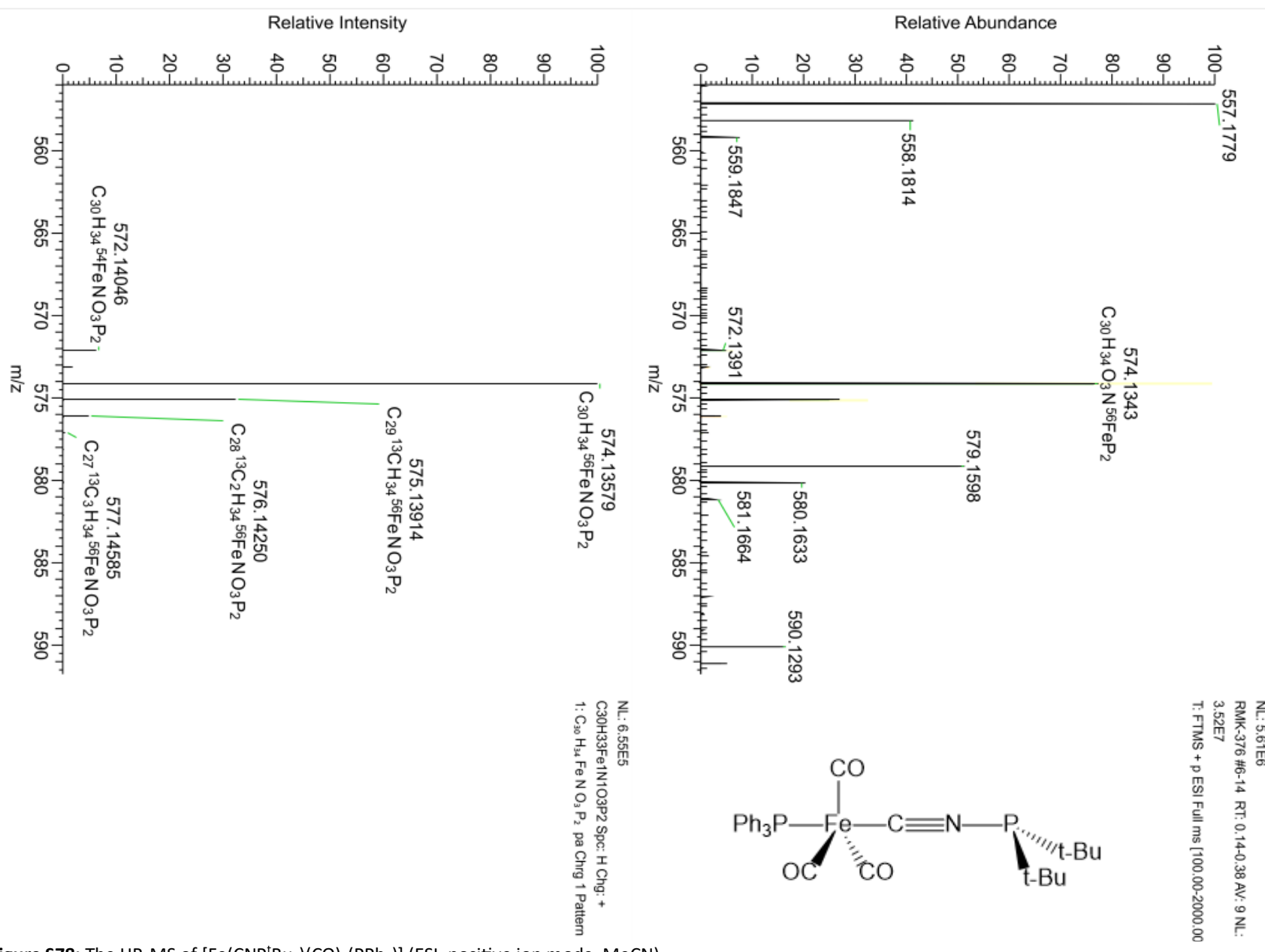
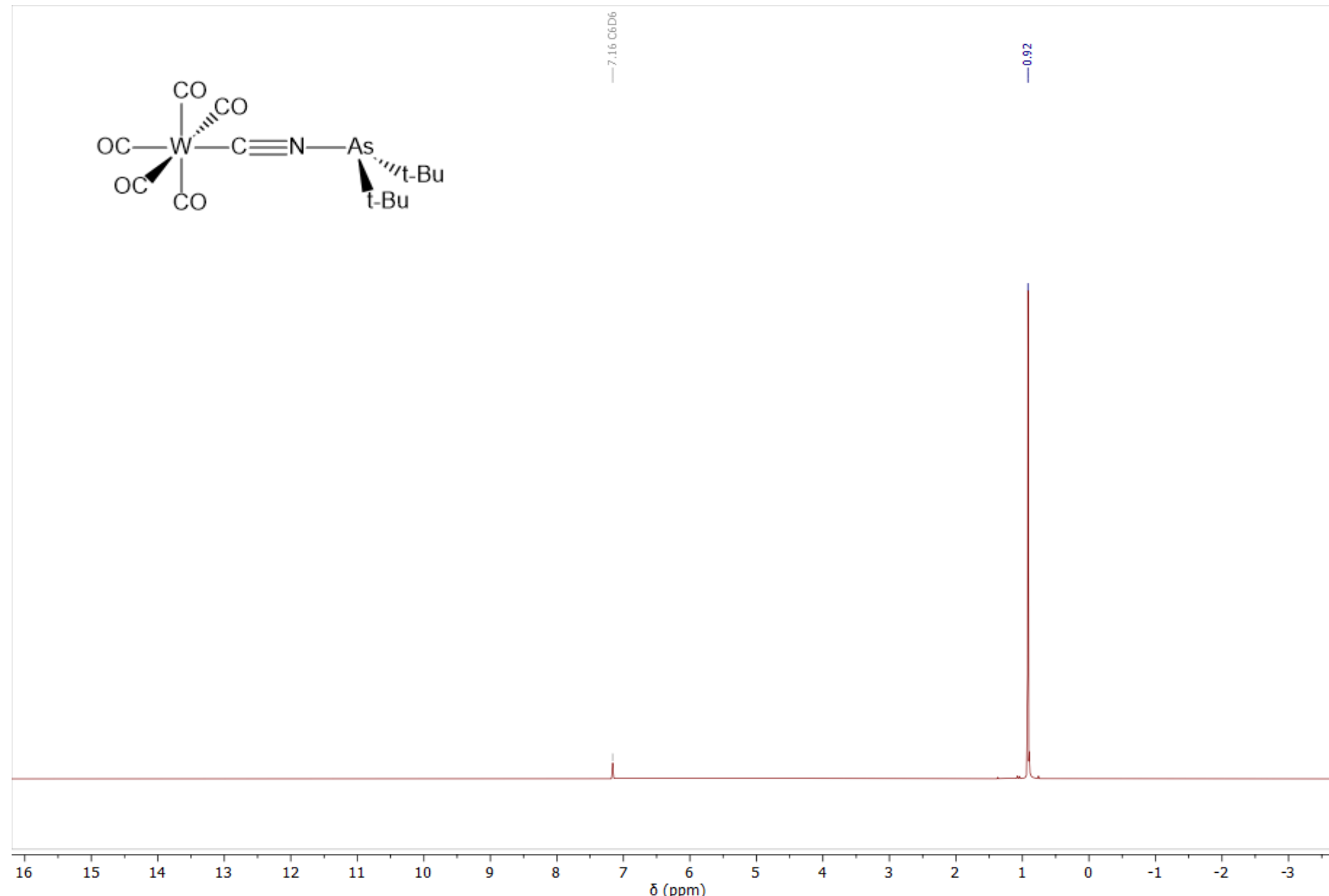
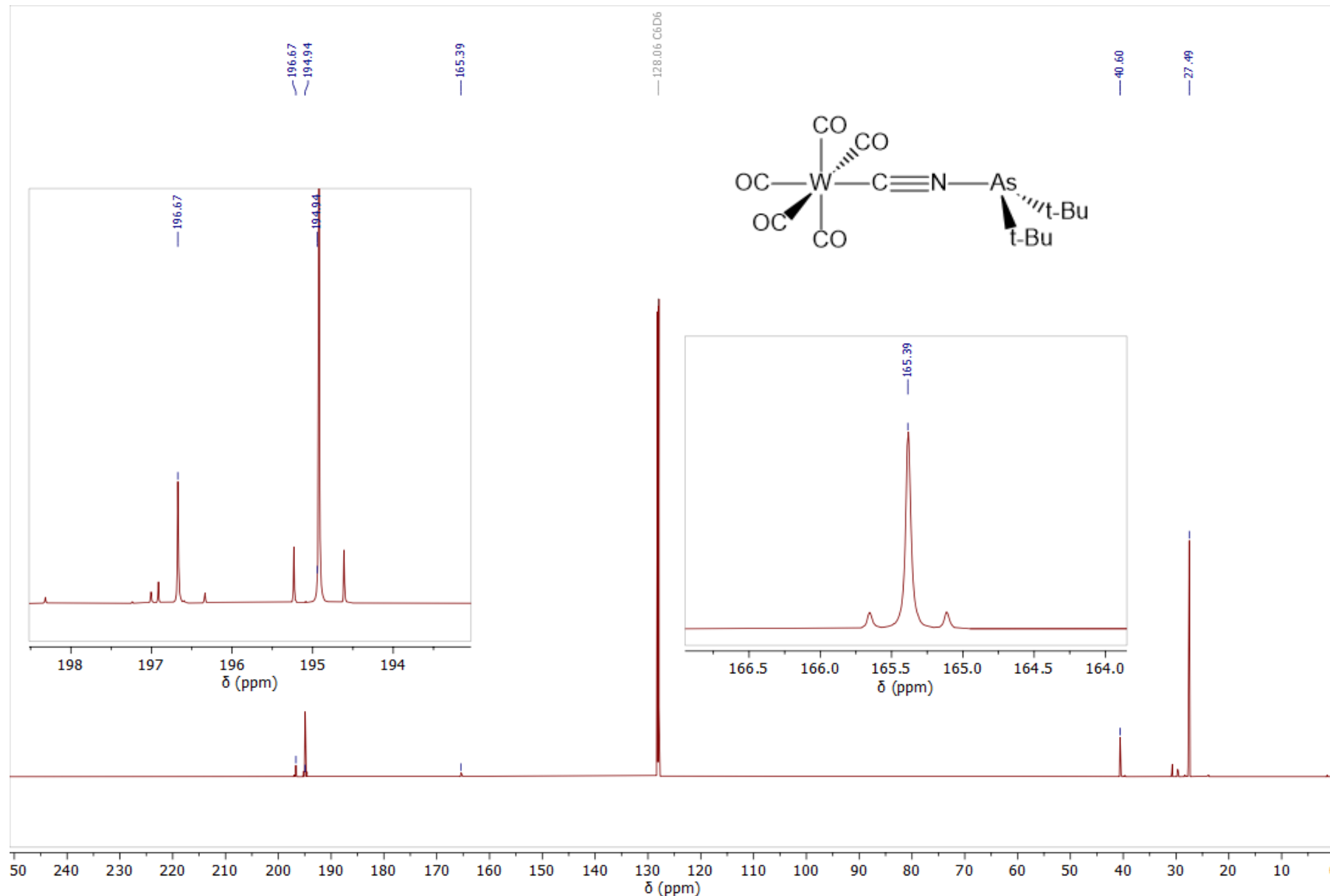


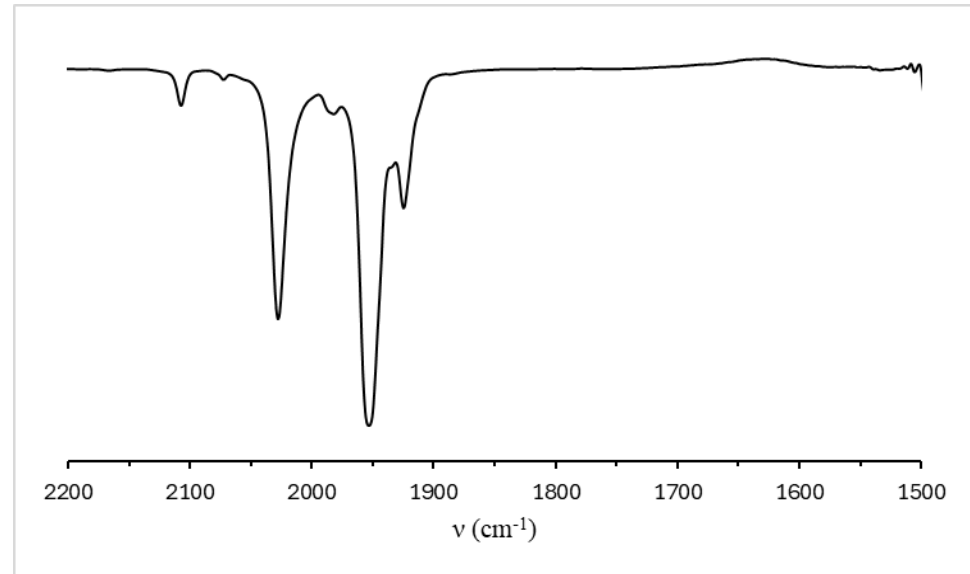
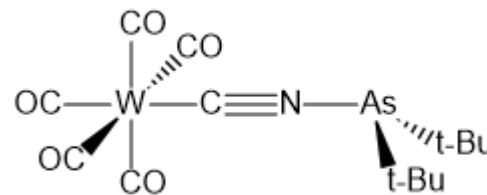
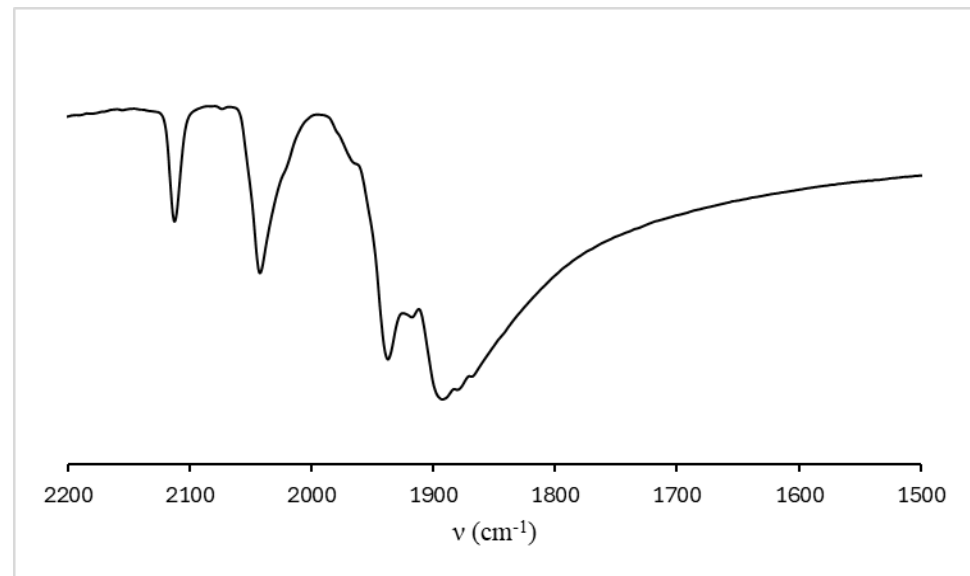
Figure S78: The HR-MS of  $[\text{Fe}(\text{CNP}^{\text{t}}\text{Bu}_2)(\text{CO})_3(\text{PPh}_3)]$  (ESI, positive ion mode, MeCN).



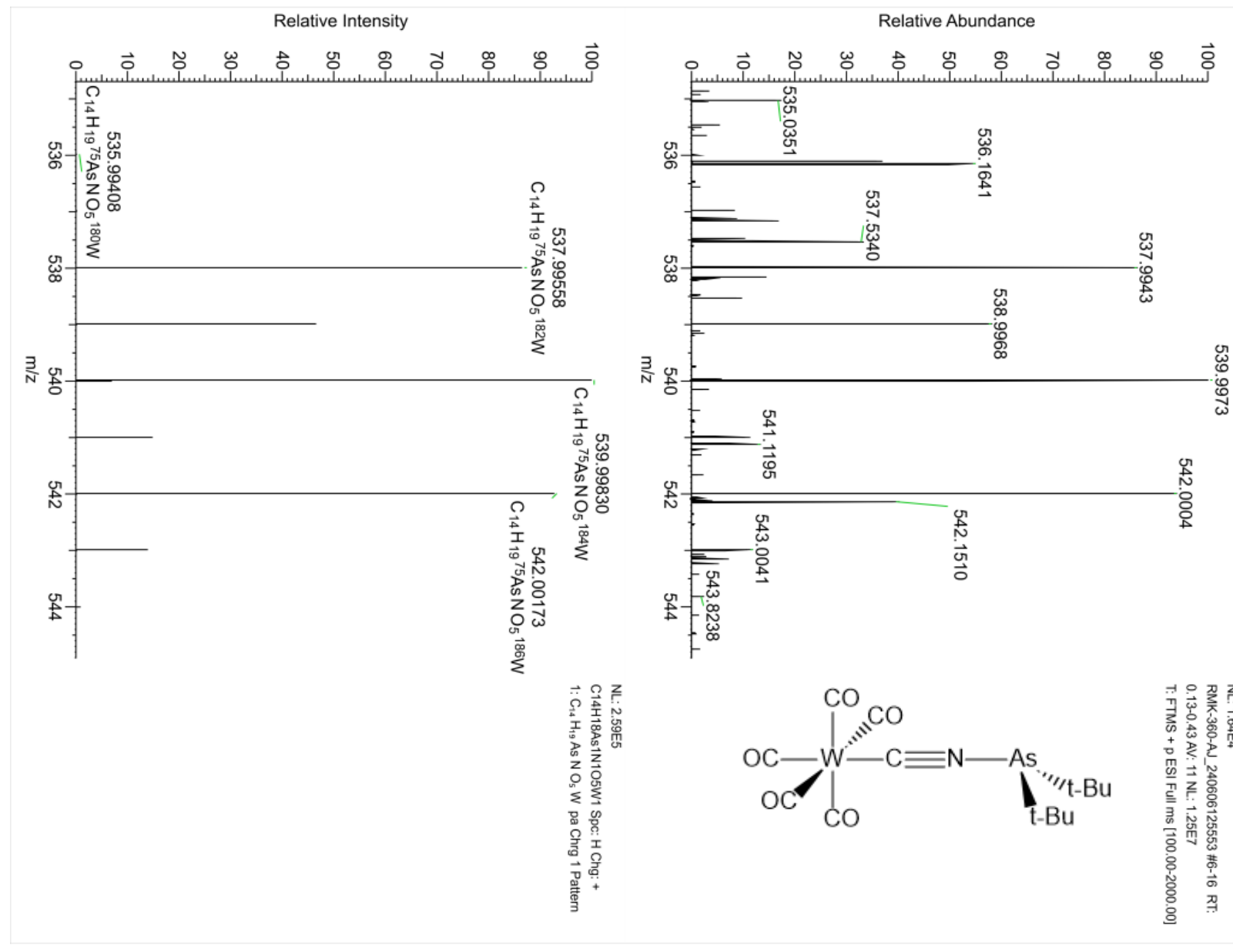
**Figure S79:** The  $^1\text{H}$  NMR spectrum of  $[W(CNAs^tBu_2)(CO)_5]$  ( $\text{C}_6\text{D}_6$ , 400 MHz, 25 °C).



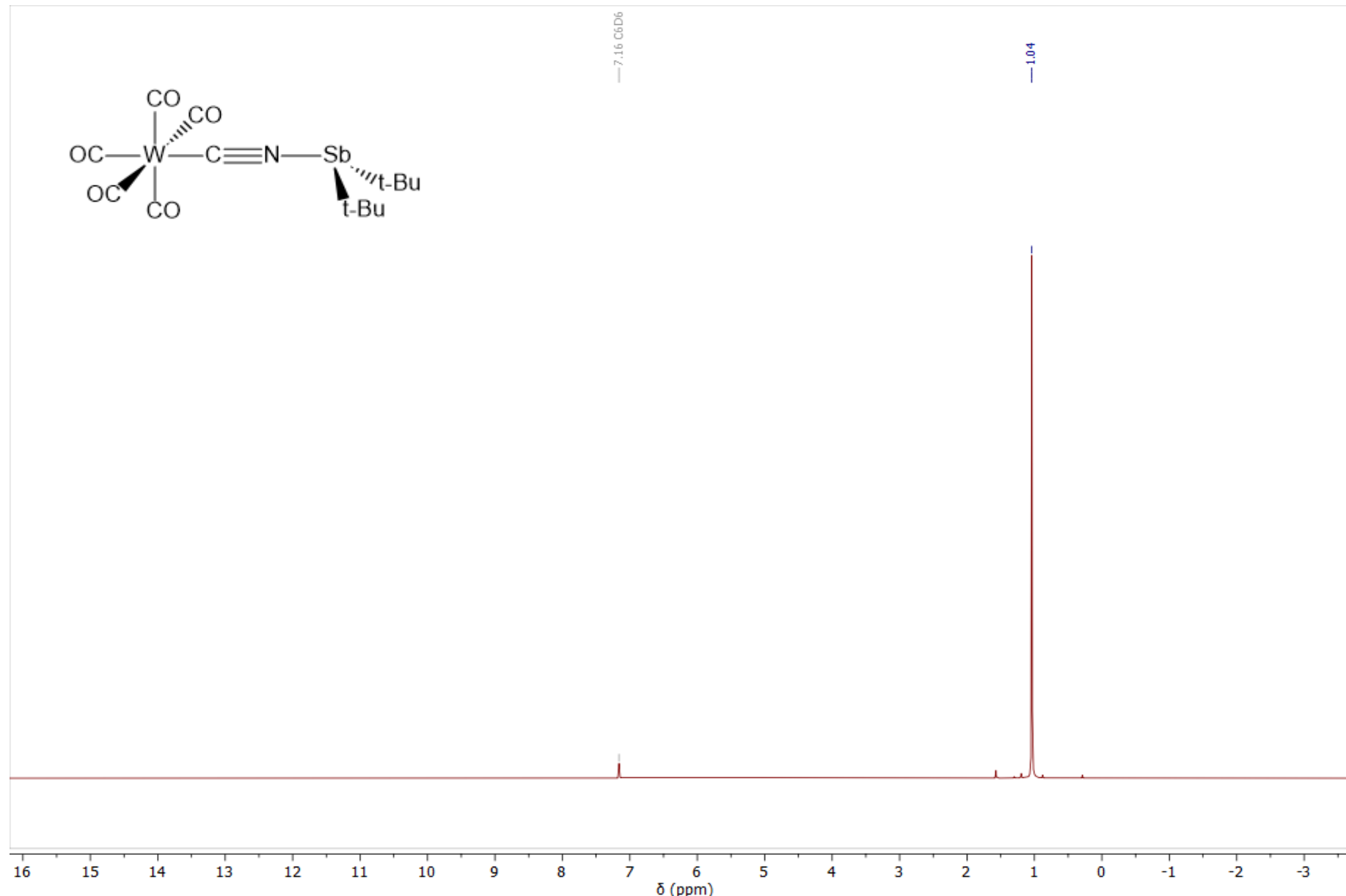
**Figure S80:** The  $^{13}\text{C}\{^1\text{H}\}$  NMR spectrum of  $[\text{W}(\text{CNAs}^{\text{t}}\text{Bu}_2)(\text{CO})_5]$  ( $\text{C}_6\text{D}_6$ , 201 MHz, 25 °C).



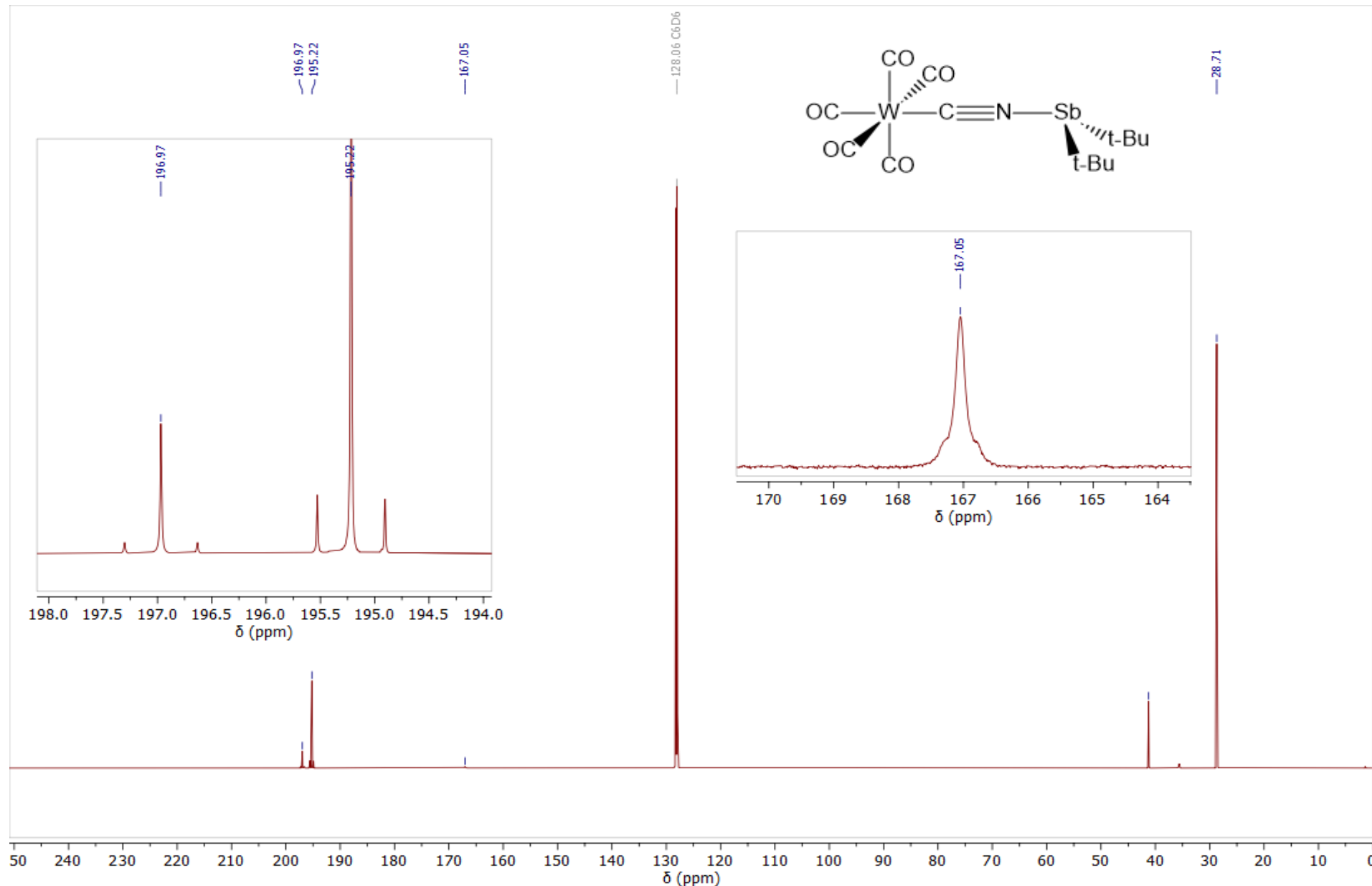
**Figure S81:** The solid state ATR-IR (top) and solution FT-IR (*n*-hexane; bottom) spectra of  $[W(CNAs^tBu_2)(CO)_5]$  in the carbonyl region (25 °C).



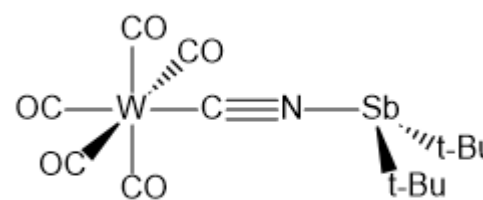
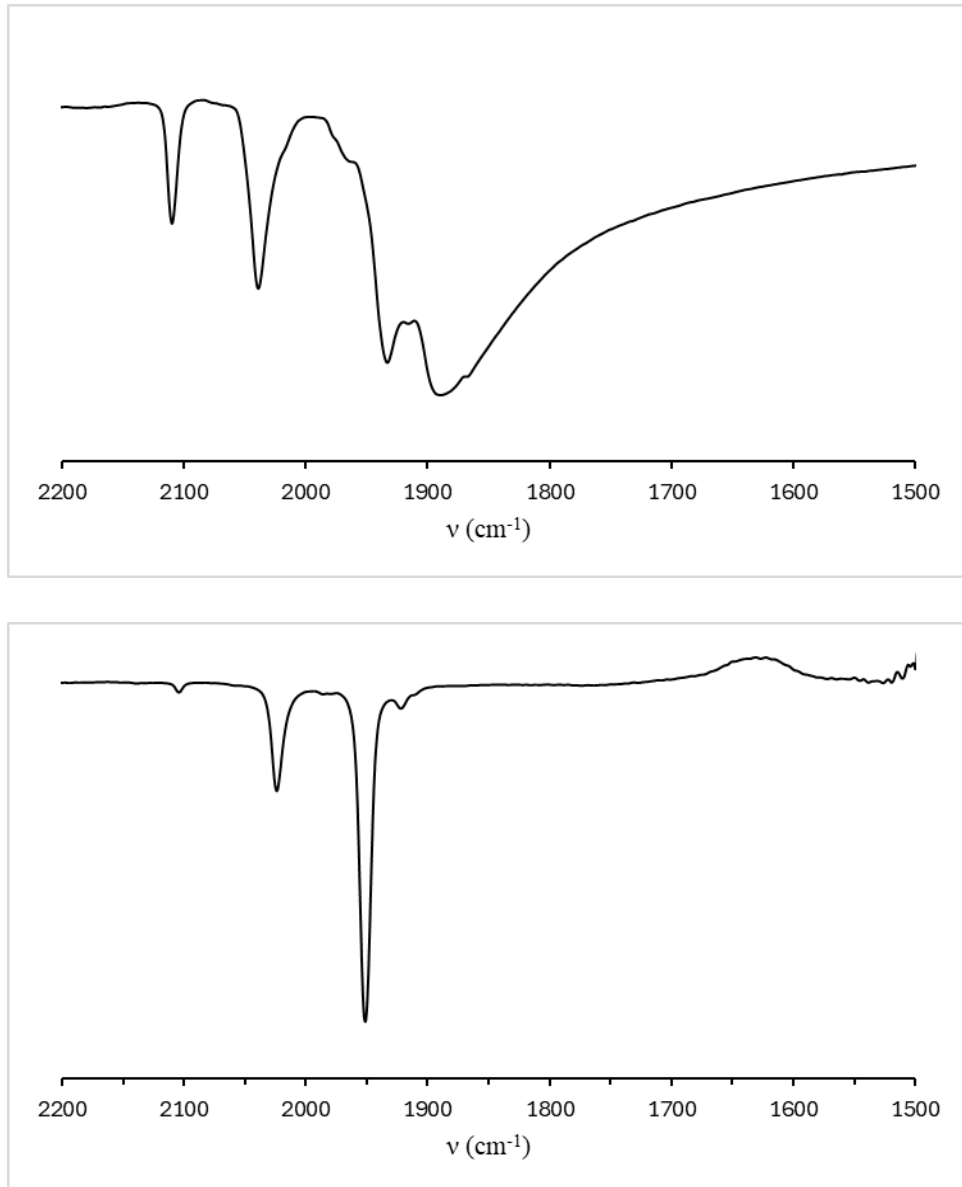
**Figure S82:** The HR-MS of  $[W(CNAs^tBu_2)(CO)_5]$  (ESI, positive ion mode, MeCN).



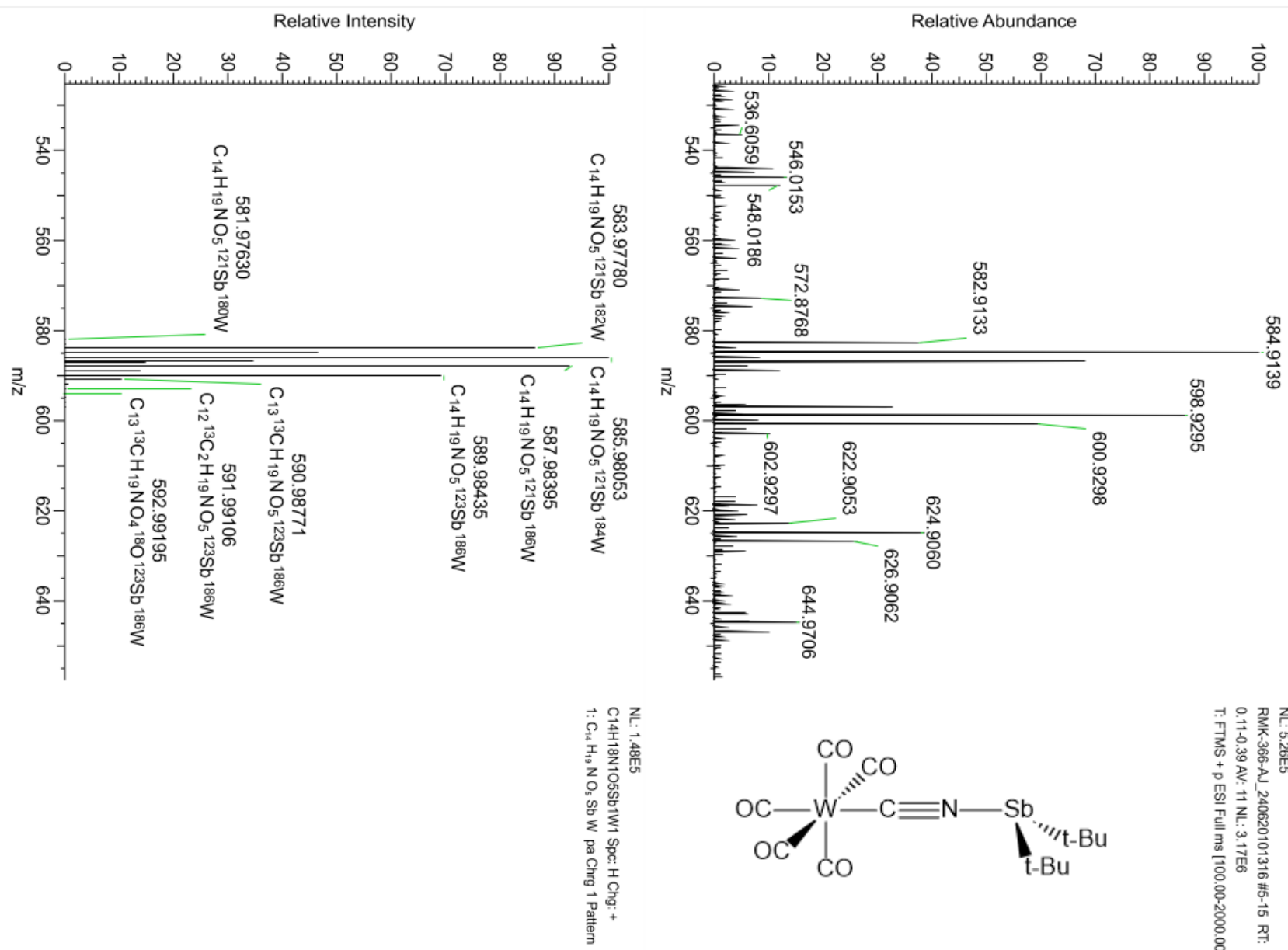
**Figure S83:** The  $^1\text{H}$  NMR spectrum of  $[W(CNSb^tBu_2)(CO)_5]$  ( $C_6D_6$ , 400 MHz, 25 °C).



**Figure S84:** The  $^{13}\text{C}\{^1\text{H}\}$  NMR spectrum of  $[\text{W}(\text{CNSb}^t\text{Bu}_2)(\text{CO})_5]$  ( $\text{C}_6\text{D}_6$ , 201 MHz, 25 °C).



**Figure S85:** The solid state ATR-IR (top) and solution FT-IR (*n*-hexane; bottom) spectra of  $[\text{W}(\text{CNSb}^{\text{t}}\text{Bu}_2)(\text{CO})_5]$  in the carbonyl region (25 °C).

**Figure S86:** The HR-MS of  $[W(CNSb^t\text{Bu}_2)(CO)_5]$  (ESI, positive ion mode, MeCN).

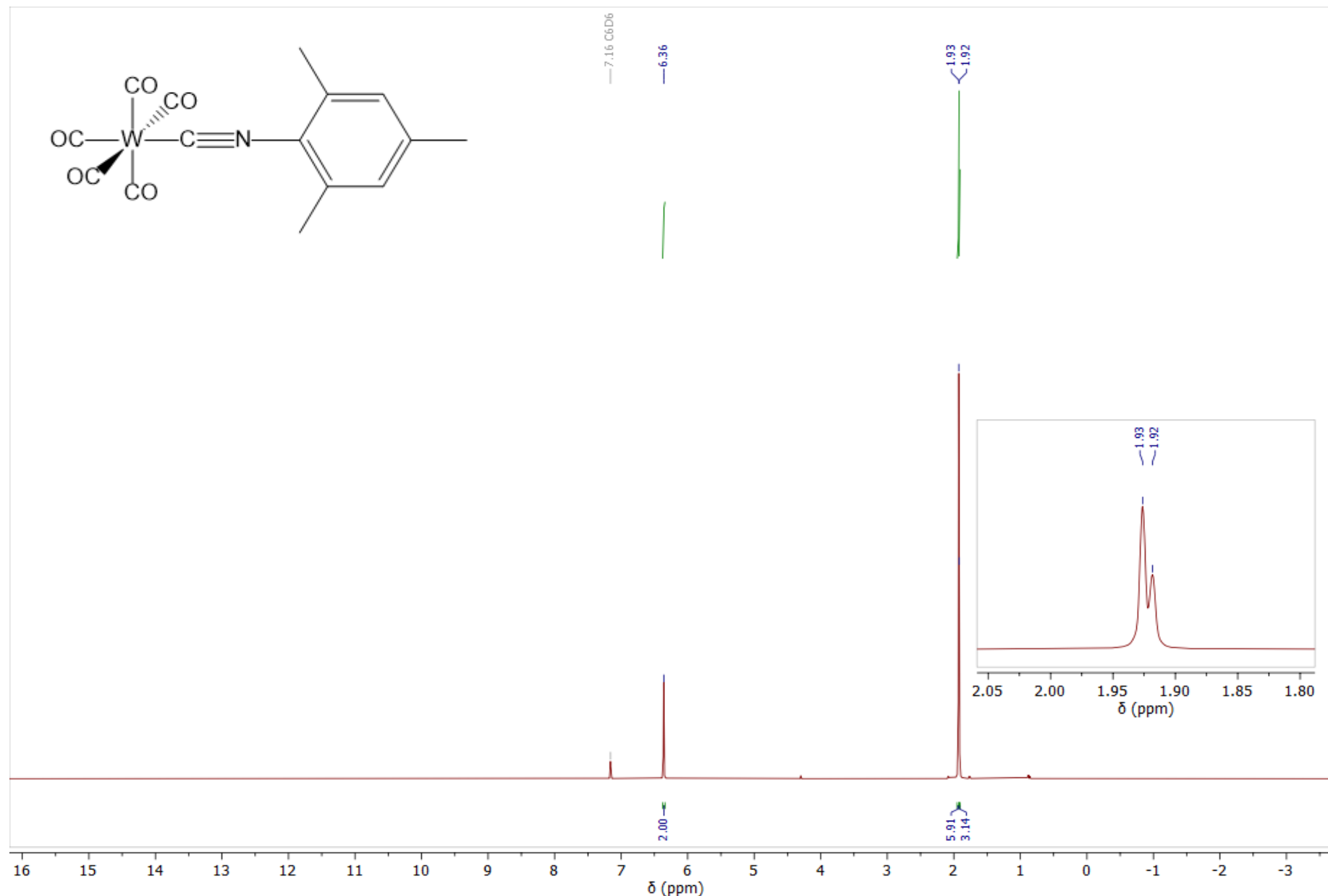
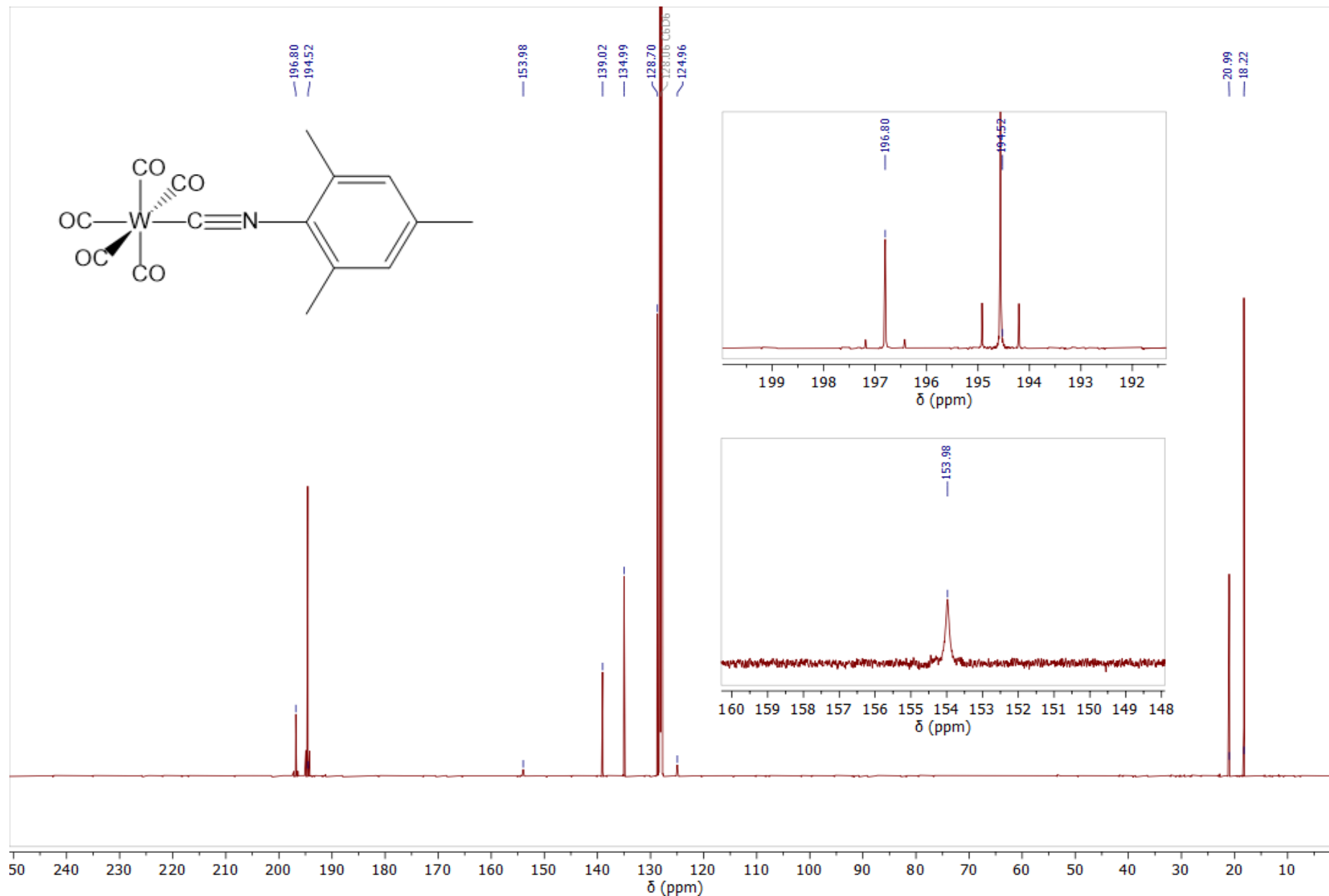
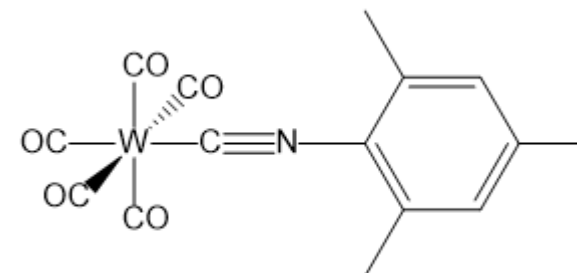
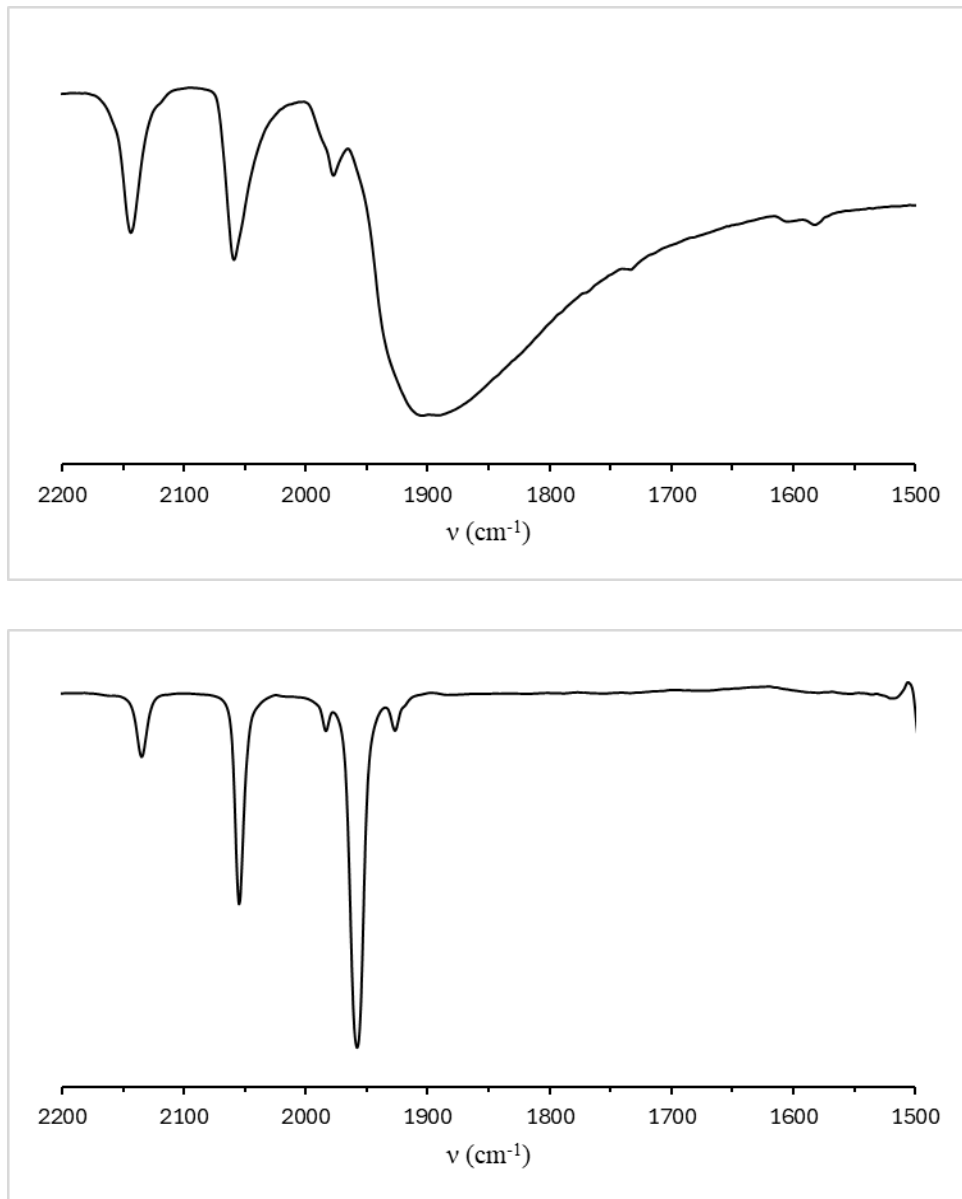


Figure S87: The  $^1\text{H}$  NMR spectrum of  $[\text{W}(\text{CNMes})(\text{CO})_5]$  ( $\text{C}_6\text{D}_6$ , 400 MHz, 25 °C).



**Figure S88:** The  $^{13}\text{C}\{^1\text{H}\}$  NMR spectrum of  $[\text{W}(\text{CNMes})(\text{CO})_5]$  ( $\text{C}_6\text{D}_6$ , 176 MHz, 25 °C).



**Figure S89:** The solid state ATR-IR (top) and solution FT-IR (*n*-hexane; bottom) spectra of  $[\text{W}(\text{CNMes})(\text{CO})_5]$  in the carbonyl region (25 °C).

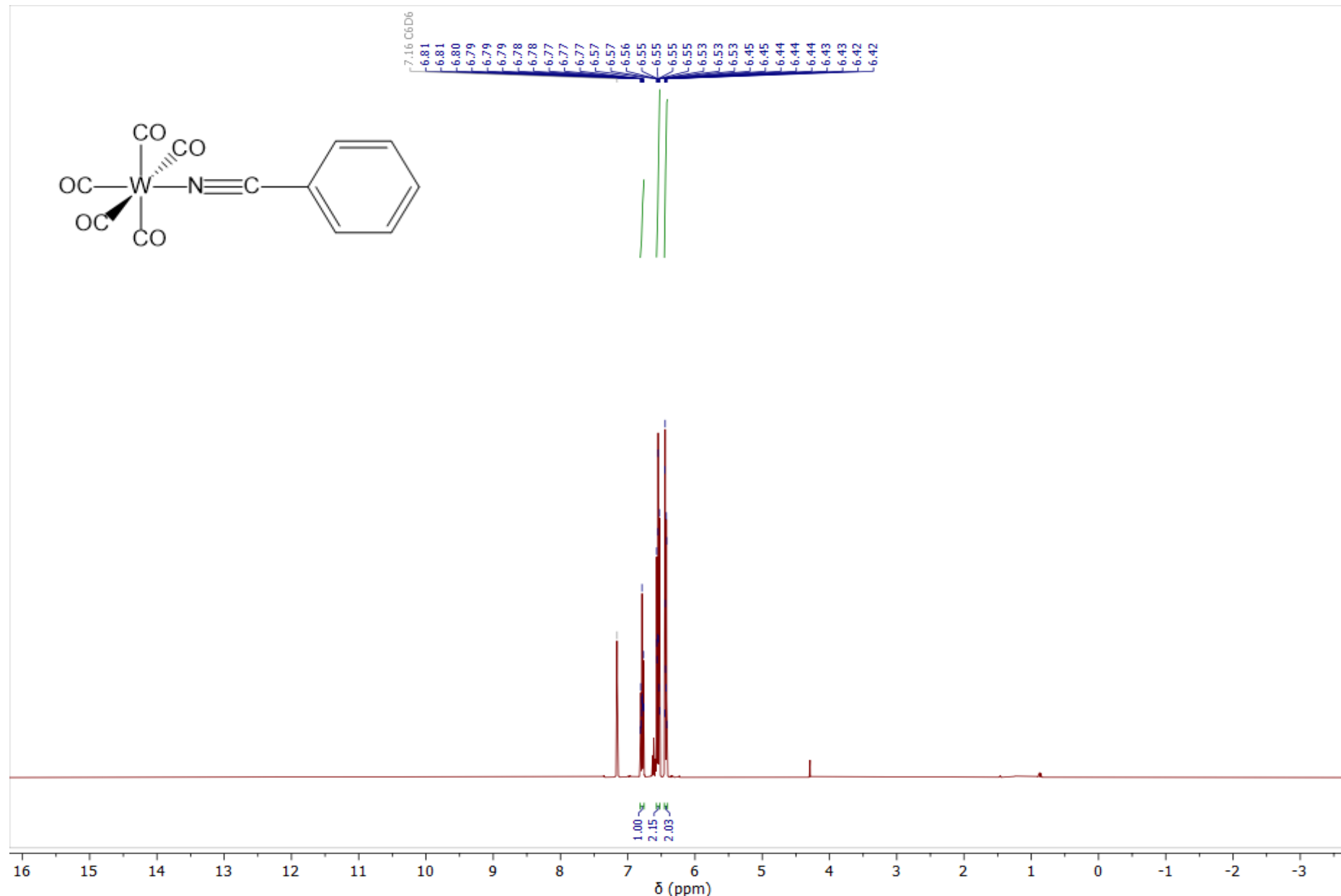


Figure S90: The  $^1\text{H}$  NMR spectrum of  $[\text{W}(\text{NCPh})(\text{CO})_5]$  ( $\text{C}_6\text{D}_6$ , 400 MHz, 25 °C).

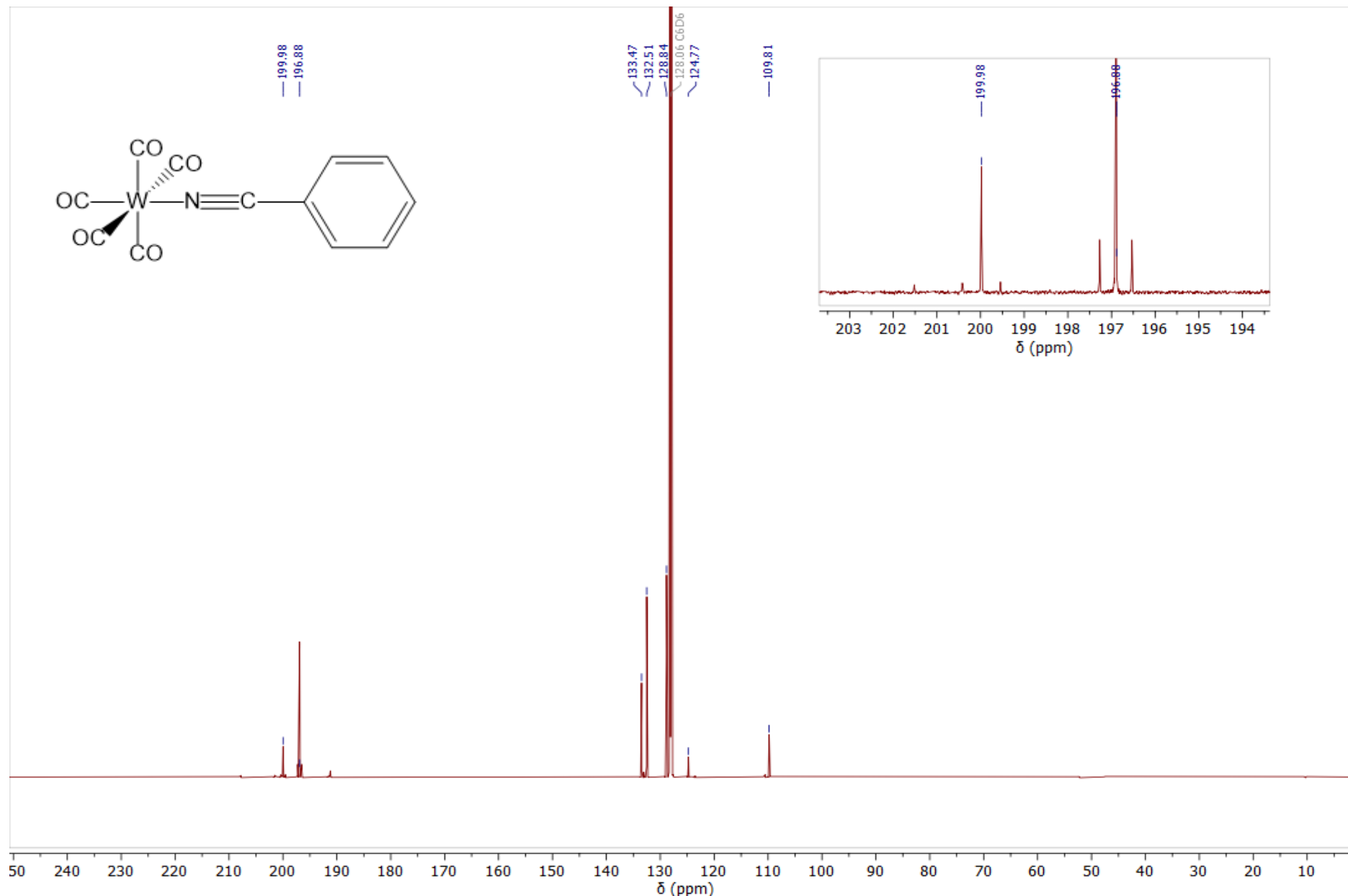
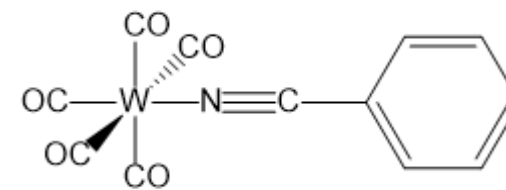
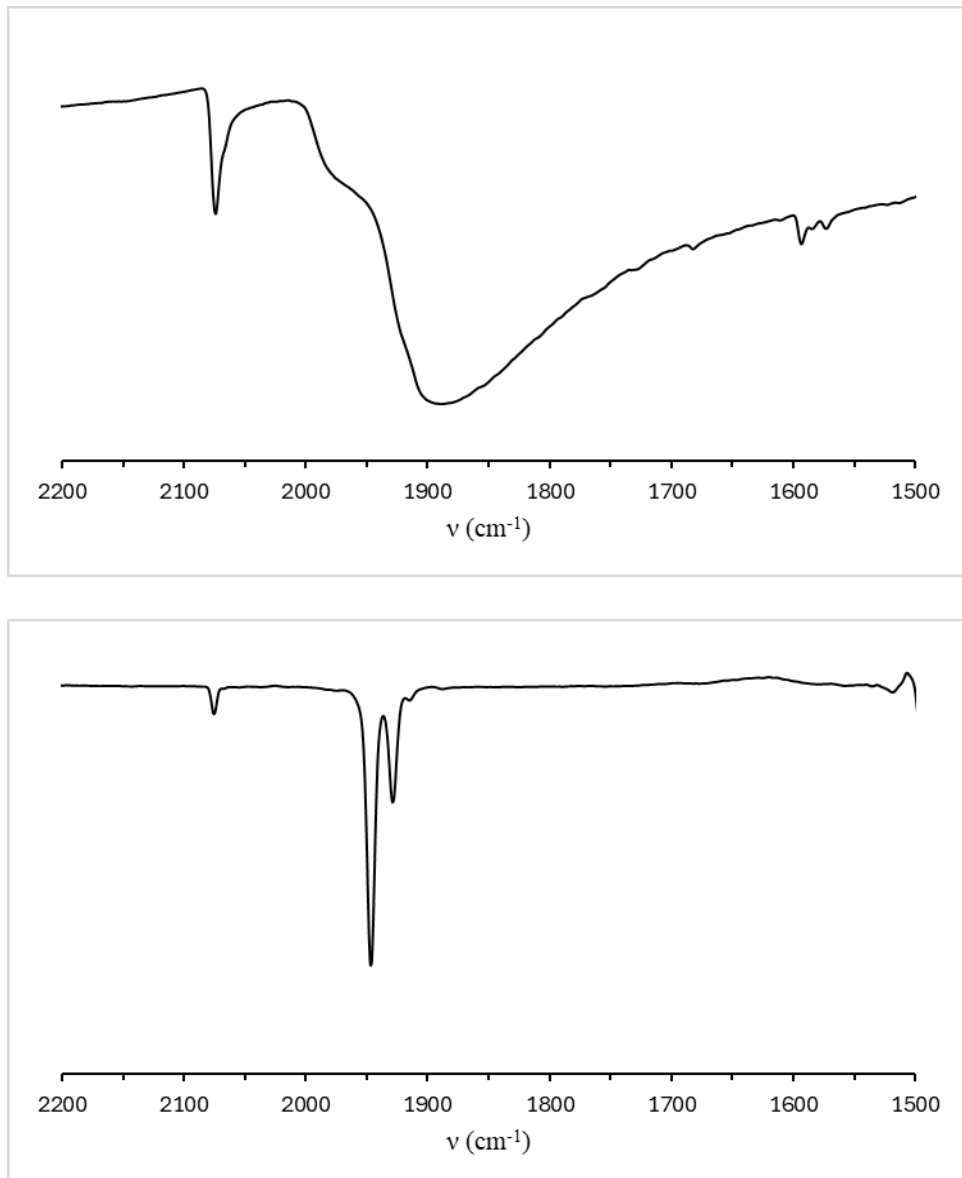


Figure S91: The  $^{13}C\{^1H\}$  NMR spectrum of  $[W(NCPh)(CO)_5]$  ( $C_6D_6$ , 176 MHz, 25 °C).



**Figure S92:** The solid state ATR-IR (top) and solution FT-IR (*n*-hexane; bottom) spectra of  $[W(NCPh)(CO)_5]$  in the carbonyl region (25 °C).